UNIVERSITÀ DEGLI STUDI DI PADOVA
DIPARTIMENTO DI INGEGNERIA INDUSTRIALE DII

TESI DI LAUREA MAGISTRALE IN INGEGNERIA AEROSPAZIALE

Theoretical Study of an MPD Thruster

Relatore: Prof. Daniele Pavarin
Correlatore: Prof. Josep Oriol Lizandra Dalmases

Laureanda: VERONICA BOTTI

ANNO ACCADEMICO 2016 – 2017

RINGRAZIAMENTI

Come prima cosa vorrei ringraziare il professor Oriol Lizandra per l'aiuto datomi nello scrivere il codice Matlab, per il supporto datomi nello svolgimento di questa tesi e per l'infinita disponibilità ogni volta che ne avessi bisogno e vorrei poi ringraziare moltissimo anche il Prof. Daniele Pavarin per il suo supporto.
Ringrazio tutti i professori di Ingegneria Aerospaziale dell'Università di Padova per tutto ciò che mi hanno insegnato in questi anni e per la pazienza e l'aiuto datomi soprattutto durante lo svolgimento degli ultimi esami.

Ringrazio infinitamente il Gab (e con lui l'OV), il Grande Forch, il Renna e la Giulia per le infinte risate fatte in questi ultimi anni, per aver sopportato le mie crisi e i miei dubbi e per avermi aiutata ogni volta che ne avessi bisogno, sia dal punto di vista pratico, sia moralmente. Loro non sono solo dei compagni di corso per me, ma gli amici che tutti vorrebbero avere.
Ringrazio anche il mio amico Alessio, con il quale mi laureo oggi e con cui ho condiviso un sacco di momenti importanti e divertenti e il quale non mi perdonerà mai per averlo portato alla via della perdizione!
Ringrazio tutto il team di EUROAVIA Padova e in modo particolare Mattia per tutte le serate passate a lavorare per EUROAVIA bevendo uno spritz al bar come solo tra amici si fa e ringrazio Simone, Andrea, Riccardo e gli altri rappresentanti degli studenti per il supporto e per tutto il loro impegno nel portare avanti gli interessi dell'università e in particolare del nostro corso.
Questi sono i momenti che di sicuro mi mancheranno di più di questi anni all'Università.

Ringrazio Eleonora, Lisa ed Elena per le tutte le belle serate passate a ridere al De Gusto e per essere sempre state presenti per me, anche quando ero via, Edoardo, che riesce sempre a farmi morire dal ridere quando ci vediamo, Sandro che è l'unica persona con cui mi sento libera di dire qualsiasi cosa senza mai vergognarmi, Matzu, per essere sempre presente nel momento del bisogno e Giampiero, perché anche se non ci vediamo mai, mi ascolta come solo un vero amico sa fare.
Voglio ringraziare Francesco, che mi ha vista crescere, un amico prezioso che mi ascolta e mi dà sempre ottimi consigli e che a volte mi ha anche tirata fuori dai guai. Poi vorrei ringraziare tantissimo Jessica, che conosco da quando sono nata, e Juan per essermi stati sempre vicini e non posso mancare di ringraziare Emily, che da quando è nata riesce sempre ad illuminarmi la giornata con la sua allegria, anche quando va tutto storto.
Ringrazio moltissimo Beatrice, la mia coscienza, che anche se ora non ci vediamo mai rimane per me una delle persone più importanti della mia vita, Chiara, una delle mie più care amiche, che è sempre presente per me ma soprattutto ringrazio di cuore Lisa, la sorella che non ho mai avuto, per tutte le esperienze pazze e meravigliose passate assieme in questi anni, per le risate e le chiacchierate durate ore ed ore al telefono e perché quando sono via mi manca immensamente.

Ringrazio infinitamente Margot per avermi fatto da seconda mamma per tutto il tempo passato in Belgio e con essa ringrazio Fanny e Gerardo e le loro famiglie per tutto l'aiuto che mi hanno dato in quei mesi lontana da casa e Marie, per i bei 9 mesi di convivenza a Redu.

Infine, mi rivolgo alle mie due famiglie, quella di origine e quella che mi sto creando ora e a questo proposito dovrò scrivere due ringraziamenti separati:
Della mia famiglia d'origine un ringraziamento speciale va alle seguenti persone: mia nonna Azzurrina, che ogni volta che vado da lei mi coccola e mi prepara sempre tutto quello che piace a me, mio zio Claudio, che

per me è come un secondo padre, per avermi supportato sia moralmente che economicamente in questo mio percorso, per la sua infinita bontà, per la sua generosità e il suo altruismo, per la sua allegria, per tutte le volte che vado da lui e che fa di tutto per rendermi felice. Ringrazio mio fratello Federico, che per me rimane sempre il mio fratellino Kikko, per tutte le volte che mi ha dato una mano, e il mio fratellone Ricky, che si preoccupa sempre che io stia bene. Da quando sono partita sono le persone che mi mancano di più. Infine, voglio ringraziare le due persone più importanti della mia vita: mia madre e mio padre. Non ci sono parole per descrivere tutto ciò che hanno fatto per me e cosa significhino per me e quindi l'unica cosa che posso fare è dedicare questa laurea a loro. Senza di loro non avrei mai potuto raggiungere nessuno dei traguardi che ho raggiunto e per questo posso solo dire GRAZIE MAMMA! GRAZIE PAPA'! VI VOGLIO BENE!

Infine vorrei ringraziare la mia seconda famiglia, quella che mi sto costruendo ora, ma per farlo dovrò scrivere le prossime parole in inglese:

I would like to thank Johan's family: Nele, Veronique and Pierre, for having accepted me in their family and in particular Veronique and Pierre for their help and support all along these months. Thanks to them I felt at home even if I was far from my original family!
Finally, the biggest thanks goes to my amazing boyfriend Johan for all the help he gave me for my thesis, for always being there for me, even in the hardest moment. I have no words to describe what he did for me and how much this meant to me. Since I've met him my life has totally changed and I could not be happier than this. I love you, Johan!

Ci sono moltissime altre persone che vorrei ringraziare, ma non basterebbe un libro per nominarle tutte, quindi l'unica cosa che posso dire ora è:

A tutti voi che oggi siete qui, GRAZIE!

Veronica Botti

INDEX

TABLE OF FIGURES

TABLE OF TABLES

INTRODUCTION

The purpose of this thesis is to describe the operations of a Magneto Plasma Dynamic thruster (MPD thruster), thanks to the analyse of the conclusions drown by Professor Martinez Sanchez in the paper "***The Structure of Self-Field Accelerated Plasma Flows***".

In order to do that, a MatLab code has been created, to reproduce the results he presented in that paper, but beforehand, an analysis of the physics that stands behind electrical propulsion and, in particular, this thruster will be done.

In Chapter 1, a brief description of the basic equations of propulsion and a comparison between chemical and electrical thrusters will be made, showing the cases in which, electrical propulsion is more convenient than Chemical one.

Then, in Chapter 2, a brief description of the main electrical thrusters at the state of the art will be given, describing their operations and performances.

A theoretical description of the basics of Plasma Physics will follow in Chapter 3 with a focus on the basic equations of the magneto hydro dynamics.

In Chapter 4 we will describe with a simple model how to calculate the main parameters of an MPD thruster, such as thrust, efficiency, and current density.

In Chapter 5 will finally take a look in the mathematical equations behind the MatLab code and in Chapter 6 we will present some notable results, comparing them with those presented by Professor Martinez Sanchez.

CHAPTER 1: SPACE PROPULSION GENERALITIES

The word "***Propulsion***" derives from the Latin words "***pro***"- that means "**on**"- and "***pellere***"- that means "**push**" and represents the act that you have to do to give a material body the energy needed for his own motion- i.e. "***push-on***". This action is made by a device called "***Propeller***" that is dynamic to its own essence, so it shows with the generation of a force called "***Thrust***", that is responsible for its motion.

THE EQUATION OF THE THRUST

Let's start with the mathematical analysis of the problem: the only way to accelerate something in free space is by reaction. Considering the following system:

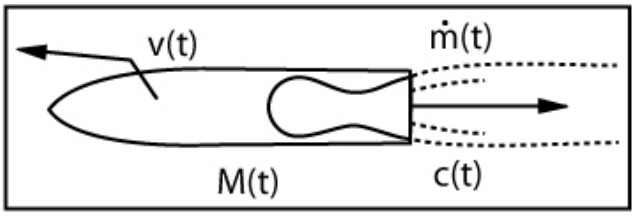

Figure 1-1: Simplified model of a thruster.

The ***Equation of the Thrust*** in vacuum derives from:

$$M_{tot}(t) = m(t)\vec{v}(t) + \int_0^t \dot{m}(t')[\vec{v}(t') - \vec{c}(t')]dt' = \ Cost. \qquad (1\text{-}2)$$

where we are writing $m(t)$ instead of $M(t)$. We put it constant because we're considering no drug or interaction of molecules with ambient air. Thus, it derives:

$$\frac{dM_{tot}}{dt} = 0 \qquad (1\text{-}3)$$

$$m\frac{d\vec{v}}{dt} + \vec{v}\frac{dm}{dt} + \dot{m}(\vec{v} - \vec{c}) = 0 \qquad (1\text{-}4)$$

but we know that:

$$\dot{m} = -\frac{dm}{dt} \leftarrow (Mass\ Flow\ Rate) \tag{1-5}$$

$$\Longrightarrow m\frac{d\vec{v}}{dt} = \dot{m}\vec{c} = \vec{F} \leftarrow (\boldsymbol{Thrust}) \tag{1-6}$$

$$\Longrightarrow \frac{d(m\vec{v})}{dt} = \vec{F} - \vec{v}\dot{m} = \dot{m}(\vec{c} - \vec{v}) \tag{1-7}$$

We can do the same to calculate the ***Kinetic Energy-*** $\boldsymbol{E_k}$- of the system rocket-jet:

$$E_k = \frac{1}{2}m|\vec{v}|^2 + \int_0^t \frac{1}{2}\dot{m}(t')[\vec{v}(t') - \vec{c}(t')]^2 dt' \tag{1-8}$$

$$\Longrightarrow \frac{dE_k}{dt} = m\vec{v}\frac{d\vec{v}}{dt} + \frac{1}{2}|\vec{v}|^2\frac{dm}{dt} + \frac{1}{2}\dot{m}\left(|\vec{v}|^2 + |\vec{c}|^2 - \overrightarrow{2\vec{v}\vec{c}}\right) = \frac{1}{2}\dot{m}|\vec{c}|^2 \tag{1-9}$$

since

$$m\vec{v}\frac{d\vec{v}}{dt} = \dot{m}\vec{c}\vec{v} \tag{1-10}$$

$$\frac{dm}{dt} = -\dot{m} \tag{1-11}$$

so, if some energy is expended internally at the rate $\dot{E}$ and converted to total kinetic energy with ***Efficiency-*** $\boldsymbol{\eta_{th}}$ we have that:

$$\frac{dE_k}{dt} = \eta_{th}\dot{E} \tag{1-12}$$

so that:

$$\eta_{th}\dot{E} = \frac{1}{2}\dot{m}|\vec{c}|^2 \leftarrow (Jet\ kinetic\ Power) \tag{1-13}$$

If we then define the ***Useful Propulsive Work*** as:

$$\vec{F}\vec{v} = \dot{m}|\vec{v}||\vec{c}| \tag{1-14}$$

we can find the ***Propulsive Efficiency-*** $\boldsymbol{\eta_{prop}}$:

$$\eta_{prop} = \frac{\vec{F}\vec{v}}{\eta_{th}\dot{E}} = \frac{\dot{m}|\vec{v}||\vec{c}|}{\frac{1}{2}\dot{m}|\vec{c}|^2} = 2\frac{|\vec{v}|}{|\vec{c}|} \tag{1-15}$$

This value is arbitrary high (if $|\vec{v}| > \frac{|\vec{c}|}{2} \Longrightarrow \eta_{prop} > 1$), so it's not typically used for rockets, but it's still true that if we thrust at high speed we increase the Kinetic Energy more.

Considering now the well-known ***Formula of the Thrust***:

$$F = \dot{m}v_e + A_e(p_e - p_a) = \dot{m}c \tag{1-16}$$

(and remembering that from this moment we are evaluating just the modules of the quantities and defining):

- v_e- Jet Speed far from the Exhaust;
- A_e- the Exhaust Nozzle Area;
- p_e- the Exhaust Pressure;
- p_a- the Ambient Pressure;
- c- Effective Exhaust Speed;

and:

$$c = \frac{F}{\dot{m}} \tag{1-17}$$

we have that for finite p_a, in thermal rockets, increasing A_e we increase also v_e, towards a limit represented by:

$$v_{e,max} \sim \sqrt{2c_p T_0} \tag{1-18}$$

where T_0 represents the Total Temperature of the exhaust. Then, it can be $A_e(p_e - p_a)$ negative. So the best A_e is the one that makes $\boldsymbol{p_e = p_a}$. When we have this condition we can say that we are in ***"Perfect Adaptation"***.

Other very important parameters are:

- c_F- *Thrust Coefficient*- It represents what happens in the nozzle;
- c^*- *Real Exhaust Velocity*- it represents the velocity of the sound into the Combustion Chamber;
- I_{sp}- *Specific Impulse*- it represents the Effective Exhaust Velocity;
- I_{tot}-*Total Impulse*- it tells me how big is the engine;
- I_{ss}- *Specific Impulse of the System*;
- ${}^{F}/_{W} - \ Thrust\ level$- it tells me the relation between the thrust and the system weight;

and we know that:

$$c = c^* \cdot c_F \tag{1-19}$$

where:

$$c^* = \frac{\sqrt{RT_0}}{\Gamma(\gamma)} \tag{1-20}$$

$$\Gamma(\gamma) = \sqrt{\gamma}\left(\frac{2}{\gamma+1}\right)^{\frac{\gamma+1}{2(\gamma-1)}} \tag{1-21}$$

$$c_F = \frac{F}{p_0 A_t} \tag{1-22}$$

so c^* depends on the properties of the propellant. To quantify instead the performances of a nozzle analyzing the $c_F - \varepsilon$ graphic:

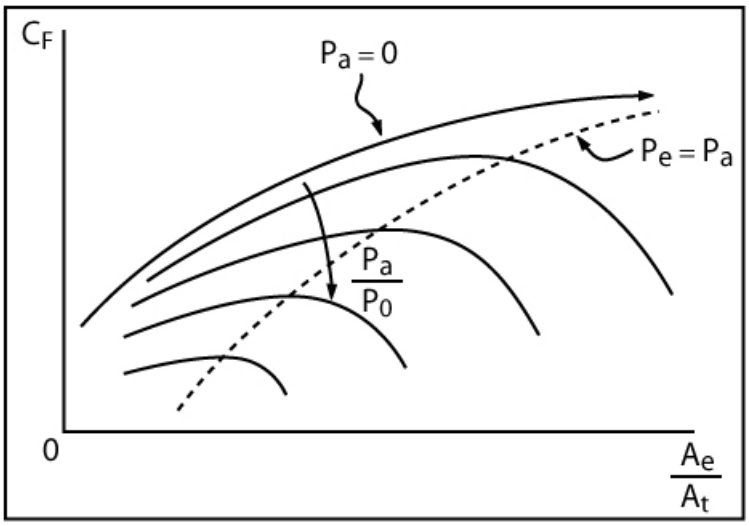

Figure 1-2: $c_F - \varepsilon$ graphic

The most typical values of c_F are included between 1.5 and 2.
The bigger is the Effective Exhaust Velocity, the better is the engine. So, the two "players" are the combustion chamber- that is represented by c^*- because it warms the gases, and the nozzle- that is represented by c_F- because it transforms the thermal energy in ordered energy.

$$I_{sp} = \frac{F}{\dot{m}g} = \frac{c}{g^*} = \frac{c^* c_F}{g^*} \tag{1-23}$$

The I_{sp} in general should be high to have better performances.

$$I_{tot} = \int_0^{t_{burning}} F dt \tag{1-24}$$

$$\Longrightarrow I_{sp} = \frac{F \cdot t_{burning}}{m \cdot g^* \cdot t_{burning}} = \frac{I_{tot}}{m_{prop} \cdot g^*} \tag{1-25}$$

$$I_{ss} = \frac{I_{tot}}{m_{tot} \cdot g^*} \tag{1-26}$$

Then:

$$\dot{m} = \rho_t v_t A_t = \rho_0 A_t \left(\frac{2}{\gamma+1}\right)^{\frac{1}{\gamma-1}} \sqrt{\gamma R T_0 \left(\frac{2}{\gamma-1}\right)} \quad (1\text{-}27)$$

$$\rho_0 = \frac{p_0}{R T_0} \quad (1\text{-}28)$$

where the subscript "t" represents the *Throat* of the Nozzle and the subscript "0" indicates the total variables. Finally, we can calculate the Δv that the rocket needs to reach the requested altitude. To do it we first define the following parameters:

- m_0- *Initial mass*;
- $m_{P/L}$- *P/L mass*;
- m_{in}- *Inert mass*;
- m_s- *mass of the structure*;
- m_{prop}- *mass of the propellant*;
- m_f-*Final mass*;

We have:

$$m_0 = m_{P/L} + m_{in} + m_{prop} \quad (1\text{-}29)$$

$$m_f = m_{P/L} + m_{in} \quad (1\text{-}30)$$

$$k_u = \frac{m_{P/L}}{m_0} \leftarrow (P/L\ Ratio) \quad (1\text{-}31)$$

$$k_p = \frac{m_{prop}}{m_0} \leftarrow (Propellant\ Ratio) \quad (1\text{-}32)$$

$$k_m = \frac{m_0}{m_f} \leftarrow (Masses\ Ratio) \quad (1\text{-}33)$$

$$\epsilon = k_s = \frac{m_{in}}{m_{in} + m_{prop}} \leftarrow (Inert\ \ Mass\ Fraction) \tag{1-34}$$

This last parameter increases with the decreasing of the propellant.
As we said in the introduction, Tsiolkovsky was the first one that theorized the ***Rocket Equation***. Starting by the definition of the ***Thrust***:

$$F = \dot{m}c \tag{1-35}$$

and remembering that:

$$\dot{m} = -\frac{dm}{dt} \tag{1-36}$$

$$m\frac{dv}{dt} = F = -\frac{dm}{dt}c \tag{1-37}$$

$$-cdm = mdv \tag{1-38}$$

$$dv = -c\frac{dm}{m} \tag{1-39}$$

$$\Longrightarrow \Delta v = -\int_{m}^{m_f} c\frac{dm}{m} = c\ ln\left(\frac{m_0}{m_f}\right) = c\ ln(k_m) = g^* I_{sp} ln(k_m) \tag{1-40}$$

$$\Longrightarrow m_0 = m_f \cdot e^{\frac{\Delta v}{I_{sp} \cdot g^*}} \tag{1-41}$$

$$\Longrightarrow m_{prop} = m_f\left(e^{\frac{\Delta v}{I_{sp} \cdot g^*}} - 1\right) = m_{P/L}\frac{\left(e^{\frac{\Delta v}{I_{sp} \cdot g^*}} - 1\right)(1-\epsilon)}{(1 - \epsilon e^{\frac{\Delta v}{I_{sp} \cdot g^*}})} \tag{1-42}$$

From this last equation we can find the ***Condition of Realization of the Mission***:

$$(1 - \epsilon^{e^{\frac{\Delta v}{I_{sp} \cdot g^*}}}) > 0 \tag{1-43}$$

$$\Longrightarrow I_{sp} > \frac{\Delta v}{ln\left(\frac{1}{\epsilon}\right) \cdot g^*} \tag{1-44}$$

Where the Δv calculated is the theoretical one, calculated by Tsiolkovsky.

As we told above, for chemical rockets *c* is limited by chemical energy/mass in fuel:

$$c_{max} = \sqrt{2E} \tag{1-45}$$

In fact, since:

$$\frac{1}{2}\dot{m}{v_e}^2 = \eta_{th}\dot{E} = \eta_{th}\dot{m}E \tag{1-46}$$

$$\Longrightarrow v_e = \sqrt{2\eta_{th}E} \tag{1-47}$$

And making a replacement of *E* by the *Enthalpy H* and remembering that, for a Brayton cycle we have:

$$H = c_p T_0 \tag{1-48}$$

$$\eta_{th} = 1 - \left(\frac{p_e}{p_0}\right)^{\frac{\gamma-1}{\gamma}} \tag{1-49}$$

we get:

$$v_e = \sqrt{2c_pT_0\left[1-\left(\frac{p_e}{p_0}\right)^{\frac{\gamma-1}{\gamma}}\right]} \tag{1-50}$$

Thus, what we want is to get high value of the ratio $\frac{p_0}{p_e}$, that means getting high value of the pressure in the Combustion Chamber- p_0. Higher $p_0$in fact can increase T_0 by inhibiting dissociation, so getting higher I_{sp}. But the main reason to get higher p_0 is to reduce weight for a given thrust, in fact, as we can see from the figure below:

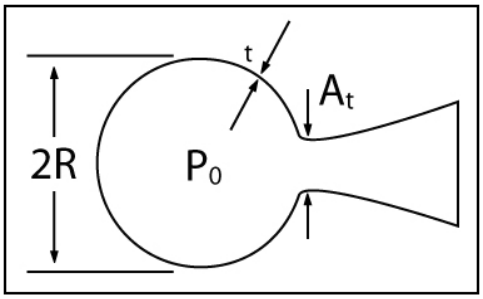

Figure 1-3: Simplified model of a thruster

$$\frac{m}{F} \cong \frac{4\pi R^2 t\rho_w}{c_F p_0 A_t} \tag{1-51}$$

$$2\pi Rt\sigma = \pi R^2 p_0 \Longrightarrow t = p_0\frac{R}{2\sigma} \tag{1-52}$$

$$A_t = KR^2 \tag{1-53}$$

$$\Longrightarrow \frac{m}{F} \cong \frac{4\pi p_0 R\rho_w}{2\sigma c_F p_0 K} \tag{1-54}$$

$$\Longrightarrow \frac{m}{F} \cong \frac{2\pi}{Kc_F}\frac{\rho_w}{\sigma}R \tag{1-55}$$

$$F = c_F p_0 KR^2 \tag{1-56}$$

$$\Longrightarrow R = \sqrt{\frac{F}{c_F p_0 K}} \tag{1-57}$$

$$\Longrightarrow \frac{m}{F^{3/2}} \cong \frac{2\pi}{(K c_F)^{3/2}} \frac{\rho_w}{\sigma} \sqrt{\frac{1}{p_0}} \tag{1-58}$$

Thus, for a given thrust level, the engine mass scales like $\frac{1}{\sqrt{p_0}}$. So, for a given I_{sp} it may be better to reduce p_0, reducing thrust and operating longer.
However, even if we did it and we maximized the thermal efficiency η_{th} by minimizing the pressure ratio $\frac{p_e}{p_0}$, we would get the same value of the velocity we wrote before:

$$v_{e,max} = \sqrt{2 c_p T_0} \tag{1-59}$$

that is about $v_{e,max} \cong 4500\ m/s$.
That's the main reason for what sometimes we'd rather use Electric Thrusters even though the trust they perform is much lower than the one performed by a Chemical Rocket: Electrical Rockets break the v_e limit, allowing any I_{sp}. In few words, Electrical Rocket are very fuel efficient Rockets.
However, the power requested by an Electrical Rocket to work well is very high, in fact:

$$P = \frac{1}{\eta_c} \frac{1}{2} \dot{m} c^2 = \frac{F c}{2 \eta_c} \tag{1-60}$$

$$\frac{P}{m} = \frac{F}{m} \frac{c}{2 \eta_c} = \frac{a c}{2 \eta_c} \tag{1-61}$$

Roughly, if we have $0.5\ W/kg \rightarrow 2\ kg/W = 2000\ kg/KW$.
So, with reasonable mass/power ratios for Electric Power, we can get just very low accelerations. A graphic that shows well this point is the following one:

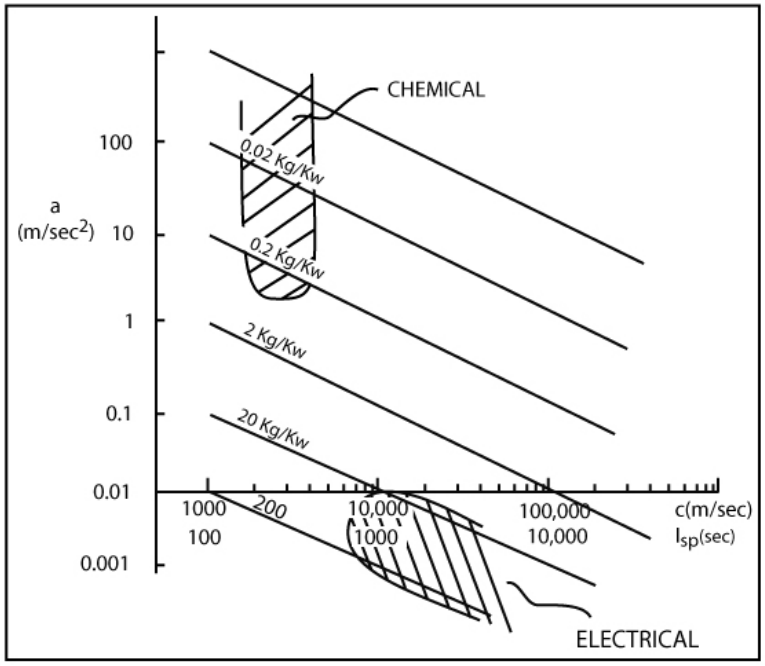

Figure 1-4: a-I_{sp} graphic for chemical and electrical thrusters

CHEMICAL VS ELETRIC PROPULSION AND LOW THRUST SPIRAL CLIMB

In electric propulsion systems, large amounts of energy can be transferred to propellant mass to increase the exhaust velocity. In these systems, thrust is generated in by using electric or magnetic processes to accelerate propellant so, as we said above, this makes electric thrusters, unlike chemical one, not energy limited when neglecting component lifetime, but just power limited: in fact, the rate at which energy can be provided is limited by the mass of the power system so, they typically have a low thrust to mass ratio.
However, the interesting thing of these thrusters is that they tend to have higher I_{sp}, so they can operate for significantly longer periods of time than chemical one.

So, let's make an example to show in which case an electrical thruster is better than a chemical one when we go away from the Earth.

To reach Mars for example, leaving from a LEO and using a Hohmann Transfer, we need a $\Delta\vec{v}\sim 5\ km/s$. In fact the total $\Delta\vec{v}$ will be the result of the sum between two impulses: the first one is given by the difference between the transfer velocity at perigee and the initial orbital velocity around the Earth- Δv_1- and the second one is given by the final orbital velocity around Mars and the Transfer apoapsis velocity- Δv_2:

$$v_E = \sqrt{\frac{\mu}{r_E}} \qquad (1\text{-}62)$$

$$v_{E,p} = \sqrt{2\mu\left(\frac{1}{r_E} - \frac{1}{r_E + r_M}\right)} \tag{1-63}$$

$$\Longrightarrow \Delta v_1 = v_{E,p} - v_E = \sqrt{\frac{\mu}{r_E}}\left(\sqrt{\frac{2r_M}{r_E + r_M}} - 1\right) \tag{1-64}$$

$$v_M = \sqrt{\frac{\mu}{r_M}} \tag{1-65}$$

$$v_{M,a} = \sqrt{2\mu\left(\frac{1}{r_M} - \frac{1}{r_E + r_M}\right)} \tag{1-66}$$

$$\Longrightarrow \Delta v_2 = v_{M,a} - v_M = \sqrt{\frac{\mu}{r_M}}\left(1 - \sqrt{\frac{2r_E}{r_E + r_M}}\right) \tag{1-67}$$

Where:

- μ is the Gravitational Constant of the Sun;
- r_E is the distance Earth-Sun;
- r_M is the distance Mars-Sun;

The total impulse will be given, as we said, by their sum:

$$\Delta v_{TOT} = \Delta v_1 + \Delta v_2 = 5.4\ km/s \tag{1-68}$$

Now, as we said, we know that the maximum exhaust velocity that a chemical thruster can reach is about $4.5\ km/s$ so, knowing the Rocket Equation, it has been calculated that a conventional chemical rocket should use more than $2/3$ of the vehicle mass only for the fuel (it has been calculated about 73% of the vehicle mass) for a mission like this.

For even longer mission, where the required Δv are in the range of $35 - 70\ km/s$ the chemical rockets should use more or less 99.98% of their mass just for the fuel. This is not taking into account any swing-by that can be done using different planets.
Hence, such situations require the use of different engines, like the Electrical Thrusters.
However, Electrical Thrusters, cannot provide high Thrusts so, a Hohmann Transfer is not possible; in these cases it's preferable to use a ***Spiraling Transfer Trajectory***.

Let's now make an approximation of the Δv ***for a Low-Thrust Spiral Climb***.
Assume an initial circular orbit with a velocity:

$$v = v_{co} = \sqrt{\frac{\mu}{r_0}} \tag{1-69}$$

with the Thrust applied tangentially and being:

$$a = \frac{F}{m} \tag{1-70}$$

By the Conservation of the Energy, assuming the orbit remains near-circular we can write:

$$\frac{d}{dt}\left(-\frac{\mu}{2r}\right) = a\sqrt{\frac{\mu}{r}} = \frac{\mu}{2r^2}\frac{dr}{dt} \tag{1-71}$$

$$\Longrightarrow \mu^{1/2}\frac{r^{-3/2}}{2}dr = adt \tag{1-72}$$

Integrating it:

$$\int_0^{t_b} adt = \Delta v \tag{1-73}$$

$$\Longrightarrow -\mu^{1/2}r^{-1/2}\Big|_0^{t_b} = \Delta v \tag{1-74}$$

$$\Longrightarrow \Delta v = \sqrt{\frac{\mu}{r_0}} - \sqrt{\frac{\mu}{r(t_b)}} = v_{co} - v_{c_{fin}} \tag{1-75}$$

The velocity increment Δv is equal to the decrease in orbital velocity. The rocket is pushing forward, but the velocity is decreasing, because in a r^{-2} force field, the kinetic energy is equal in magnitude but of the opposite sign as the total energy.
Thus, the general formula for the Δv is:

$$\Delta v = |\Delta v_c| \tag{1-76}$$

Rewriting the formula that we found:

$$\sqrt{\frac{\mu}{r_0}} - \sqrt{\frac{\mu}{r}} = at \tag{1-77}$$

And solving for r, we get:

$$r = \frac{r_0}{\left(1 - \frac{at}{\sqrt{\frac{\mu}{r_o}}}\right)^2} = \frac{r_0}{\left(1 - \frac{at}{v_{co}}\right)^2} \tag{1-78}$$

This formula shows how ***the radial distance "spirals out" in time***, in fact one can say that $r \to \infty$ for $t = \frac{v_{co}}{a}$, that is another way to refer to the "***escape velocity***". In this case, anyway, the orbit is no longer circular, so the result is not very precise, but it gives an idea of the problem.
If we now calculate the radial and the tangential component of the velocity:

$$v_r = \dot{r} = \frac{\frac{2a}{v_{co}} r_0}{\left(1 - \frac{at}{v_{co}}\right)^3} \tag{1-79}$$

$$v_\theta = r\dot{\theta} = \sqrt{\frac{\mu}{r}} = \sqrt{\frac{\mu}{r_0}} - at = v_{co}\left(1 - \frac{at}{v_{co}}\right) \tag{1-80}$$

we can get the ***Overall Kinetic Energy***:

$$\frac{v^2}{2} = \dot{r}^2 + \left(r\dot{\theta}\right)^2 = \frac{{v_{co}}^2}{2}\left[\left(1 - \frac{at}{v_{co}}\right)^2 + \frac{4\left(\frac{ar_0}{{v_{co}}^2}\right)^2}{\left(1 - \frac{at}{v_{co}}\right)^6}\right] \qquad (1\text{-}81)$$

and knowing that the ***Escape Point*** is defined having ***Zero Total Energy***, after some passages we find:

$$1 - \frac{at}{v_{co}} = (2\nu)^{1/4} \qquad (1\text{-}82)$$

Where we defined the ***Ratio of Thrust to Gravity*** :

$$\nu = \frac{a}{\frac{\mu}{r_0^2}} \qquad (1\text{-}83)$$

Hence, finally, since $at = \Delta v$ we get:

$$\Delta v_{esc} = v_{co}\left[1 - (2\nu)^{1/4}\right] = v_{co}\left[1 - 0.79\nu^{1/4}\right] \qquad (1\text{-}84)$$

With these equations we just gave an idea of the Δv required to perform a Low-Thrust Spiral Climb to the point you can escape the Gravitational Force of the planet.

LAST CONSIDERATION ABOUT ELELCTICAL THRUSTERS

We have just calculated some important parameters like the Efficiency and the Specific Impulse of a Rocket. Until now we have considered the efficiency- η- as a constant, independent of the choice of the Specific Impulse- I_{sp}. This is not correct, in general, for Electric Thrusters where the physics of the gas acceleration process can change significantly as the power loading (hence the jet velocity) is increased.
In general, we can typically establish a connection between η and *c*: so that $\eta = \eta(c)$. For example, η increases with *c* in both ion and MPD thrusters, whereas it typically decreases with *c* in arcjets (beyond a certain *c*).
Just to have an idea, we can calculate the efficiency for Ion Engine: Ion Engine can be fairly well characterized by a constant voltage drop per accelerated ion. If we call this $\Delta\,\phi$ and singly charged ions are assumed, the energy spent per ion- E_i- is:

$$E_i = \frac{1}{2} m_i c^2 + \Delta\,\phi \tag{1-85}$$

where we consider:

- m_i- Ion Mass;
- e- Electron Charge;

and where only the first part of the Energy- $\frac{1}{2} m_i c^2$ is useful.
So, the efficiency- η - is:

$$\eta = \frac{c^2}{c^2 + \frac{2e\Delta\,\phi}{m_i}} \tag{1-86}$$

However, we should also include a factor- $\eta_0 < 1$ to account for power processing and other losses. We then have:

$$\eta = \eta_0 \frac{c^2}{c^2 + {v_L}^2} \tag{1-87}$$

where v_L is a "***Loss Velocity***", equal to the velocity to which one ion would be accelerated by the voltage drop $\Delta\,\phi$. With this last expression we can notice, first of all, the importance of a high atomic mass propellant: $\Delta\,\phi$ is insensitive to propellant choice, and so v_L can be reduced if m_i is large. Then, we can also notice the rapid loss of efficiency when *c* is reduced below v_L.

Hence, as we anticipated, the efficiency of an electrical thruster highly depends on the exhaust speed.

In this chapter, we have seen some general equations about Propulsion and made a comparison between chemical and electrical thrusters. This lead us to the conclusion that, in specific cases and depending on the requirements, such as interplanetary transfers, electrical thruster are more convenient than chemical ones because they provide higher Specific Impulses and therefore need less propellant.
In the next chapter, we will give an overview of the current state of the art of electrical thursters.

CHAPTER 2: ELECTRIC PROPULSION

As discussed before, the Electric Propulsion shows multiple advantages compared with the chemical one.
The idea of Electric Propulsion for spacecraft dates back to ***1911***, from a publication made by ***Konstantin Tsiolkovsky***. Earlier***, Robert Goddard*** has noted such a possibility in his personal notebook, but ***the first design of an electric thruster*** was made just in ***1948*** and ***the first experiments*** in the 50s, just in laboratory and with a reduced power.
It was in the 60s that the interest of the scientific community for that field grew up and numerous research centers started to develop this kind of thrusters: the first in-space demonstration of Electric Propulsion was one of the two engines carried on board the ***SERT-1 (Space Electric Rocket Test 1)*** spacecraft, launched on the ***20th of July 1964***, which produced the expected thrust, showing the applicability of that new technology. It was an ion engine and it operated for 31 minutes.
Then, on the ***3rd of February 1970*** the ***SERT-2*** was launched, carrying on two ion thrusters that operated for a long time: one for more than 5 months and one for almost 3 months.
In ***1973 Dr. Tony Martin considered electrically powered propulsion with a nuclear reactor for the interstellar Project Dedalus***, but the novel approach was rejected because of the very low thrust, the big weight needed to convert nuclear energy into electrical equipment and a small acceleration.
Then, because of the reduction of money given for the space research after the conclusion of the Apollo Program, also the Electric Propulsion was set aside in the Occident, but luckily, in the 90s they restarted to study it again, and finally, from the following decade the use of Electric Thrusters started to become concrete: by the early 2010s, many satellite manufacturers were offering electric propulsion options on their satellites (especially for *Attitude Control*), while some commercial communication satellite operators were beginning to use them for *GEO insertions*.

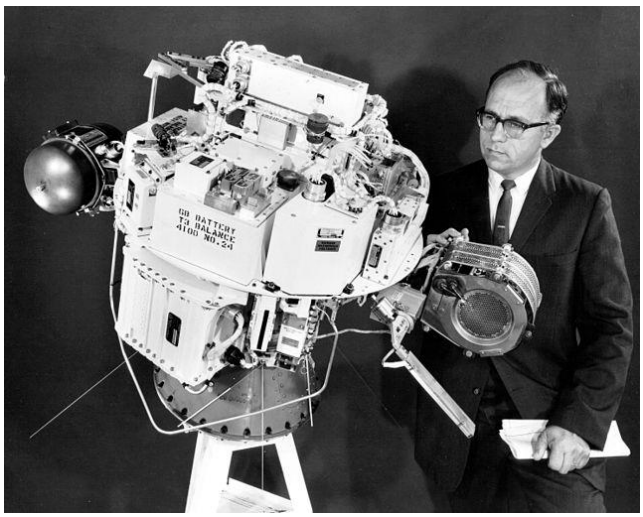

Figure 2-1: *A picture of the **SERT-1**: we can see, on the sides, the two Electric Thrusters tested in the mission are visible*

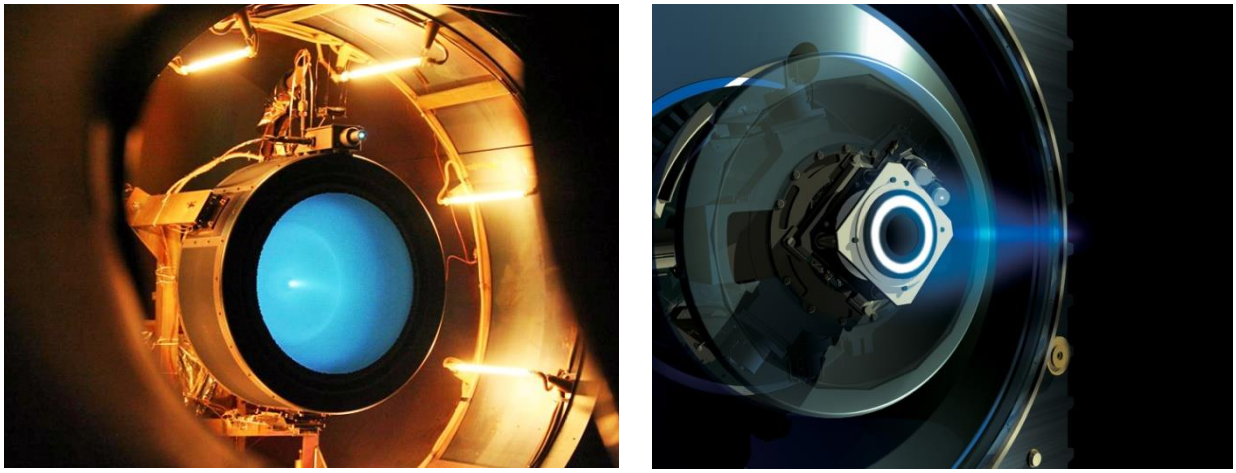

Figure 2-2: An Ion Thruster (at the left) and o an artist's impression of the SMART-1 Ion Engine (at the right)

Figure 2-3: An electric thruster

CLASSIFICATION OF THE ELECTRIC THRUSTERS

Electrical Thrusters can be classified based upon *three categories*:

1. based on **the acceleration mechanism** adopted:
    - ***Electrothermal***;
    - ***Electrostatic***;
    - ***Electromagnetic***;
2. based on **the operating regime** adopted:
    - ***Stationary***: if the thruster works continuously for a certain duration;
    - ***Pulsed***: if it works for brief intervals that can be thought as impulses (so with a duration minor than a second), and separated by longer periods of accumulation of the energy;

3. based on **the fluid** used. The two definitions almost overlap:
    - ***ionic thrusters***: they use an electrostatic acceleration mechanism;
    - ***plasma thrusters***: the acceleration is mostly electromagnetic;

    There's an exception represented by the Hall Thrusters that are considered plasma thrusters.

The most interesting characterization for us is the first one.
The table below shows some important performances of the Electric Thrusters currently realized.

Table 2-1: Electrical Thrusters at the state of the art

ACCELERATION MECHANISM	THRUSTER	FUEL	EFFICIENCY	$I_{sp}\ (s)$	$\overline{F}\ (N)$
Electrothermal	***Resistojet***	$Hydrazine - (N_2H_4)$	$65 - 90\%$	$\sim 300\ (< 500)$	-
	Arcojet	$Hydrazine - (N_2H_4)$	$25 - 45\%$	~ 700	$10^{-5} - 2.5 \cdot 10^{-6}$
Electrostatic	***FEEP***	$Liquid\ Cs, In, Hg$		$5000 - 8000$	$10^{-5} - 2.5 \cdot 10^{-6}$
	Ion	$Xe\ Gas$	$40 - 80\%$	3000	$3 \cdot 10^{-2}$
	RIT	-	-	$3400 - 3700$	$3.5 \cdot 10^{-3}$
	Helicon Double Layer	$Ar, Kr, Xe, He, H\ Gas$	-	~ 10000	$\sim 10^{-3}$
	Hall (SPT, PPT, ALT)	$Xe, Bi\ Gas$	$35 - 60\%$	$1000 - 3000$	$10^{-2} - 1.5$
	Colloidal	$Plexiglas - (C5O2H8)_n$ $Teflon - (C2F4)_n$ $Polymid,$ $Siliconorganics$	$60 - 70\%$	$1000 - 2000$	-
Electromagnetic	***MPD, LFA***	$H, Ar, Na, Al\ Gas$	-	$1000 - 10000$	$20 - 200$
	ElPT	-	-	$1000 - 10000$	$10^{-3} - 100$
	PPT	$Teflon - (C2F4)_n$	$7 - 13\%$	$850 - 1200$	

Now we're going to describe the most used of them.

2.1.1.2. Electrothermal Thrusters

In the old URSS ***Electrothermal thrusters*** had been used from the 1971.
As we said, the acceleration mechanism of these systems is the same of the chemical thrusters: the fuel is heated in a proper compartment inside the engine- very similar to the combustion chamber- and, then, expanded in a nozzle; hence the thermal energy is converted in kinetic energy and finally transformed into Thrust.

The main difference between an Electrothermal Thruster and a Chemical one is about the way the gas is heated: in the former by a resistance in contact with the engine- ***Resistojet***- or by an electric arc produced in the gas through the application of a ΔV- ***Arcojet***- while in the latter by a chemical reaction of the fuel. These systems are characterized by low I_{sp} even though much higher than those of the cold fuel thrusters and of some chemical rockets and, in general, it's preferred to have gases with a low molecular weight (like *Hydrogen*- H-, *Helium*- He-, and *Ammonia*- NH_3).

Resistojet

The ***Resistojet*** was first used in 1965 on board of the military spacecrafts ***VELA***, then, for commercial use, from the 1980 with the launch of the first satellite of the ***INTELSAT-V*** program and, currently, it's used mostly for:

- *Orbit Insertions*;
- *Attitude Control*;
- *De-orbit of LEO satellites*;
- In situation where energy is much more plentiful then mass and where propulsion efficiency needs to be reasonably high but low thrust is acceptable;

It's a thruster where the fuel is heated by a resistance that consists of a hot glowing filament in a proper chamber before entering the nozzle and being exhausted from it as Thrust.

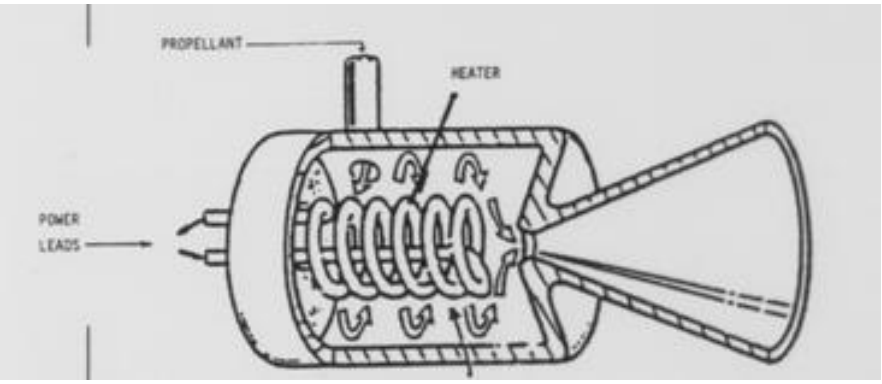

Figure 2-4: A Resistojet scheme

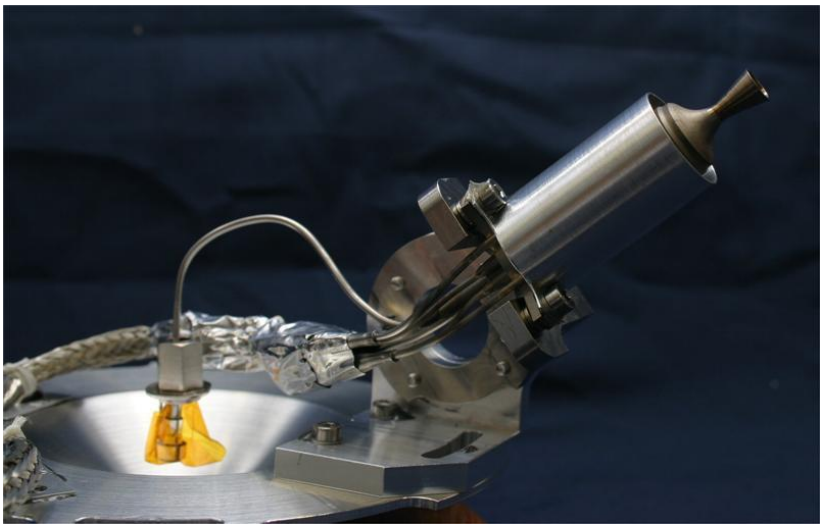

Figure 2-5: A Resistojet

Arcjet

In the ***Arcjet*** an electric discharge or "arc" is generated on the fuel (Hydrazine- N_2H_4 or Ammonia-NH_3), so more energy is supplied to extract more work from every kg of propellant at the expense of an increased power consumption.

The thrust is low respect to the chemical thrusters. If the electric energy available on board is enough, an arcjet adapts to maintain the position of the vehicle in orbit and may replace the rockets monopropellant.

In German, at the Institute of Space Systems Aviation of the University of Stoccarda the researchers developed various arcjets powered by hydrogen that can produce from $1\ to\ 100\ km/s$ of Power. The heated hydrogen can reach velocities slightly lower than $16\ km/s$.

Arcjets can acquire power from solar cells or batteries.

The Hydrazine is the most used fuel because it can be used in a chemical thruster of the same spacecraft as a backup of the arcjet.

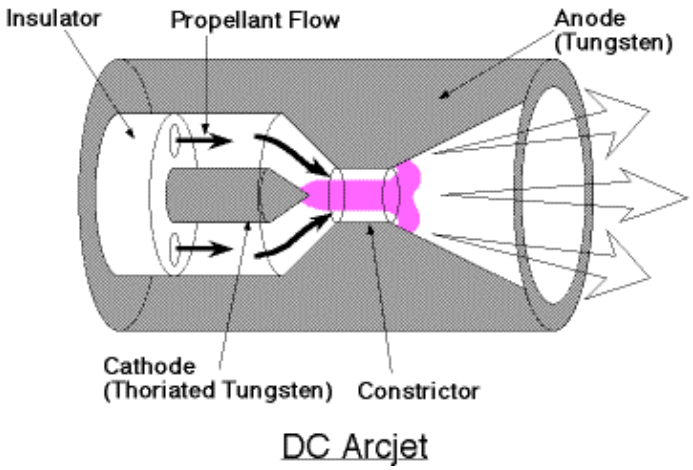

Figure 2-6: An Arcjet scheme

Figure 2-7: An Arcjet

2.1.1.3. Electrostatic Thrusters

In the ***Electrostatic Thrusters*** the fuel, after being ionized, is accelerated mostly by the ***Coulomb Force***, so after the application of an electrostatic field in the direction of the acceleration. Magnetic fields are used only for auxiliary purposes in the ionization chamber.

The electrostatic force, per unit area (or energies per unit volume) are of the order of $\frac{1}{2}\varepsilon_0 E^2$, where E is the strength of the field V/m and ε_0 the Permittivity of the vacuum, that values $\varepsilon_0 = 8.85 \cdot 10^{-12}\ F/m$.

Typical maximum fields are of the order of $10^6\ V/m$, yielding maximum force densities of roughly $5\ N \cdot m = 5 \cdot 10^{-5}\ atm$.

The production of ***ions***- *electrically charged particles*- for acceleration is achieved through several methods, like the more conventional ***electron bombardment*** or the ***electron cyclotron resonance***, or others like ***contact ionization***, ***radiofrequency ionization***, which electrically charges atoms from an onboard fuel supply. This fuel supply is an inert gas, mostly *Xenon* or *krypton*, which is injected into the ionization chamber and then expelled for propulsion.

These kind of systems provide relatively high I_{sp}, which have a value included between $1000\ s$ and $10000\ s$, high efficiencies ranging between $55\% - 98\%$, but low thrusts.

All the ion thrusters take advantage from the charge-mass rate of the ions. This rate mean that also relatively low ΔV can create high exhaust velocities. This reduces the quantity of mass requested, but increases the necessary specific power so, in these systems, the I_{sp} is high and the Thrust $\vec{F}$ is low and, consequently, few acceleration is provided because the masses of the charge electric units are directly proportional to the quantity of energy furnished.

So, the ion thrusters are not suitable for vehicle launches, but just for deep space missions.

Then, most of them, can manage just little quantity of fuel: the electrostatic grid ion thrusters, for instance, suffer from "*Space Charge Effects*" in big flows.

The low acceleration implies the need to have a continuous Thrust for a long time so that to have an acceptable Δv, so the these thrusters should last from weeks to years.

The most used fuels are characterized by molecules or atoms with high mass to ionizing energy rate. The ionizing rate, in fact, has to be low.

They mustn't contaminate the vehicle and they mustn't have a high erosive rate.

They can be divided in Electrostatic and Electromagnetic thrusters and the difference between them is about the way the ions are accelerated.

Field Emission Electric Propulsion- FEEP

The ***Field Emission Electric Propulsion*** is an ionic thruster that uses liquid metal- mostly Cesium- Cs- or Indium-In- as a fuel.
It consists of *two electrodes*: an *emitter* and an *accelerator*.
A $\Delta V \sim 10\ kV$ is applied between the two electrodes to generate a very high electric field on the tip of the metal surface.
The electric field extracts the ions that are then accelerated at high velocity (usually more than $100\ km/s$).
A separated electron source is requested to maintain the vehicle electrically neuter.
The Thrust, as we said, is very low ($\sim \mu N - mN$).
The ***FEEP*** is mostly used for very accurate attitude control ($\sim \mu rad$) on space vehicles. It usually represents the only valid option for ***drag-free satellite applications*** like ***LISA***, where the Thrust requests high precisions ($\sim \mu N$) and a wide range ($0.1 - 150 \mu N$).
The higher thrusts are used for the attitude control and for the orbital maintenance in little commercial spacecrafts.

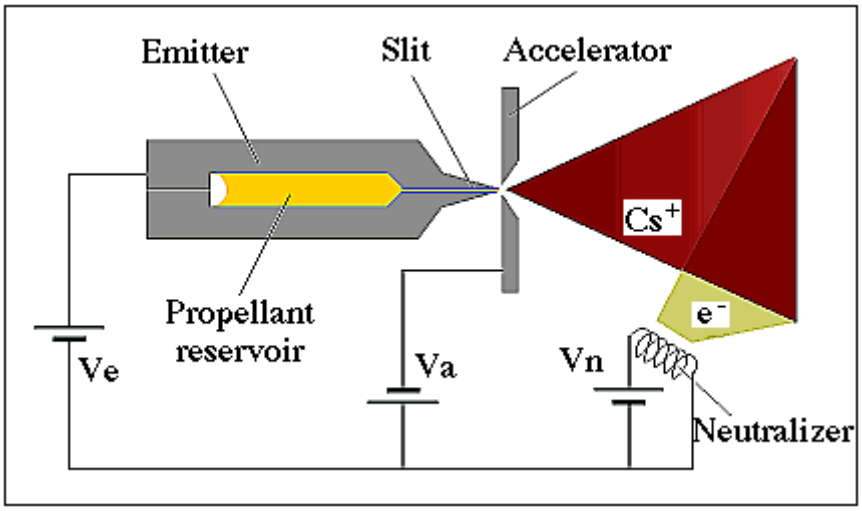

Figure 2-8: A FEEP scheme

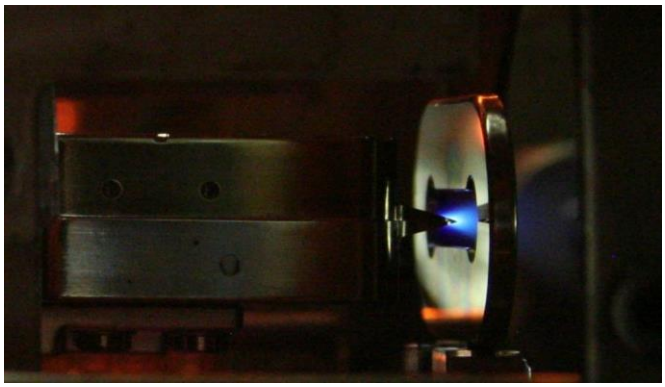

Figure 2-9: The EVT3

Ion Thruster

These thrusters typically use *Xenon* gas that has no charge and is ionized after being bombarded with electrons coming from a very hot cathode. The ionization creates ions positively charged thanks to the loss of one electron. These ions then diffuse through the positive grid and enter in a zone that is characterized by a ΔV between the positive and negative grids (the anode is the positive grid and the cathode is the negative one). This ΔV accelerate the ions at very high high velocity, which cross the negative grid creating the Thrust. In the external part of the thruster there's a ***neutralizer***, that is a device that emits electrons that will couple with the retiring ions to neutralize them. This operation is made to avoid the ion beam to come back to the vehicle and so annulling the thrust.
So we can summarize the main steps as follows:

1. The atoms of the fuel are injected into the propulsion chamber and then bombarded by electrons with an electric gun, so causing the loss of one electron per atom (or two sometimes), transforming them in ions. The walls and the grid absorb the lost electrons;
2. The ions move to the exit of the combustion chamber thanks to the diffusion, then they exit in a plasma shell or over the positive grid;
3. After entering the shell, the ions are between the two grids at the exit of the chamber and they are accelerated electrostatically in the from the positive grid to the negative;
4. The positive grid has a potential V^+ higher than the negative (that attracts the ions). Those, when get close to the negative grid, are then attracted to its aperture and they finally exit;
5. The expelled ions push the spacecraft in the direction opposite to their motion, thanks to the ***3rd Newton Law: Principle or Action and Reaction***;
6. A cathode, called neutralizer shoots electrons to the ions to have the same quantity of positive and negative charges expelled to avoid a net gain of charge;

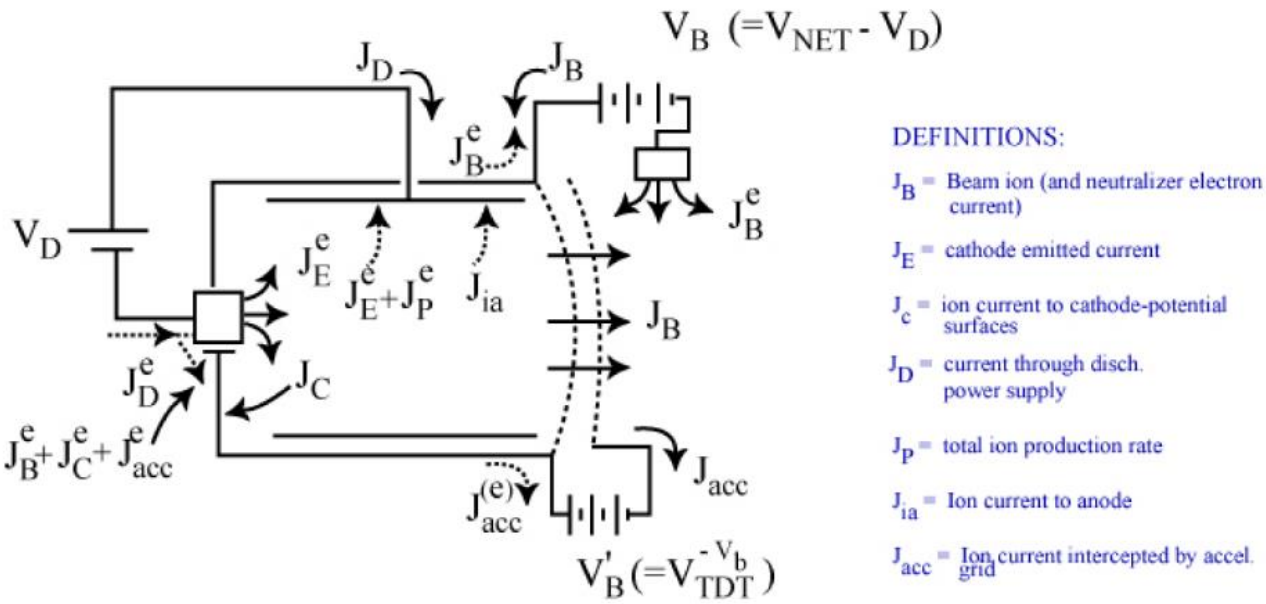

Figure 2-10: An Ion Thruster Scheme

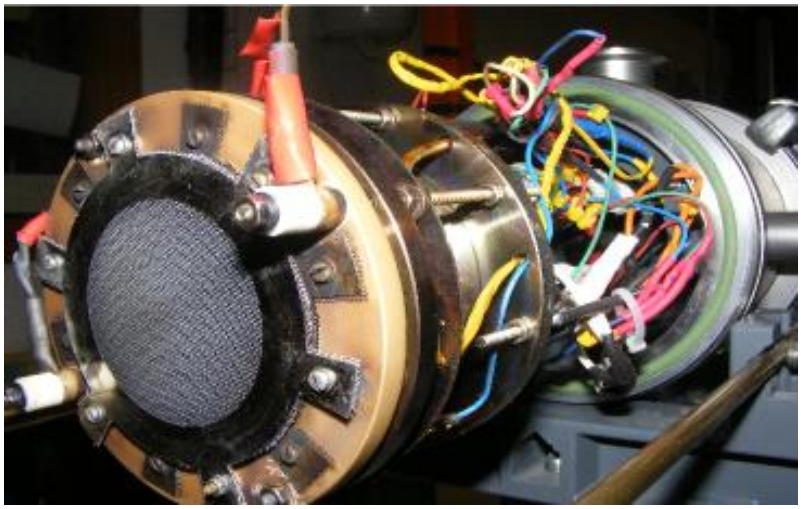

Figure 2-11: An Ion Thruster

We can spend few words about the *performance* of this thrusters: the ***Ion Thruster*** accelerates ions to a velocity close to $100\ km/s$. However, the ion optics are constantly bombarded by the ions of the fuel, so after a certain period they start to erode or they detach, reducing the duration of the operation of the engine. That's a problem because ion engine must last for many years efficiently and continuously.
That's why, for example, is used *Xenon*, that, even if it's very difficult to find in nature and so very expensive, is less erosive of *Mercury* or *Cesium*, that were used in the first tests made in the 60s and 70s.

Some variation of this thruster have been created. One, in particular, is interesting: it's an engine created thanks to the partnership between the ***European Space Agency- ESA-*** and the ***Australian National University*** that has improved the performances of the classic model. This engine in fact can accelerate the exhausts to a velocity close to $210\ km/s$ and create an I_{sp} that is 4 times the one of the previous model.

The conventional Ion Thrusters use only two grids: one at high voltage and one at low. These grids, as we said, can accelerate and extract the ions. However, when the ΔV between them reaches $5\ kV$ some of the particles extracts by the chamber collide with the low voltage grid, eroding it and compromising le longevity of the engine.
This problem has been by-passed successfully using two couples of grids: the first one, that has a $\Delta V \sim 3\ kV$ (so, high voltage), extracts the particles, while the second one, that operates at a low voltage, accelerates the particles, creating the Thrust.
Another advantage is a more compact design, so that it's possible to create a bigger thruster to have a higher Thrust. In this way, the exhaust plume can be thinner and less divergent of about $3°$ (so 5 times thinner than the previous model).

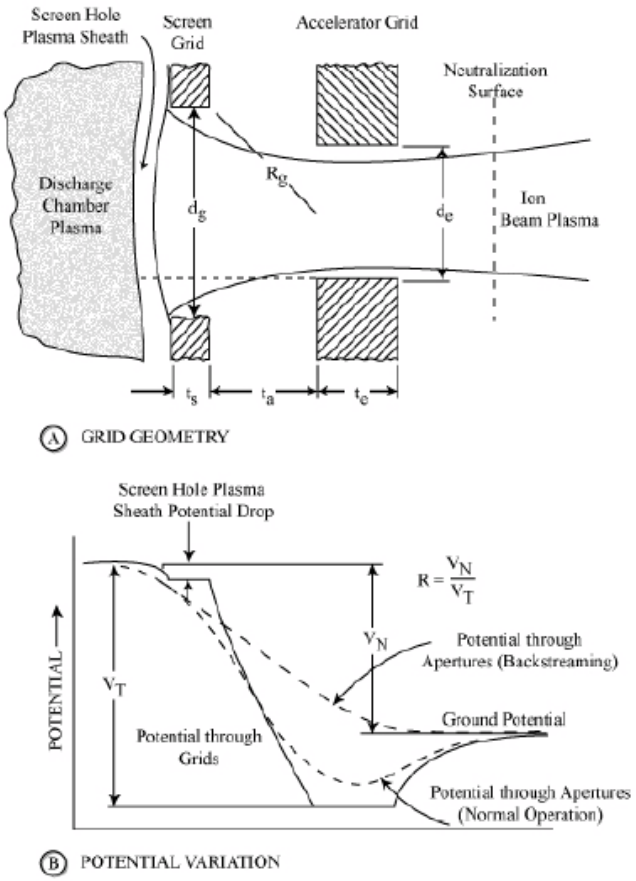

Figure 2-12:A Grid Geometry (at the top) and a Potential Variation (at the bottom) of an Ion Thruster

Other variants of the Ion Thruster depend on the way the atoms are ionized. They're developing different techniques, as the use of microwaves to heat the fuel enough to obtain the plasma: the advantage is about the absence of the cathode (that can break or erode) increasing in this way the time of life of the thruster.
Other improvements are focused on the grid, so it does not break.

Radio Frequency Ion Thruster-RIT

A variant of the Ion Thruster is the ***Radio Frequency Ion Thruster (RIT)***, that combines the principal advantages of any gridded ion engine with those given by the ion generation provided by high frequency electromagnetic fields.

This Thruster, unlike the gridded ion version, don't need a hot cathode inside the thruster's ionization unit. The propellant is ionized by electromagnetic fields, so the ionizer chamber, that is a vessel made of an isolating material, is surrounded by an *RF-coil*, that induce an axial magnetic field. The primary magnetic field induces a secondary one, according to the ***Maxwell's Law***, in which the electrons gain the energy to ionize the fuel.

The mostly used fuel is *Xenon*, and the mass flow can be varied over an extremely wide range. The frequency is in the range of Hz.

This thruster is suitable for systems where fast changes of thrust level are necessary. The desired Thrust, in fact, is reachable faster than milliseconds by simply changing the applied RF-power.

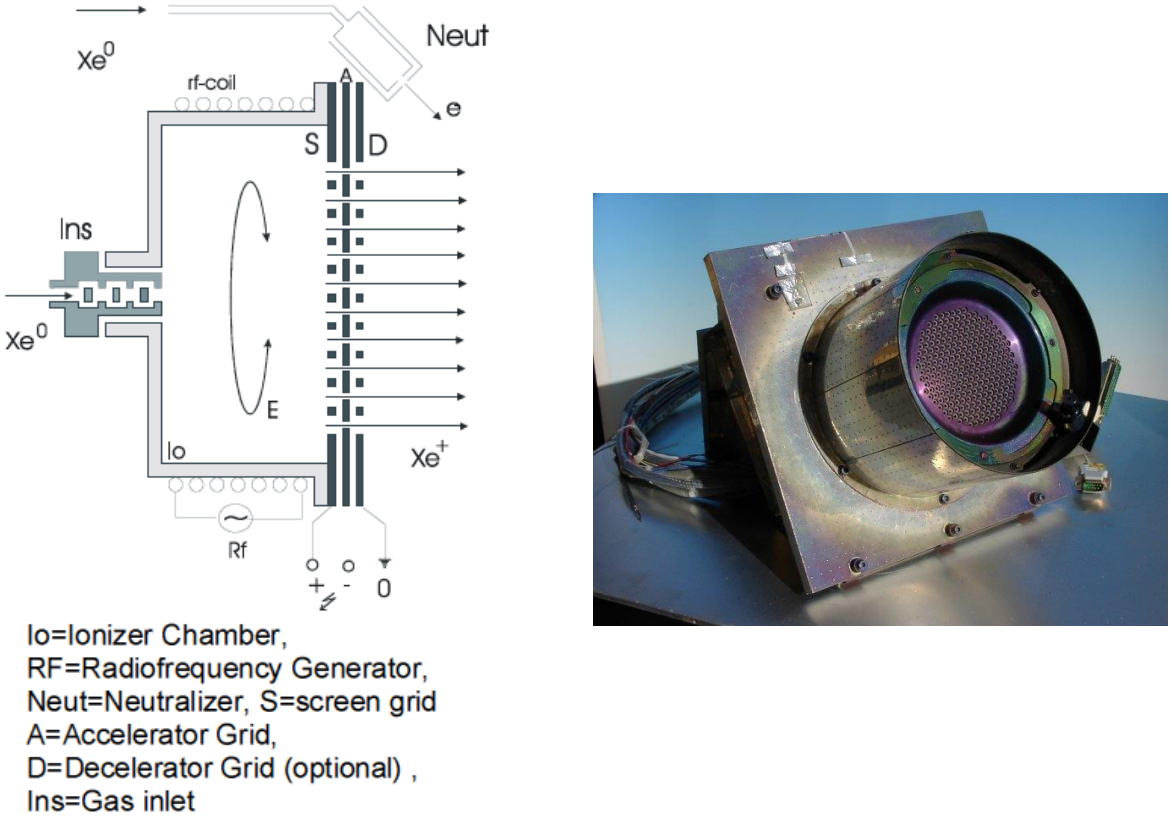

Figure 2-13: A RIT Thruster (at the right) and a RIT Thruster scheme (at the left)

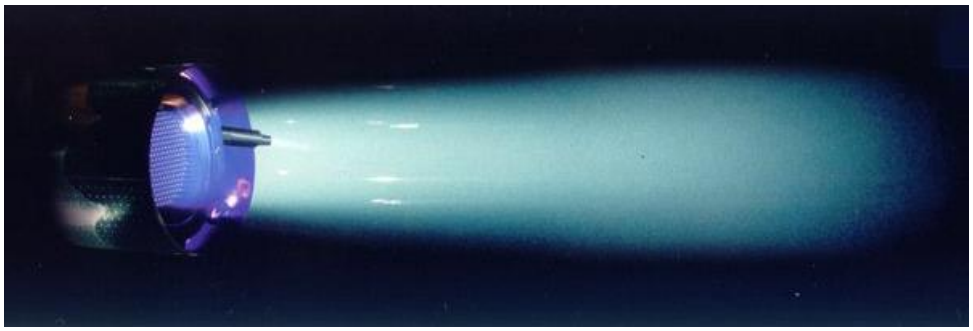

Figure 2-14: A RIT Thruster

Helicon Double Layer Plasma Thruster

A Helicon Double-Layer Thruster (HDLT) is a plasma thruster that works thanks on the so called "***Double-Layer Plasma***", a structure in a plasma that consists of two parallel layers with opposite electrical charge. The sheets of charge cause a strong electric field and so a sharp change in electrical potential across the double layer. In the double layer, ions and electrons are accelerated, decelerated, or reflected by the electric field.
Thus, the main consequence of a double layer, is to separate regions of plasma with different characteristics. The double layers can be classified in three categories, depending on:

- *the **Strength** of the Double-Layer-* that is expressed as the ratio of the potential drop in comparison with the plasma's equivalent thermal energy. A double layer is said to be "***strong***" if the potential drop across the layer is greater than the equivalent thermal energy of the plasma's components, otherwise it is considered "***weak***".
- *the **Potential Drop** of the Double-Layer-* that differentiate Double-Layers in Relativistic and Non-Relativistic: a Double-Layer is said to be "***Relativistic***" if the potential drop over the layer is so large that the total gain in energy of the particles is larger than the rest mass energy of the electron, otherwise, the Double-Layer is said to be "***Non-Relativistic***". In case it is Relativistic, it results in the location of the charge density in two very thin layers inside which the double layer the density is constant at and very low compared to the rest of the plasma.
- *The **Way this double layer is generated***- that divides Double-Layers in "***Current carrying***" and" *Current-**free***". The former may be generated by current-driven plasma instabilities which amplify variations of the plasma density. The latter, instead, forms on the interface between two plasma regions with different characteristics, and its associated electric field maintains a balance between the penetration of electrons in either direction (so that the net current is low).

In a Helicon Double-Layer Thruster a very high ionized gas is ejected to provide Thrust. The gas- that can be *Argon*, *Krypton*, *Helium*, *Hydrogen* or *Xenon*- is injected into a tubular chamber with an open end, while radio frequency AC power is coupled into a specially shaped antenna wrapped around the chamber. The antenna emits an electromagnetic wave, causing the breaking down of the gas and the consequent formation of a plasma. The antenna then excites a helicon wave in the plasma, heating it more. The device is characterized by a constant magnetic field in the source tube but, away from the source region, it rapidly decreases in magnitude, behaving like a sort of "*magnetic nozzle*". This causes a sharp boundary between the high-density plasma inside the source region, and the low-density plasma in the exhaust, which is associated with a sharp

change in electrical potential. The plasma properties change rapidly across this boundary, as a ***current-free electric double layer***.

The electrical potential, much higher inside the source region than in the exhaust, confines most of the electrons and accelerate the ions away from the source region. In the end of this process, part of the electrons escapes the source region to neutralize the plasma.

Like the others Electrostatic Thrusters, the HDLT is characterized by a high I_{sp} and low Thrust.

Its primary application is for station-keeping maneuvers, long LEO to GEO orbit transfers and deep space applications.

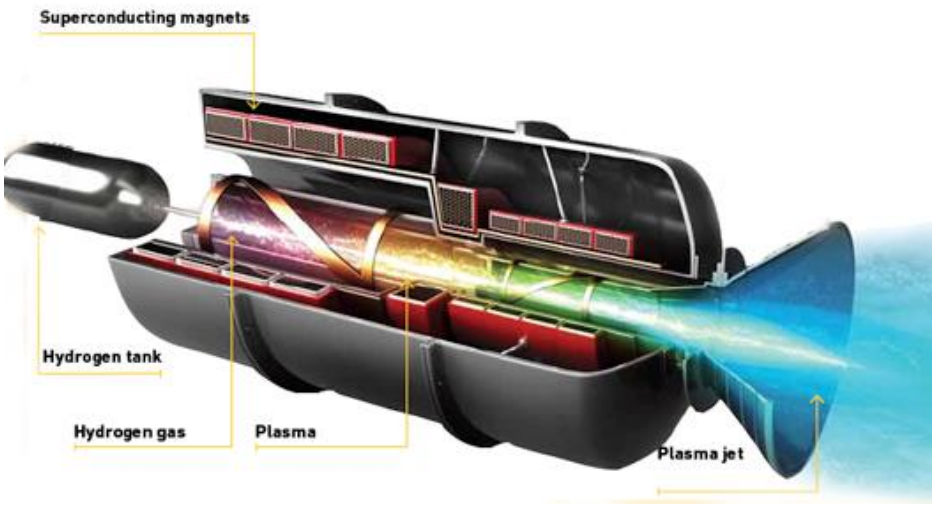

Figure 2-15: An HDL Thruster scheme

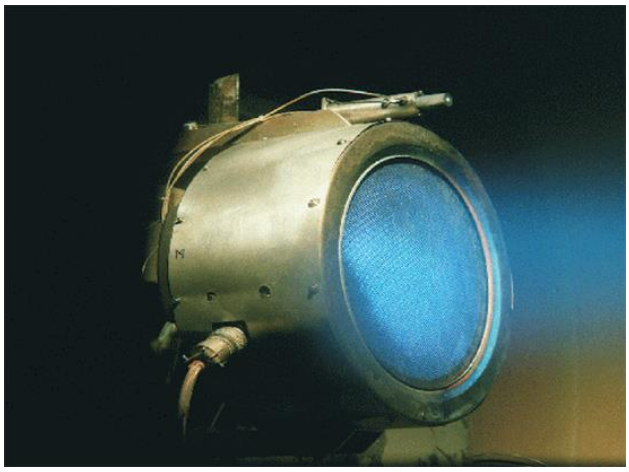

Figure 2-16: An HDL Thruster

Hall Thrusters

The ***Hall Thruster*** is one of the most efficient Thrusters currently used. It's an electrostatic ion accelerator in which the grid system is replaced with a relatively strong magnetic field perpendicular to the flow, that blocks the counter-flow of electrons in the accelerating field.

It was studied independently in USA and URSS in the 50s and 60s, but it was developed in a very efficient thruster just in the ex URSS, while in USA they were abandoned when it became apparent that there were strong instabilities which could not have been completely and, when, some additional work in Germany indicated higher effective plasma collisionality than had been expected.
The URSS developed two kind of Hall Thrusters:

- Thrusters with wide acceleration zone- SPD/SPT (Stationary Plasma Thrusters);
- Thrusters with narrow acceleration zone- DAS/TAL (Thrusters with Anode Layer);

The SPT, mostly developed by ***I. Morozov*** in the ***Kurchatov Institute of Moscow***, has been used since 1972 and mostly for satellite stabilization N-S, E-W direction. Progressively more efficient configurations evolved there, and it was realized that the instabilities, while present and annoying, did not materially interfere with performance.
The thrust of the first generation SPT was about $20 - 30\,mN$ (they were called SPT-50 and SPT-60 respectively). In 1982 the SPT-70 and the SPT-100 have reached a Thrust of about $40\,mN$ and $83\,mN$.
In the post URSS Russia high power thrusters that could reach few kW were introduced (SPT-140, SPT-160, SPT-180, T-160), and also low power thrusters that reached a power of about that could reach few $< 500W$ were introduced (SPT-35).
By the early 1980's, these thrusters have flown in over 50 missions of the URSS, which, however, were limited to relatively small total impulses. Starting in 1991, with the complete removal of the earlier communications barrier, development has re-started in USA greatly improving its performances.

The Hall Thruster consists of a coaxial annular cavity where plasma is created by passing current between the annular anode on the upstream end of an otherwise dielectric cavity and the externally located cathode.
The propellant enters this plasma cavity via an annular manifold at the anode. A radial magnetic field is applied, either by ring-shaped permanent magnets, or through coils and soft iron yokes. The magnetic field greatly slows down the axial mean velocity of the electrons which, due to the low collisionality prevailing, are forced to execute an $\vec{E} \times \vec{B}$ drift around the annulus, while being radially confined by sheaths on the insulating walls.
The ions instead, are only weakly affected by the magnetic field, because of their higher mass and, if the density is low enough that collisions are rare, are simply accelerated by the electrostatic field to an exit velocity:

$$c_i = \sqrt{\frac{2eV}{m_i}} \qquad (2\text{-}2)$$

where V is the potential where the ion is created (respect to the outside potential).
Because of its quasi-neutrality, thanks of the presence of the electrons, no space-charge limitation arises in this type of thruster (unlike the gridded ion thrusters), and the acceleration distance can be several centimeters, compared to the typical $0.5 - 1\,mm$ gap used in electrostatic gridded ion engines. This is one of the main advantages of the Hall Thruster and, then, it also removes the strong thrust density limitation dictated by the Child-Langmuir Law in Electrostatic Gridded Ion Engines.
Electrons also travel axially across the B field under the influence of the applied axial $\vec{E}$ field. They are then collected by the upstream anode, and pumped by the power supply to an external cathode. The emitted

electrons mainly couple with the accelerated ions to neutralize the beam, but a fraction, that must be minimized, also diverts upstream into the accelerator section.

As we said, the ions are simply accelerated by the electrostatic field $\vec{E}$ but, since the ions are in a quasi-neutral plasma, an equal and opposite electrostatic force is applied to the free electrons in that zone that, thanks to the applied radial magnetic field $\vec{B}$, drift azimuthally (so perpendicular to $\vec{E} \times \vec{B}$) with enough velocity to create an equal and opposite magnetic field on themselves. So, calling x the forward axial direction:

$$-e\left[\vec{E} + \vec{v}_e \times \vec{B}\right] = 0 \tag{2-3}$$

$$\Longrightarrow \vec{v}_{e,Drift} = -\frac{\vec{E} \times \vec{B}}{B^2} \tag{2-4}$$

$$\Longrightarrow \vec{v}_{e,\theta} = -\frac{\vec{E}_x}{\vec{B}_r} \tag{2-5}$$

with $B = \left|\vec{B}\right|$.

As we said above, the ions doesn't have this azimuthal drift motion, so a net azimuthal current density called ***Hall Current*** arises:

$$\vec{J}_{Hall} = -en_e\vec{v}_{e,Drift} = en_e\frac{\vec{E} \times \vec{B}}{B^2} \tag{2-6}$$

Given a $\vec{J}_{Hall}$ current in a plasma, the magnetic force density- called ***Lorentz Force***-acting on it is:

$$\vec{f} = \vec{J}_{Hall} \times \vec{B} == -en_e\vec{v}_{e,Drift} \times \vec{B} \tag{2-7}$$

$$\Longrightarrow \vec{f} = +en_e\vec{E} \tag{2-8}$$

The duality of this system is just in this last formula: the device is a Hall Thruster, but an Electrostatic accelerator.

The performances and the characteristics of this thruster are the following:

- *Efficiency*: High-50-60 %;

- I_{sp}~$1200 - 1800\ s$ $(12 - 18\frac{kNs}{kg})$;
- $\frac{\vec{F}}{P}$ rate: $50 - 70\ mN/kW$;
- ΔV~$300\ V$ between the cathode and the anode;
- The electrons that ionize the fuel has an energy of about $10 - 20eV$ $(or\ 100000 - 250000\ °C)$. Once ionized most of the ions has a charge that is $+1$, while a little fraction (about $10\ \%$) has a charge that is $+2$;
- About the 30% of the discharge current is an electronic current that doesn't produce Thrust. The other 70% of the current is an ion current. Since most of the electrons is trapped by the Hall Current, they have a long parking period inside the thruster and so they can ionize about ~90% of the fuel. So:
  - $Ionization\ Efficiency$~90%;
  - $Discharge\ Efficiency$~70%;
  - $Total\ Efficiency$~63%;
- The thrust is low respect to the chemical thrusters ~$80\ mN$;
- $I_{sp}|_{Hall\ Thruster} > I_{sp}|_{Ion\ Thrusters}$;
- The acceleration and the generation of the ions happen in a quasi-neutral plasma so there's no ***Child-Langmuir Charge*** (Space Charge) saturated current limitation on the Thruster. This allows for much smaller thrusters compared to gridded ion thrusters.
- The fuel is injected through the anode that has multiple little wholes to work as a gas distributor. The *Xenon* is the most used because of its high molecular weight and low ionization energy. Many different fuels can be injected (also the *Oxygen*) in the anode, but the cathode needs a fuel that can be easily ionized. Now they're starting using the Bismuth because is cheap, it has a high molecular weight and a low partial pressure;

The Hall Effect Thruster has been used in the SMART-1 of the ESA (Snecma PPS-1350-G1), with a life time of 13 months, 289 impulses of the engine, 58.8 kg of Xenon spent and a $\Delta v = 2737\frac{m}{s}(46.5\frac{m}{s}per\ kg\ of\ Xenon)$ and it will be used in the Bepi Combo mission.

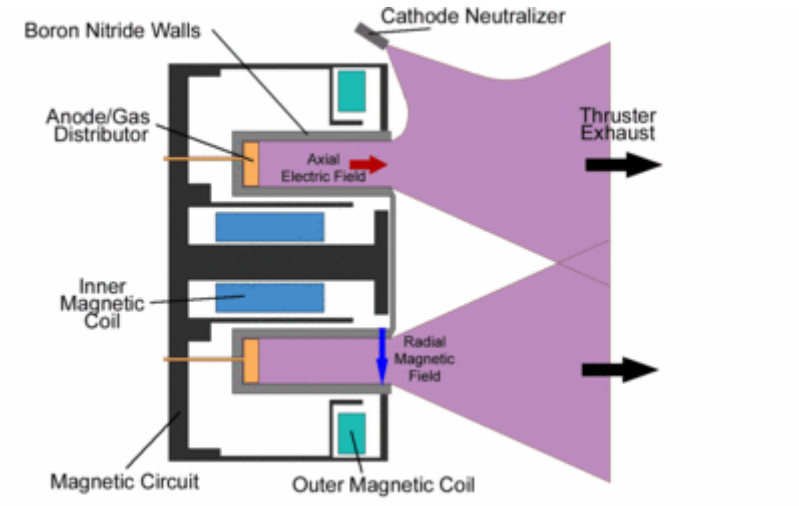

Figure 2-17: A Hall Thruster scheme

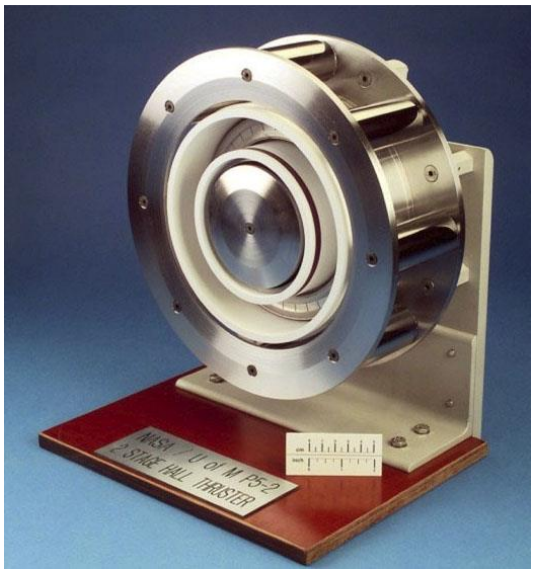

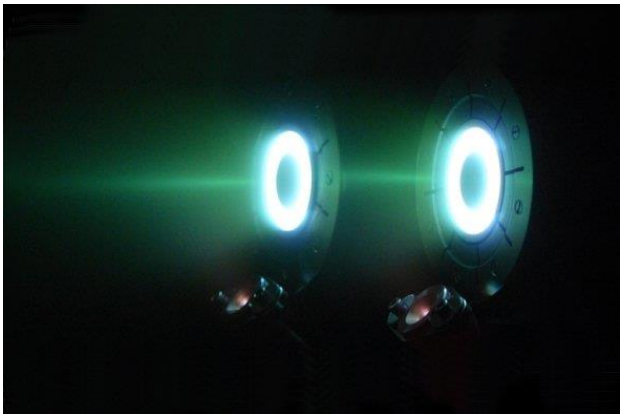

Figure 2-18: Hall Effect Thrusters

Colloidal Thruster

A new type of Electrostatic Thruster has been developed: the ***Colloidal Thruster***. It works thanks of charged liquid droplets produced by an ***electro-spray process*** and then accelerated by a static electric field. The fuels typically used for this application are cheap and convenient- *Plexiglas*, *Teflon*, *Poly-mid* and *Silicon-organics*- and they tend to be a low-volatility ionic liquid.
The performances, like all the Electrostatic Thrusters, are:

- Micro Thrust;
- Low Thrust cost;
- High Thruster Efficiency: $\eta \sim 60 - 70\%$;
- High Specific Impulse: I_{sp} $\sim 1000 - 2000\ s$;
- Moderate exhaust velocities: $v \sim 40 - 400\ m/s$;
- Potential: $\Delta V \sim 15 - 25\ kV$;
- Temperature Density: $\sim 200 - 10000\ C/kg$;
- Life time: $t \sim 2000 - 3000\ h$;

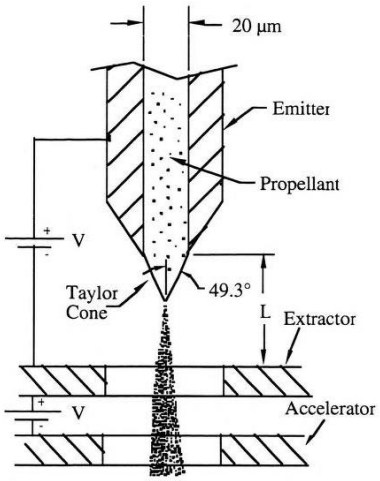

Figure 2-19: A Colloidal Thruster scheme

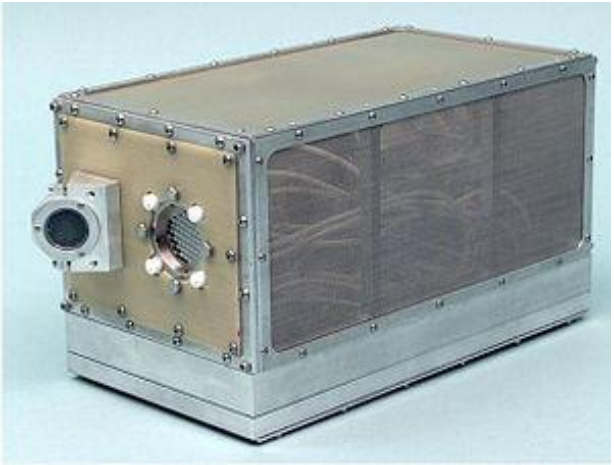
Figure 2-20: A Colloidal Thruster

2.1.1.4. Electromagnetic Thrusters

As we said previously, Ion Engine and Colloidal Thrusters are Electrostatic Thrusters because the electrostatic forces that accelerates ion (or droplets in case of Colloidal Thrusters) are also directly felt by some electrode and this is how the structure receives thrust. Considering that the ***Thrust Density*** of an Ion Engine has a magnitude of:

$$F_A = \frac{1}{2}\varepsilon_0 E_a^2 \qquad (2\text{-}9)$$

being E_a the field on the surface of the extractor electrode and having a magnitude of:

$$E_a = \frac{4}{3}\frac{V}{d} \qquad (2\text{-}10)$$

Since $\varepsilon_0 = 8.85 \cdot 10^{-12}\,\frac{F}{m}$ and E_a is not usually more than $2000\ \frac{V}{mm}$, we are limited to ***Electrostatic Pressure*** of about $20\ \frac{N}{m^2}$ (and due to various inefficiencies more like $1-2\ \frac{N}{m^2}$).
Hall Thrusters occupy an intermediate position, because ions are accelerated electrostatically but electrons, which see the same (and opposite) electrostatic force because of the quasi-neutrality of the plasma- $n_i = n_e$-, are essentially stopped axially by an interposed magnetic field. So, at the end, most of the force is magnetically transmitted. In this case there's still an electrostatic field in the plasma and, so, there will be some electrostatic pressure acting on various surfaces, with a magnitude of:

$$F_N = \frac{1}{2}\varepsilon_0 E_n^2 \qquad (2\text{-}11)$$

But because of the quasi-neutrality of the plasma these fields are much weaker than they are between the grids of an ion engine and it's just thanks of the magnetic mechanism that we can reach thrust densities 10 times higher than those of ion engines, despite the weak electrostatic fields.
Hence, we can ask how much stronger can be the force per unit area on some structure when it is transmitted magnetically as compared to electrostatically.
The counterpart of the Electrostatic pressure is the ***Magnetic Pressure***- $\frac{B^2}{2\mu_0}$-, were B is the Field Strength and $\mu_0 = 1.256 \cdot 10^{-6}\ \frac{H}{m}$ is the ***Permeability of Vacuum***.
If we don't recourse to superconductive structures B can be of the order $0.1\ T$ so, the Magnetic Pressure can be of the order of $\frac{B^2}{2\mu_0} \cong 8000\ \frac{N}{m^2}$.
Thrusters that can exploit these magnetic forces are called ***Electromagnetic***.
The Magnetic field can be external or self-induced (when plasma becomes large enough) and it can be steady or varying very fast in time.
Let's now describe the most important Electromagnetic Thrusters.

MPD/LiLFA Thrusters

The ***Magneto Plasma Dynamic*** (***MPD***) and the ***Lithium Lorentz Force Acceleration*** (**LiLFA**) ***Thrusters*** are constructively similar.
The operation principle of these thrusters is that the ionized gas enter the acceleration chamber where the magnetic and electrical fields are created using a power source. The particles are then propelled by the Lorentz Force resulting from the interaction between the current flowing through the plasma and the magnetic field (that can be externally applied or self-induced, as we said above) out through the exhaust chamber. So, in these thrusters, there's no combustion.

The only two differences that the ***LiFLA*** and the ***MPD Thrusters*** have are:

- While the most used propellants used by the MPD Thrusters are Hydrogen- H-, Xenon- Xe-, Lithium- Li-, Argon- Ar-, Sodium- Na-, Neon- Ne-, Aluminum- Al and Lithium- Li- (for the best performances), gases, the LiLFA uses Lithium Vapor- Li- that can be stored in a solid form;
- The main cathode of an MPD thruster is replaced by several little vents inserted in a cathodic hollow tube. In the MPD the cathode erodes very easily because of the constant contact with the plasma; in the LiFLA, instead, the Lithium Vapor is injected into the hollow cathode and is not ionized into its erosive plasma form until it goes out of the tube. The plasma is then accelerated by the Lorentz Force.

The ***Specific Impulse***- I_{sp}- and the ***Thrust***- $\vec{F}$- increase with the ***Magnetic Pressure***, while the ***Specific Thrust***- $\frac{\vec{F}}{W}$- decreases.

As already said several times, there are two kind of MPD Thrusters:

- With an ***External Magnetic Field***;
- With a ***Self-Induced Magnetic Field***;

The former is equipped with magnets or solenoids that surround the acceleration chamber to produce an additional component of the Magnetic Field while in the latter the Magnetic Field is entirely generated by the intensity of the current flowing through the cathode placed in the center of the chamber, thanks to the ***Biot-Savart Law***.

The need for Applied Magnetic Fields arises from the demand of more efficiency when the pressure is low, and the Self-Induced configuration is too weak; in fact, when the Magnetic pressure is too low, the Magnetic Field cannot reach the required intensity to get the minimum efficiency for the acceleration process.

The advantages connected to the use of an MPD Thruster are:

- Very high Specific Impulse: $I_{sp} \sim 1000 \div 10000$;
- High Exhaust Velocities: $v \sim 110\ km/s$;
- High Thrusts: $\vec{F} \sim 200\ N$

This last point is the one that differentiates the MPD Thrusters from all the other Electric Thrusters; in fact, as we know, despite the big advantage of the Electric Thrusters of having very high I_{sp}, we noticed that unfortunately they cannot provide big thrusts. Thus, the MPD has a very high potential because it combines both the advantages of the Electric and the Chemical Thrusters. However, everything has a cost: in fact, the Power required from the MPD to provide that Thrust is of the order of $100\ kW$ to have good performances. Of course, the current RTGs and the solar panels cannot provide such a high Power.

Another disadvantage connected to the MPD is the erosion of the cathode due to the evaporation of the fuel guided by the high current density (that is more than $100\ A/cm^2$).

For this reason, the use of mixtures of propellants of multiple vacuum channel cathodes of Li/B have been tested in laboratory and it seems to be a very hopeful solution for the erosion.

In the next chapters we'll enter more in detail of the physics of an MPD Thruster.

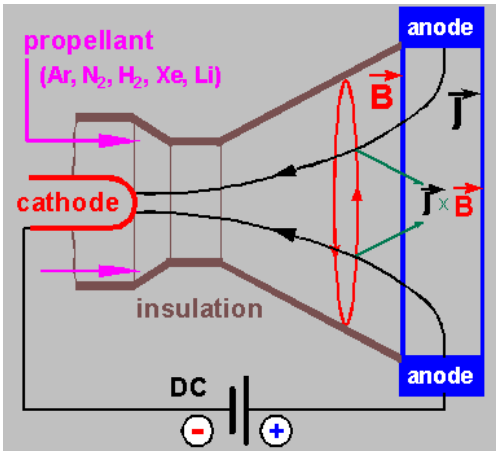

Figure 2-21: Examples of MPD Thrusters (at the top and at the bottom left) and a MPD Thruster scheme (at the bottom right)

ElPT Thrusters

The ***Electrode-less Plasma Thruster***- ***ElPT***- has two unique characteristics:

- The Electrodes removal, that solves the problem of the erosion and so increases the life time of the thruster respect to other Ionic Thrusters;
- The capacity to regulate he Thrust;

The neutral gas is ionized by electromagnetic radiations and then transferred in another chamber where it's accelerated with electric and magnetic oscillating fields using the physics behind the "***Ponderomotive Force"***: in case of interaction between matter and high intensity radiations the magnetic term of the Lorentz Force can be neglected because of the relativistic velocities conferred to the electrons by the high frequency fields. This force represents a non-linear term in the interaction because the velocity used to calculate it depends itself on them.

In this thruster, the separation of the ionization and acceleration sections gives the engine the capability to regulate the velocity of the propellant flux combining, in this way, the amplitude of the Thrust and the I_{sp}.

PIT Thrusters

The **Pulse Inductive Thrusters**- **PIT**- has a nozzle that release a puff of gas of Ammonia- NH_3- or Argon- Ar- that diffuse through an induction flat coil in a wire of $1\ m$ of diameter. Then, a group of capacitors release an electric current impulse that lasts about $10\ ms$ on the coil, generating a radial magnetic field that then induces a circular electric field on the gas, ionizing it and causing the movement of ions in the opposite direction respect to the one of the original current impulse. Since their motion is perpendicular to the magnetic field, the ions are accelerated and expelled into space.
This device doesn't need any electrode (that erode very easily) and its power can be increased just increasing the number of impulses for seconds. A system of $1\ Mb$ could pulse for 200 times for seconds.

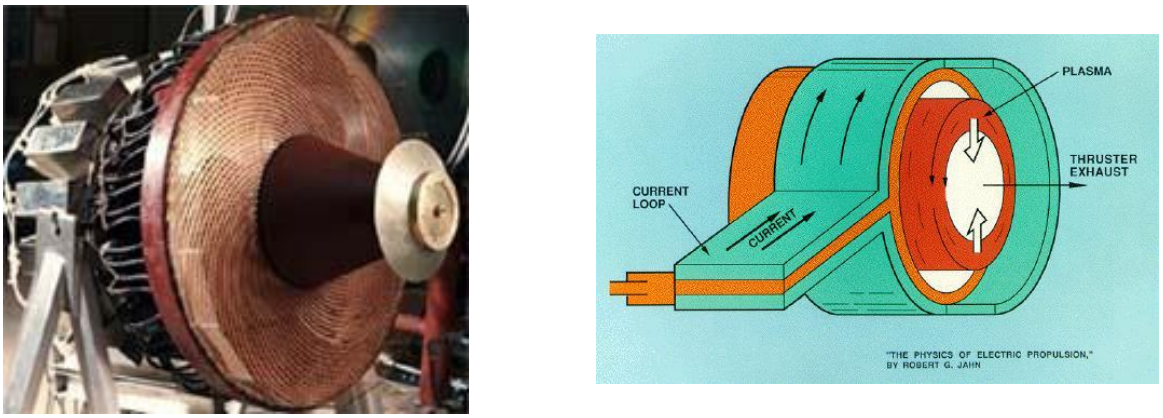

Figure 2-22: A PIT Thruster (on the left) and a PIT Thruster scheme (on the right)

PPT Thrusters

A ***Pulsed Plasma Thruster***- ***PPT***- is much different from the other Electromagnetic Thrusters for its low realization costs, low weight, its simplicity and reliability.
It's called "Pulsed" because it's based on brief impulsive discharges (so of very high intensity) that let it have high I_{sp} even for moderate powers. The absorbed power can be managed just regulating the frequency of repetitions of the impulses without modifying the performances of the engine.
It's mostly used in Micro-Propulsion where you need a very accurate attitude control and brief impulses but exact.
His performances are:

- $I_{sp} \sim 1000\ s$
- Impulsive bit $\sim 30\ \mu N/s$
- $P \sim 100\ W$

The most used material is ***Solid Teflon-*** $(\boldsymbol{C2F4})_{\boldsymbol{n}}$- and the working principle is the following: a pipeline boot generates a spark on the surface of the propellant producing enough electric conductivity inside the acceleration chamber so as to allow the capacitors to release the energy they'd stored and then to allow the Teflon ablation.

The operating cycle starts when the ***Processing Power Unit*** (***PPT***) picks power from the Bus of the Spacecraft and charges the capacitors bench to the desired voltage. These capacitors are connected to a couple of electrodes in which the Teflon bar is powered.
Once the PPT discharge is trigged, it quickly becomes an arc and the ΔV between the electrodes reaches few hundreds of Volts.
Ideally, the spread arc covers the entire surface of the propellant. The charge flows from the capacitors through the electrodes and the arc, creating a ***Charge Loop*** that induces a Magnetic Field.
Thanks to the interaction of this Magnetic Field with the arc the Lorentz Force is generated, accelerating the thin layer of the surface of the ionized Teflon.
A big fraction of the ablated mass remains neutral feeling the gas-dynamic effects of the acceleration.
So, the acceleration is due to the combined effect of the gas-dynamic and electromagnetic forces.
The gas mass reaches the exit of the channel and is expelled with a minimum heat and electromagnetic energy loss.
Finally, once the capacitors bench has downloaded all the energy it was loaded, the cycle restart from the beginning, generating the pulsed behavior of the PPT.
The way the propellant is injected into the Combustion Chamber should be fixed to get the desired density distribution and when the discharge is generated it's important that it quickly reaches the intensity desired as to get a stable current layer, highly conductive and impermeable to the gas.

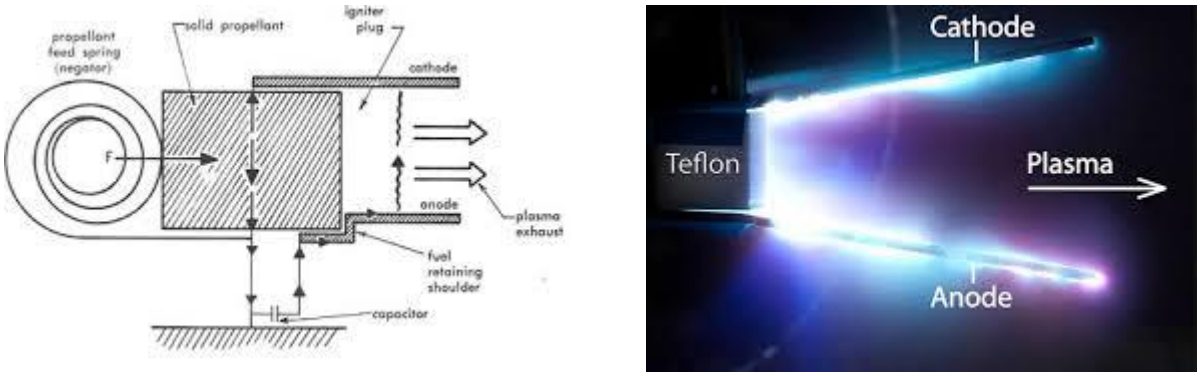

Figure 2-23: A PPT Thruster (at the right) and a PPT Thruster scheme (at the left)

With this the PPT the description of the main Electric Thrusters is over.
The aim of this thesis is to make an analysis of an MPD thruster so in the next chapters we're going into detail of the Plasma Physics and, in particular, in the Physics of the MPD Thruster.

CHAPTER 3: PHYSICS OF THE ELECTRIC THRUSTERS

As we said in the introduction, one of the main advantages of the Electric Propulsion is that the Electric Thrusters break the v_e limit due to the temperature and the chemical characteristics of the fuel.
The most efficient and powerful Electric Thrusters works thanks to the plasma.
So let's start with a description of plasma physics and to continue then with the MHD equation, that are more suitable for the description of an MPD Thruster.

PLASMA PHYSICS GENERALITIES

Plasma is considered as the fourth state of matter and, even if on the Earth is very rare to find it in nature - except for the Ionosphere, Boreal and austral Auroras and the lightning- it represents the quasi totality of the mass of the Universe, most of which is in the rarefied intergalactic regions, in particular the intracluster medium and stars, including the Sun.
On the contrary, in the last decades artificial plasma has been created and used more frequently: an example can be represented by the neon signs.
It is used in Space Propulsion for many reason:

- It is globally neuter $\Longrightarrow$ we can abandon the neutralizers;
- It is an easy storable propellant;
- It is throttlable;

It can be produced in various way, like with a capacitive-inductive source, or a wave source, it can be accelerated in many way, as we saw in the previous chapter, and it can be detached by a magnetic nozzle or a neutralizer.

Figure 3-1: TheNorthen Lights

Plasma is an ionized gas, consisting of a set of charged and neutral particles, quasi-neutral and which exhibits a collective behavior.

It is important to note that, although they are unbound, these particles are not “free” in the sense of not experiencing forces. When the charges move, generate electrical currents with magnetic fields, and as a result, they are affected by each other's fields and they respond to the main ***Electromagnetic Laws*** that, for vacuum, are:

$$\vec{F} = \vec{j} \times \vec{B} \leftarrow \boldsymbol{Lorentz\ Force} \tag{3-2}$$

$$\left.\begin{aligned} \varepsilon_0 \nabla \cdot \vec{E} = \rho \leftarrow \boldsymbol{Gauss\ Law} \\ \nabla \times \vec{E} = -\frac{\partial \vec{B}}{\partial t} \leftarrow \boldsymbol{Faraday\ Law} \\ \nabla \cdot \vec{B} = 0 \leftarrow \boldsymbol{Non-existance\ of\ magnetic\ monopoles} \\ \nabla \times \vec{B} = \mu_0 \left(\vec{j} + \varepsilon_0 \frac{\partial \vec{E}}{\partial t} \right) \leftarrow \boldsymbol{Ampére\ Law} \end{aligned}\right\} \leftarrow \boldsymbol{Maxwell\ Equations\ in\ vacuum} \tag{3-3}$$

If we consider just the electrostatic case, with a negligible variation of the magnetic field $\vec{B}$, so:

$$\vec{B} = Const; \tag{3-4}$$

$$\Longrightarrow \nabla \times \vec{E} = 0 \tag{3-5}$$

$$\Longrightarrow \vec{E} = -\nabla\bar{\phi} \tag{3-6}$$

where $\bar{\phi}$ is a scalar potential.
If we substitute in the Gauss Law, we then have:

$$\nabla^2\bar{\phi} = -\frac{\rho}{\varepsilon_0} \leftarrow \boldsymbol{Poisson\ Equation} \tag{3-7}$$

As we said, plasma is an ionized gas and the ***Saha Ionization Equation***- also known as ***Saha Langmuir Equation***- describes its ionization state relating it to the temperature and the pressure.
It represents the equilibrium between the ionization rate (that depends on the temperature- T) and recombination rate (that depends on the density- ρ):

$$\frac{n_i}{n_n} = 2.4 \cdot 10^{21} = \frac{T^{3/2}}{n_i} e^{\left(-\frac{U_i}{kT}\right)} \tag{3-8}$$

For temperatures in the range of $300\ K$, with a ionization grade per Newton of about $U_i = 14.5\ eV$ and a density of $3 \cdot 10^{25}\ m^{-3}$, the percentage of ionized particles is very low $\frac{n_i}{n_n} \sim 10^{-122}$, so on the Earth we cannot observe the presence of the Plasma except for few cases.

3.1.1.2. Quasi-Neutrality of the Plasma

Saying that plasma is ***quasi-neuter*** means that the plasma is overall neuter, thus:

$$-q_e n_e = q_i n_i \pm \Delta \tag{3-9}$$

where the subscripts e and i indicates the electrons and the ions, respectively, and Δ is very small.
This is one of the main characteristic of the plasma, which reflects its capacity to remain electrically neuter. In fact the plasma can balance the positive negative and the charges so that $n_i \sim n_e$ in any macroscopic element of the plasma itself. An imbalance on the local charge density will create an electrostatic force that will restore the charge equilibrium.

To understand better this concept, consider an initial stationary state where $n_i = n_e = n_0$ and let's assume that the plasma is cold, which means that the excitement thermal motion of the electrons and ions is negligible.
Suppose now to perturb the system moving some electrons from a region to another adjacent to the first one: this motion will create a net positive charge behind them and, thus, an electric field- E- between ions and electrons. This electric field will exert a force to them to reduce their distance.
Let's calculate the effect of an electric field- E_x-, directed on the x axis, on a single electron with a mass- m_e and an electric charge q_e:

$$F_{el,x} = m_e a_x = m_e \frac{d^2x}{dt^2} = q_e E_x \tag{3-10}$$

Now, applying the Gauss Theorem for a close rectangular surface, it can be shown that:

$$E_x = -\frac{x N_e q_e}{\varepsilon_0} \tag{3-11}$$

where N_e is the electronic density at the equilibrium. So, substituting, we obtain:

$$\frac{d^2x}{dt^2} = -\omega_p^2 x \tag{3-12}$$

where:

$$\omega_p = \sqrt{\frac{N_e q_e^2}{\varepsilon_0 m_e}} \tag{3-13}$$

and ω_p is the ***Plasma Frequency***. This means that every perturbation to the equilibrium of plasma create an oscillation with frequency ω_p. Then, the oscillations of the plasma seem to interest just the zone where the charge imbalance has happened, without propagating in other zones of the plasma. However, in reality, the oscillations propagate because of thermal effects and "***finite boundaries***": the electrons in fact arrive in quite adjacent zones, transporting an information that is closely linked to the perturbation itself.
In a partially ionized gas where the perturbation are important , the oscillations of the plasma can happen just if the average time τ_n between the collisions is long enough respect the oscillation of the plasma, so:

$$\omega_p \tau_n > 1 \tag{3-14}$$

This condition is fundamental to consider an ionized gas as a plasma.
Before proceeding further, we should review important notions like ***Temperature*** and ***Energy***:

Temperature

The particles of a gas that is in thermal equilibrium have very different velocities. The most likely distribution is the ***Maxwellian Distribution***:

$$f(u) = A \cdot e^{\left(\frac{-\frac{1}{2}mu^2}{K_B T}\right)} \tag{3-15}$$

where K_B is the Boltzmann Constant that is:

$$K_B = 1.38 \cdot 10^{-23}\, J/K \tag{3-16}$$

and the density n is given by:

$$n = \int_{-\infty}^{\infty} f(u)du \tag{3-17}$$

The width of the distribution is characterized by the Temperature T, while the altitude depends on the density n:

$$A = n\sqrt{\left(\frac{m}{2\pi K_B T}\right)} \tag{3-18}$$

and, in presence of an external potential- ϕ - the distribution will become:

$$f(u) = A \cdot e^{\left(\frac{-\frac{1}{2}mu^2 - e\phi}{K_B T}\right)} \tag{3-19}$$

This last equation shows that there are less electrons where the potential ϕ is higher because, if we integrate respect u, not all the particles have enough energy to be there.
Knowing that for $\phi \to \infty \Longrightarrow n_i = n_e = n_\infty$, then:

$$\Longrightarrow\ n_e = n_\infty e^{\left(\frac{e\phi}{K_B T}\right)} \tag{3-20}$$

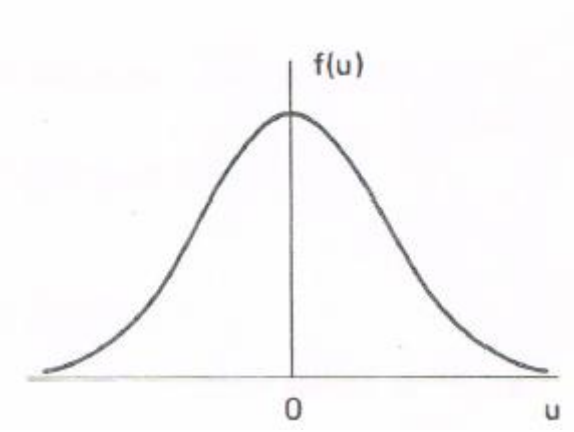

Figure 3-2: f(u)-u graphic

Average Kinetic Energy

To see the exact meaning of T we can compute the average Kinetic Energy of the particles in this distribution.

$$E_{av} = \frac{\int_{-\infty}^{\infty} \frac{1}{2} m u^2 f(u) du}{\int_{-\infty}^{\infty} f(u) du} \tag{3-21}$$

that, for a mono-dimensional distribution, after some calculations, becomes:

$$E_{av} = \frac{1}{2} K_B T \tag{3-22}$$

while, for the tri-dimensional case becomes:

$$E_{av} = \frac{3}{2} K_B T \tag{3-23}$$

So, as we can easily understand, the general result is that E_{av} is equal to $\frac{1}{2} K_B T$ per degree of freedom.
Since T and E_{av} are so closely related, it's common to indicate the Temperature T in units of energy, so, since:

$$1\ K_B T = 1\ eV = 1.6 \cdot 10^{-19} J \tag{3-24}$$

we then have:

$$T = \frac{1.6 \cdot 10^{-19}}{1.38 \cdot 10^{-23}} = 11600 \tag{3-25}$$

So, we can say that $1\ eV = 11600\ K$.
It's interesting to note that a single plasma can have different temperature at the same time. In fact, it happens often that electrons and ions have different Maxwellian Distributions inside the same plasma, because the collision rate among particles with other particles of same species is larger than the rate of collisions between ions and electrons. Thus, each species can have its own thermal equilibrium and, so, its own Temperature. However, the plasma may not last long enough for the two temperatures to equalize.
Then, when there is a Magnetic Field $\vec{B}$, even a single species can have two temperatures because the forces acting perpendicular to $\vec{B}$(due to the *Lorentz Force*) are different from those acting along $\vec{B}$, so the components of the velocity perpendicular and parallel to $\vec{B}$ could belong to different Maxwellian Distributions with different Temperatures $T_{\perp}$and $T_{/\!/}$.

3.1.1.3. Debye Shielding

A fundamental characteristic of the plasma is its ability to shield out electric potentials that are applied to it. However, this characteristic is valid just in a macro-view of the plasma. As we said in the previous paragraph, looking at a more restricted area of the plasma, we could see that some particles having the same charge are grouped into "***charged clouds***" where the electrostatic potential is strong enough to withhold them and shield them from other charges, but some particles, that are at the edge of these charged clouds (where the electric field is weak) have enough thermal energy to escape from its electrostatic potential. That "***edge***" occurs at the radius where the Potential Energy of the particles is almost equal to their Thermal Energy- $K_B T$- and the shielding is not complete.

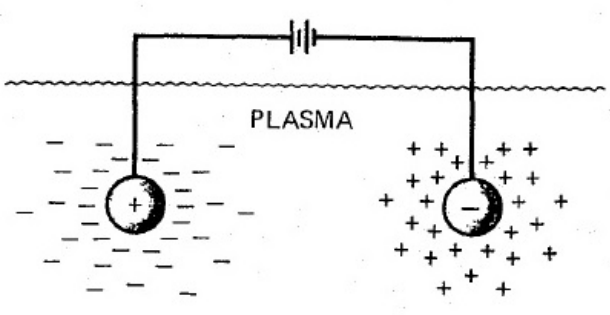

Figure 3-3: Representation of charged clouds

Let's now compute the approximate thickness of this charged cloud: imagine that the potential ϕ in the plane $x = 0$ is held at a value $\phi|_{x=0} = \phi_0$ by a perfectly transparent grid, as we can see in the figure below.

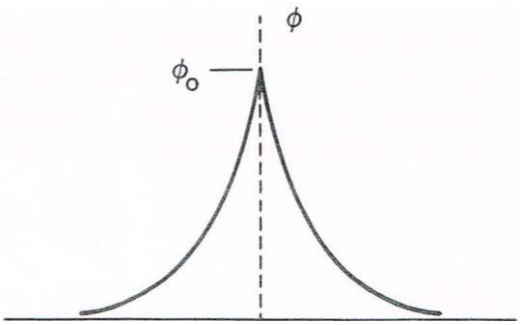

Figure 3-4: $\phi(x)$ trend

We want to compute $\phi(x)$. Assume that the ion-electron mass rate- m_i/m_e- is large enough that the inertia of the ions prevents them from moving significantly on the time scale of the experiment.
Thus, Poisson's Equation in one dimension is:

$$\varepsilon_0 \nabla^2 \phi = \varepsilon_0 \frac{d^2\phi}{dx^2} = -e(n_i - n_e) \tag{3-26}$$

where e, in this case, is the electron charge.
If the density far away is n_∞ we then have $n_i = n_\infty$.
In the presence of a Potential Energy $q\phi$, the electron distribution function is:

$$f(u) = a\mathbf{e}^{\frac{-\left(\frac{1}{2}mu^2 + q\phi\right)}{K_B T_e}} \tag{3-27}$$

where **e**, in this case, is the mathematical constant.

This equations express the physical principle that there are fewer particles at places where the potential energy is large since not all particles have enough energy to get there.
Integrating $f(u)$ over u, setting $q = -e$ and noting that

$$\lim_{\phi \to 0} n_e = n_\infty \tag{3-28}$$

we find:

$$n_e = n_\infty \mathbf{e}^{\frac{e\phi}{K_B T_e}} \tag{3-29}$$

so, substituting for n_i and n_e in the previous equation:

$$\varepsilon_0 \frac{d^2\phi}{dx^2} = e n_\infty \left(\mathbf{e}^{\frac{e\phi}{K_B T_e}} - 1 \right) \tag{3-30}$$

In the region where $\left|\frac{e\phi}{K_B T_e}\right| \ll 1$ we can expand it in a Taylor series:

$$\varepsilon_0 \frac{d^2\phi}{dx^2} = e n_\infty \left[\frac{e\phi}{K_B T_e} + \frac{1}{2}\left(\frac{e\phi}{K_B T_e}\right)^2 + \cdots \right] \tag{3-31}$$

No simplifications are possible for the region near the grid where $\frac{e\phi}{K_B T_e}$ may be large. However, these regions don't contribute much to the thickness of the cloud because the potential falls very rapidly there.
Thus, we have:

$$\varepsilon_0 \frac{d^2\phi}{dx^2} = \frac{n_\infty e^2}{K_B T_e} \phi \tag{3-32}$$

$$\Longrightarrow \frac{d^2\phi}{dx^2} - \frac{n_\infty e^2}{\varepsilon_0 K_B T_e} \phi = 0 \tag{3-33}$$

$$\Longrightarrow \frac{d^2\phi}{dx^2} - \left(\frac{1}{\lambda_D}\right)^2 \phi = 0 \tag{3-34}$$

So, we can finally define the ***Debye Length***:

$$\Longrightarrow \lambda_D = \sqrt{\frac{\varepsilon_0 K_B T_e}{n_\infty e^2}} \tag{3-35}$$

and we can finally write:

$$\phi = \phi_0 \mathbf{e}^{\left(-\frac{|x|}{\lambda_D}\right)} \tag{3-36}$$

Thus, the ***Debye Length*** is a measure of the shielding distance or thickness of the sheath.
We can do a couple of considerations about this last formula:

- As the density is increased, λ_D decreases, since each layer of plasma contains more electrons;
- λ_D increases with increasing $K_B T_e$. In fact, without thermal agitation, the charge cloud would collapse to an infinitely thin layer;
- To define λ_D we used the temperature of the electrons because they're more mobile than the ions, so they do the shielding by moving so as to create a surplus or a deficit of negative charge;

In the previous paragraph we defined the ***Quasi-Neutrality*** of the plasma. We can now relate this characteristic to the ***Debye Shielding***: if the dimensions L of a system are much larger than λ_D then, whenever local concentrations of charge arise or external potentials are introduced into the system, these are shielded out in a distance short compared with L, leaving the bulk of the plasma free of large electric potentials or fields. Outside of the sheath on the wall or on an obstacle $\nabla^2\phi$ is very small and $n_i \cong n_e$, so it's enough a small charge imbalance to give rise to potentials of the order of $\frac{K_B T_e}{e}$. The plasma is "quasi-neutral" in the sense that $n_i \cong n_e \cong n$, where n is the ***Plasma Density***.
So, at the end, an ionized gas can be considered a Plasma if it's dense enough that $L \gg \lambda_D$.

The definition of Debye Shielding we've just given it's valid, by a statistic point of view, only if there are enough particles in the charge cloud. This number can be estimated with a parameter called "***Plasma Parameter***"- Λ:

$$\Lambda = \frac{4}{3} n_0 \pi {\lambda_D}^3 \tag{3-37}$$

Λ represents the number of particles inside a Debye Sphere. Thus, an ionized gas can be considered a plasma if $\Lambda \gg 1$.
Hence, at the end, the minimal conditions to consider an ionized gas as a plasma are summarized as follows:

- $\omega_p \tau_n > 1$
- $L \gg \lambda_D$

- $\Lambda \gg 1$

3.1.1.4. Collective Behavior

As we mentioned at the beginning of this chapter, another important characteristic of the plasma is its ***Collective Behavior***. Depending on the density, a plasma behaves sometimes like a fluid where the collective effects are preponderant and, sometimes, like a collection of individual particles.
The collective behavior of the plasma is due to some phenomena that we described in the previous paragraph, like the Debye Shielding, and just in case the collision cross section between electrons and neuter particles is much lower than the collision cross section between electrons and ions. Thus, the frequency of the collisions with the neuter particles should be low enough so that the dynamic of the motion of the plasma is determined by the Electromagnetic Forces and not by those Hydrodynamic.
Hence, what makes plasmas particularly difficult to analyze is the fact that the densities fall in an intermediate range.

In the next paragraph we'll start the analysis of the Plasma Physics first describing the motion of a single particle in an electromagnetic field, then making a panoramic of the plasma as a fluid and, finally, we'll introduce the equations of the ***Magneto-Hydro-Dynamic***.

3.1.1.5. Motion of a Single Charged Particle in an Electromagnetic Field

To make this analysis we should start with the simplest case and then continue with the more complex.

Uniform $\vec{B}$ and $\vec{E}$ Fields

As we previously said, the fundamental equation of the motion, for a charged particle under the influence of the Lorentz Force is:

$$m\frac{d\vec{v}}{dt} = \vec{F}_{Lorentz} = q\left(\vec{E} + \vec{v} \times \vec{B}\right) \qquad (3\text{-}38)$$

where m is the mass of the particle and $\vec{v}$ its velocity.
We can analyze this equation studying the two different cases: $\vec{E} = 0$ or a finite $\vec{E}$.

$\boldsymbol{\vec{E} = 0}$

In this case, a charged particle has a simple cyclotron gyration. Hence, the equation of the motion is:

$$m\frac{d\vec{v}}{dt} = \vec{F}_{Lorentz} = q\left(\vec{v} \times \vec{B}\right) \tag{3-39}$$

Taking now $\hat{z}$ to be the direction of $\vec{B}$ ($\vec{B} = B\hat{z}$), we have:

$$\begin{bmatrix} m\dot{v}_x \\ m\dot{v}_y \\ m\dot{v}_z \end{bmatrix} = q \begin{vmatrix} \hat{x} & \hat{y} & \hat{z} \\ v_x & v_y & v_z \\ 0 & 0 & B \end{vmatrix} = \begin{bmatrix} qBv_y \\ -qBv_x \\ 0 \end{bmatrix} \tag{3-40}$$

$$\Longrightarrow \begin{cases} \ddot{v}_x = \left(\frac{qB}{m}\right)\dot{v}_y = -\left(\frac{qB}{m}\right)^2 v_x \\ \ddot{v}_y = -\left(\frac{qB}{m}\right)\dot{v}_x = -\left(\frac{qB}{m}\right)^2 v_y \end{cases} \tag{3-41}$$

This formulas describe a simple harmonic oscillator at the ***cyclotron frequency***, defined as:

$$\omega_c = \frac{|q|B}{m} \tag{3-42}$$

where we have chosen, by convention, ω_c as always positive.
The solution of these equations is then:

$$\begin{cases} v_x = v_\perp \cos(\omega_c t + \delta) \\ v_y = v_\perp \sin(\omega_c t + \delta) \\ v_z = v_{/\!/} \end{cases} \tag{3-43}$$

where δ is an arbitrary phase that defines the orientation of the particle.

Then, thanks to the Euler Transformations, the solution can also be written as:

$$v_{x,y} = v_\perp e^{\pm i\omega_c t \pm i\delta_{x,y}} \tag{3-44}$$

where the $\pm$ denotes the sign of the charged particle.
The positive integration constant $v_\perp$ is the velocity in the plane perpendicular to $\vec{B}$:

$$v_\perp = \sqrt{v_x^2 + v_y^2} \tag{3-45}$$

the particle, has a gyration motion with a radius- r_L-, called ***Larmor Radius***, such that:

$$r_L = \frac{v_\perp}{\omega_c} = \frac{m v_\perp}{|q|B} \tag{3-46}$$

Thus, if we chose the phase δ so that:

$$\begin{cases} v_x = v_\perp e^{i\omega_c t} = \dot{x} \\ v_y = \pm i v_\perp e^{i\omega_c t} = \dot{y} \end{cases} \tag{3-47}$$

the final solution of the motion will be:

$$\begin{cases} x - x_0 = r_L \sin(\omega_c t) \\ y - y_0 = \pm r_L \cos(\omega_c t) \\ z - z_0 = v_{/\!/} t \end{cases} \tag{3-48}$$

that describes a circular orbit in a plane that is perpendicular to $\vec{B}$, with an angular frequency ω_c and a radius r_L, around a ***Guiding Center*** $\left(x_0, y_0, z_0 + v_{/\!/} t\right)$ which is fixed.

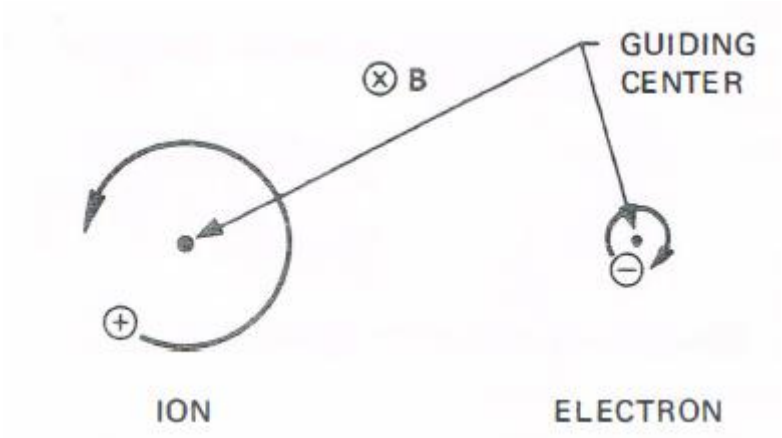

Figure 3-5: Motion of an electron around an ion

The direction of the gyration is always such that the magnetic field generated by the charged particle is opposite to the externally imposed field.
So, as we can see in the next figure, the trajectory of a charged particle in space is, in general, an helix.

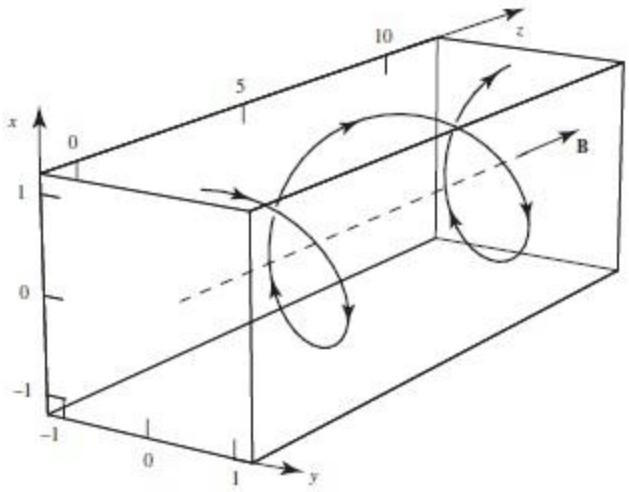

Figure 3-6: Helical trajectory of a charged particle in space

Finite $\vec{E}$

If now we add an Electric Field $\vec{E}$ to the Magnetic Field $\vec{B}$, the resulting motion will be the sum of the two basic motions: the usual circular Larmor gyration plus a drift of the guiding centre.
Assume that $\vec{E}$ lies in the $x-z$ plane (so $E_y = 0$); as in the previous case, the z component of the velocity- v_z- is unrelated to the transverse components and can be treated separately.
The equation of the motion, now, must be considered completely:

$$m\frac{d\vec{v}}{dt} = q\left(\vec{E} + \vec{v} \times \vec{B}\right) \tag{3-49}$$

The z component is simply:

$$v_z = \frac{qE_z}{m}t + v_{z,0} \tag{3-50}$$

that is a straightforward acceleration along B.
For the other two components we have:

$$\begin{cases} \dfrac{dv_x}{dt} = \dfrac{q}{m}E_x \pm \omega_c v_y \\ \dfrac{dv_y}{dt} = 0 \mp \omega_c v_x \end{cases} \tag{3-51}$$

$$\Rightarrow \begin{cases} \ddot{v}_x = -\omega_c^2 v_x \\ \ddot{v}_y = \mp\omega_c\left(\dfrac{q}{m}E_x \pm \omega_c v_y\right) = -\omega_c^2\left(\dfrac{E_x}{B} + v_y\right) = \dfrac{d^2}{dt^2}\left(\dfrac{E_x}{B} + v_y\right) \end{cases} \tag{3-52}$$

so, we can write:

$$\begin{cases} v_x = v_\perp e^{i\omega_c t} \\ v_y = \pm i v_\perp e^{i\omega_c t} - \dfrac{E_x}{B} \end{cases} \tag{3-53}$$

As we can see, the Larmor Motion is the same as before, but a drift $\vec{v}_{gc}$ is superimposed on the guiding centre in the $-y$ direction (for $E_x > 0$). The figure below expresses this concept:

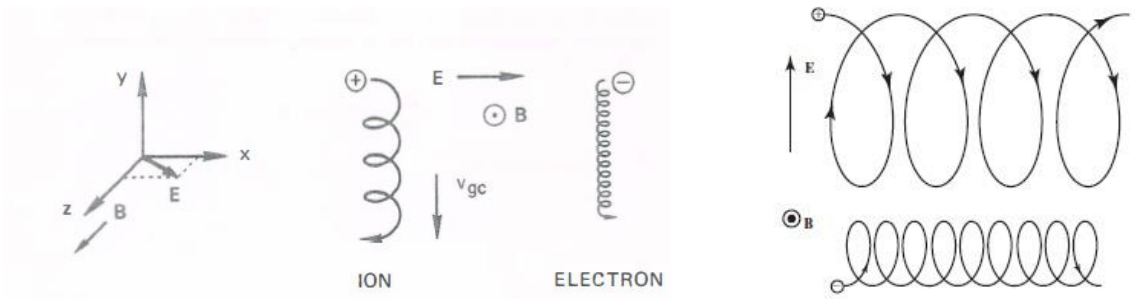

Figure 3-7: Trajectory of charged particles for a finite E field

To compute the equation for $\vec{v}_{gc}$ we can omit the term $\frac{d\vec{v}}{dt}$ in the equation of the motion, since it gives only the circular motion at ω_c. So, the equation becomes:

$$\vec{E} + \vec{v} \times \vec{B} = 0 \tag{3-54}$$

Taking the cross product with $\vec{B}$ we have:

$$\vec{E} \times \vec{B} + \left(\vec{v} \times \vec{B}\right) \times \vec{B} = \vec{E} \times \vec{B} = \vec{B} \times \left(\vec{v} \times \vec{B}\right) = vB^2 - \vec{B}\left(\vec{v} \cdot \vec{B}\right) \qquad (3\text{-}55)$$

So, the Electric Field Drift of the Guiding Centre is given by:

$$\vec{v}_{\perp,gc} = \frac{\vec{E} \times \vec{B}}{B^2} = \vec{v}_E \qquad (3\text{-}56)$$

$$v_E = |\vec{v}_E| = \frac{E}{B} \quad \left[\frac{V/m}{Tesla}\right] = [m/s] \qquad (3\text{-}57)$$

That is independent by the mass m and the charge q of the particle. In fact, in the first half cycle of the ion's orbit, it gains energy from the electric field and increases in $\vec{v}_\perp$ and, hence, in $\mathrm{r_L}$. In the second half-cycle, it loses energy and decreases in $\mathrm{r_L}$. But we know that for particles of the same velocity but different mass, the lighter one will have smaller $\mathrm{r_L}$and hence drift less per cycle.
Thus, is this difference in $\mathrm{r_L}$on the left and right sides of the orbit that causes the drift v_E.

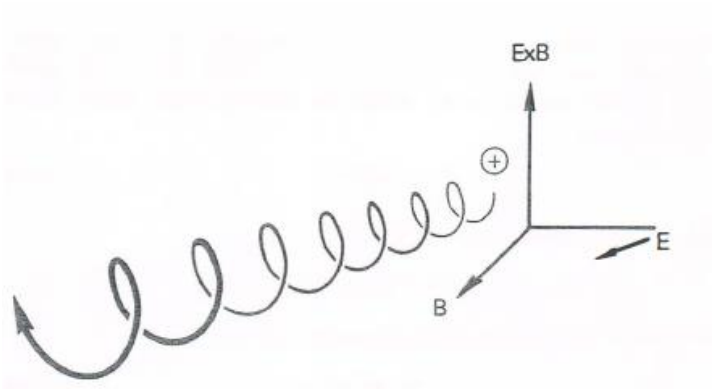

Figure 3-8 Trajectory of charged particles for a finite E field

Let's now generalize the formula considering a general force $\vec{F}$ in stand of $q\vec{E}$. In this case the guiding centre drift caused by $\overrightarrow{F}$would be:

$$\vec{v}_f = \frac{1}{q}\frac{\vec{F} \times \vec{B}}{B^2} \qquad (3\text{-}58)$$

If the force is the Gravitational Force, for example, we'll have:

$$\vec{v}_g = \frac{m}{q}\frac{\vec{g} \times \vec{B}}{B^2} \tag{3-59}$$

This is different from the previous formulas for one thing: the drift $\vec{v}_g$ changes sign with the particle's charge, so under a Gravitational Force ions and electrons will drift in opposite directions, causing a net current:

$$\vec{j} = n(M+m)\frac{\vec{g} \times \vec{B}}{B^2} \tag{3-60}$$

The magnitude of $\vec{v}_g$ is usually negligible, but when the lines of force are curved there's an effective gravitational force due to the centrifugal force, that is not negligible, is independent of the mass and will create a plasma instability called "***Gravitational Instability***".

Now we can study the case of particles in motion in inhomogeneous fields- $\vec{E}$ or $\vec{B}$- that can vary in space or time.

Non-Uniform $\vec{B}$ Field

Introducing inhomogeneity the problem becomes too complicated to be solved exactly so, to get an approximate solution, we should expand in the small ratio r_L/L, where L is the scale length of the inhomogeneity. This approach is called "***Orbit Theory***".
Let's examine the simplest cases where only one inhomogeneity occurs at time.

$\nabla B \perp \vec{B}$: *Grad-$\vec{B}$ Drift*

In this case, the lines of force are straight, but their density increases in the y direction, as we can see in the figure above.

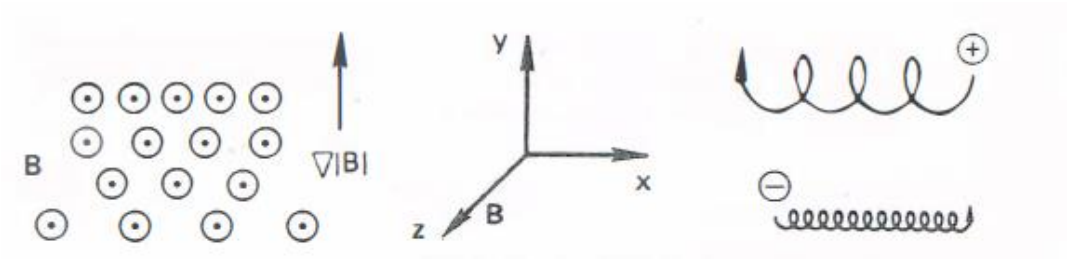

Figure 3-9: Trajectory of charged particles for a non-uniform B Field

The gradient in $|\vec{B}|$ causes he Larmor Radius to be larger at the bottom of the orbit than at the top and this shuld lead to a drift, in opposite directions for ions and electrons, perpendicular to both B and $\nabla\vec{B}$. This drift then should be proportional to r_L/L and $\vec{v}_\perp$.
Considering now the Lorentz Force averaged over a gyration:

$$\vec{F} = q\vec{v} \times \vec{B} \tag{3-61}$$

we can calculate F_y, approximately, by using the ***undisturbed orbit*** for a uniform $\vec{B}$ Field (while $F_x = 0$ since the particle spend as much time moving up as down):

$$F_y = -qv_x B_z(y) = -qv_\perp \cos(\omega_c t)\left[B_0 \pm r_L \cos(\omega_c t)\frac{\partial B}{\partial y}\right] \tag{3-62}$$

Making a Taylor expansion of $\vec{B}$ Field about the point $(x_0, y_0) = (0,0)$.
This expansion is valid just in case $r_L/L \ll 1$, being L the scale length of $\frac{\partial B_z}{\partial y}$. First term of the equation averages to zero in a gyration and the average of $\cos^2(\omega_c t)$ is $\frac{1}{2}$, so we have:

$$\vec{v}_{gc} = \frac{1}{q}\frac{\vec{F}\times\vec{B}}{B^2} = \frac{1}{q}\frac{F_y}{|B|}\hat{x} = \mp\frac{v_\perp r_L}{B}\frac{1}{2}\frac{\partial B}{\partial y}\hat{x} \tag{3-63}$$

Since the choice of the y axis is arbitrary we can generalize the equation as follows:

$$\vec{v}_{\nabla\vec{B}} = \pm\frac{1}{2}v_\perp r_L\frac{\vec{B}\times\nabla\vec{B}}{B^2} \tag{3-64}$$

where $\pm$ stands for the sign of the charge. The quantity $\vec{v}_{\nabla\vec{B}}$ is called $\boldsymbol{Grad\text{-}\vec{B}}$ ***Drift***. It's in opposite direction for ions and electrons and causes a current transverse to $\vec{B}$.

$\boldsymbol{Curved\ \vec{B}}$: $\boldsymbol{Curvature\ Drift}$

Suppose now that the lines of force are curved with a constant radius of curvature R_c and $|\vec{B}|$ to be constant. Here we cannot use the Maxwell's Equation in vacuum, so the $\mathrm{Grad}\text{-}\vec{\mathrm{B}}$ drift must be added to the effect derived here.
If $v_\parallel^2$ denotes the average square of the component of random velocity along B, the average centrifugal force is:

$$\overrightarrow{F_{cf}} = \frac{mv_{\parallel}^2}{R_c}\hat{r} = mv_{\parallel}^2\frac{\vec{R}_c}{R_c^2} \tag{3-65}$$

So we have:

$$\vec{v}_R = \frac{1}{q}\frac{\overrightarrow{F_{cf}} \times \vec{B}}{B^2} = \frac{mv_{\parallel}^2}{qB^2}\frac{\vec{R}_c \times \vec{B}}{R_c^2} \tag{3-66}$$

And this $\vec{v}_R$ Drift is called ***Curvature Drift***.
On the other side, if $\left|\vec{B}\right|$ decreases with the radius, so:

$$\left|\vec{B}\right| \propto \frac{1}{R_c} \tag{3-67}$$

we can demonstrate that:

$$\frac{\nabla\left|\vec{B}\right|}{\left|\vec{B}\right|} = -\frac{\vec{R}_c}{R_c^2} \tag{3-68}$$

$$\Longrightarrow \vec{v}_{\nabla\vec{B}} = \frac{1}{2}\frac{mv_{\perp}^2}{qB^2}\frac{\vec{R}_c \times \vec{B}}{R_c^2} \tag{3-69}$$

Adding this last term to $\vec{v}_R$, we get:

$$\vec{v}_R + \vec{v}_{\nabla\vec{B}} = \frac{m}{qB^2}\frac{\vec{R}_c \times \vec{B}}{R_c^2}\left(v_{\parallel}^2 + \frac{1}{2}v_{\perp}^2\right) \tag{3-70}$$

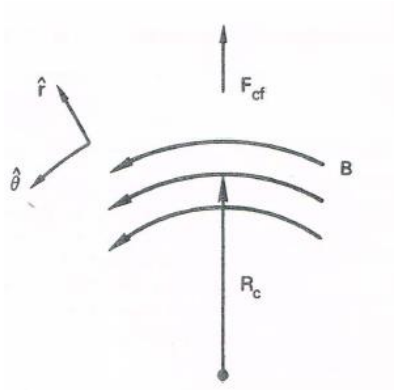

Figure 3-10: Representation of curvature drift

This case is important because it represents, for example, the case of a magnetic field into a torus: the particles will always drift out of the torus.

For a Maxwellian Distribution, as we saw in the previous paragraph, we calculated that $\overline{v_{\parallel}^2}$ and $\overline{\frac{1}{2}v_{\perp}^2}$, both equal to $K_B T_e/m$, so we have that the **Average Curved-Field Drift** is:

$$\overline{v_{R+\nabla\vec{B}}} = \pm\frac{\vec{r}_L}{R_c}v_{th}\hat{y} \qquad (3\text{-}71)$$

where $\hat{y}$ is the direction of $\vec{R}_c \times \vec{B}$. This shows that $\overline{v_{R+\nabla\vec{B}}}$ depends on the charge of the particle but not on its mass.

$\nabla B \| \vec{B}$: Magnetic Mirrors

Now consider a Magnetic Field $\vec{B}$ pointed primarily in the z direction and whose magnitude varies in the z direction. We suppose the field to be axial symmetric, with $B_\theta = 0$ and $\partial/\partial\theta = 0$. There will necessarily be a component B_r that creates a force which can trap a particle in a magnetic field.

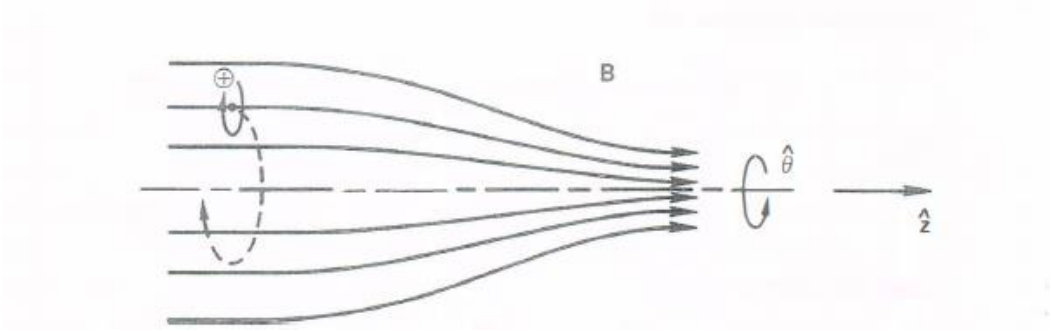

Figure 3-11: Representation of a Magnetic Field pointed in the z direction, axial symmetric whose magnitude varies with z

Thus, from $\nabla \cdot \vec{B} = 0$, we have:

$$\frac{1}{r}\frac{\partial}{\partial r}(rB_r) + \frac{\partial B_z}{\partial z} = 0 \tag{3-72}$$

If $\frac{\partial B_z}{\partial z}$ is given at $r = 0$ and doesn't vary so much with r, then we have:

$$rB_r = -\int_0^r r\frac{\partial B_z}{\partial z}dr \cong -\frac{1}{2}r^2\left[\frac{\partial B_z}{\partial z}\right]_{r=0} \tag{3-73}$$

$$\Longrightarrow B_r = -\frac{1}{2}r\left[\frac{\partial B_z}{\partial z}\right]_{r=0} \tag{3-74}$$

The variation of $\left|\vec{B}\right|$ with r causes a Grad-B Drift of guiding centers about the axis of symmetry, but there is no radial Grad-B Drift because $\partial\vec{B}/\partial\theta = 0$. So, the components of the Lorentz Force are:

$$\begin{cases} F_r = q(v_\theta B_z - v_z B_\theta) \\ F_\theta = q(-v_r B_z + v_z B_r) \\ F_z = q(v_r B_\theta - v_\theta B_r) \end{cases} \tag{3-75}$$

Since $B_\theta = 0$, two terms vanish, while the two terms containing the component B_z give rise the usual Larmor Gyration. The terms $v_z B_r$ vanishes on the axis and if it doesn't do it causes a drift in the radial direction, making the guiding centers follow the lines of force.
What we are interested in is the terms $v_\theta B_r$. We have:

$$F_z = \frac{1}{2}qv_\theta r\left(\frac{\partial B_z}{\partial z}\right) \tag{3-76}$$

So, the average over one gyration is:

$$\overline{F_z} = \mp\frac{1}{2}qv_\perp r_L\frac{\partial B_z}{\partial z} = \mp\frac{1}{2}q\frac{v_\perp^2}{\omega_c}\frac{\partial B_z}{\partial z} = -\frac{1}{2}\frac{mv_\perp^2}{B}\frac{\partial B_z}{\partial z} \tag{3-77}$$

and, defining the ***Magnetic Moment*** of the gyrating particle as:

$$\mu = \frac{1}{2}\frac{mv_{\perp}^2}{B} \tag{3-78}$$

we have:

$$\bar{F}_z = -\mu\left(\frac{\partial B_z}{\partial z}\right) \tag{3-79}$$

That is the value of the Grad-B Drift.

As the particle moves into regions with stronger or weaker $\vec{B}$ the Larmor radius changes, but ***μ remains invariant***. In fact, we the component of the equation of motion along B is:

$$mv_{\parallel}\frac{dv_{\parallel}}{dt} = -\mu\frac{ds}{dt} \tag{3-80}$$

$$\Longrightarrow mv_{\parallel}\frac{dv_{\parallel}}{dt} = \frac{d}{dt}\left(\frac{1}{2}mv_{\parallel}^2\right) = -\mu\frac{\partial B}{\partial s}\frac{ds}{dt} = -\mu\frac{dB}{dt} \tag{3-81}$$

where $\frac{dB}{dt}$ is the variation of $\vec{B}$ as seen by the particle ($\vec{B}$ itself is constant).

For the conservation of the energy we have:

$$\frac{d}{dt}\left(\frac{1}{2}mv_{\parallel}^2 + \frac{1}{2}mv_{\perp}^2\right) = \frac{d}{dt}\left(\frac{1}{2}mv_{\parallel}^2 + \mu B\right) = 0 \tag{3-82}$$

$$\Longrightarrow -\mu\frac{dB}{dt} + \frac{d}{dt}(\mu B) = 0 \tag{3-83}$$

$$\Longrightarrow \frac{d\mu}{dt} = 0 \tag{3-84}$$

This last equation is the basis for one of the primary schemes for plasma confinement: the ***Magnetic Mirror***.

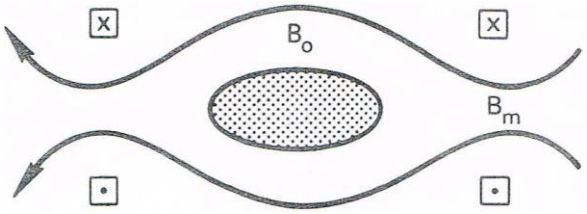

Figure 3-12: Scheme of the Magnetic Mirror

Since μ is constant, If a particle moves from a Weak-Field region to a Strong-Field region, we have:

$$\frac{1}{2}m\frac{v_{\perp,w}^2}{B_w} = \frac{1}{2}m\frac{v_{\perp,s}^2}{B_s} \tag{3-85}$$

where the subscript w indicates the *Weak-Field Condition*, while the subscript s indicates the *Strong-Field Condition*.
So, if $B_s > B_w$ we have that $v_{\perp,s}^2 > v_{\perp,w}^2$. However, the Magnetic Field B don't do any work, so the Kinetic Energy of the particle remains invariant:

$$E_K = \frac{1}{2}m\left(v_{\perp,w}^2 + v_{\parallel,w}^2\right) \tag{3-86}$$

So we'll have that:

$$v_{\parallel,s}^2 < v_{\parallel,w}^2 \tag{3-87}$$

$$\Longrightarrow v_{\parallel,s} < v_{\parallel,w} \tag{3-88}$$

that means that the axial velocity of the particle will decrease while the particle is moving into the Strong-Field region.
Thus, the axial velocity will be:

$$\frac{1}{2}mv_{\parallel}^2 = E_K - \frac{1}{2}mv_{\perp}^2 = E_K - \mu B \tag{3-89}$$

$$\Longrightarrow v_{\parallel} = \sqrt{\frac{2}{m}(E_K - \mu B)} \tag{3-90}$$

This last equation is very important because it shows that if the Magnetic Field $\vec{B}$ is Strong enough the particle can be stopped and forced by $F_{\parallel}$ the to re-enter the plasma body, into the Weak-Field region.
However, not all the particles are trapped by the Magnetic Mirror: for example, a particle with $v_{\perp} = 0$ will have no magnetic moment and will not feel any force along $\vec{B}$ and also a particle with small $v_{\perp}/v_{\parallel}$ at the mid plane $(B = B_w)$ will escape if the maximum field B_s is not strong enough. To understand in which case the particles will escape from the mirror, let's consider a particle with $v_{\perp} = v_{\perp,w}$ and $v_{\parallel} = v_{\parallel,w}$. In the mid plane we will have that $v_{\parallel} = 0$ and $v_{\perp} = v'_{\perp}$ at its turning point. Let the field be B' there. Then, the invariance of μ yelds:

$$\frac{\frac{1}{2}mv_{\perp,w}^2}{B_w} = \frac{\frac{1}{2}mv_{\perp}'^2}{B'} \tag{3-91}$$

and, for the conservation of energy, we have:

$$v_{\perp}'^2 = v_{\perp,w}^2 + v_{\parallel,w}^2 = v_w^2 \tag{3-92}$$

$$\Longrightarrow \frac{B_w}{B'} = \frac{v_{\perp,w}^2}{v_{\perp}'^2} = \frac{v_{\perp,w}^2}{v_w^2} = \sin^2(\theta) \tag{3-93}$$

where θ is the ***pitch angle*** of the orbit in the Weak-Field region. Particles with smaller θ will mirror in regions of higher B, but if θ is too small, B' will exceed B_s and the particles will not mirror at all. Replacing B' with B_s we can find the limit of θ to confine the articles:

$$\sin^2(\theta_s) = \frac{B_w}{B_s} = \frac{1}{R_m} \tag{3-94}$$

where R_m is the ***Mirror Ratio***.
The boundary defined by this equation is a cone in velocity space, independent of q and m, called "***Loss Cone***". Particles lying within the loss cone (so with $\theta < \theta_s$) are not confined. So, a mirror-confined plasma is never isentropic.

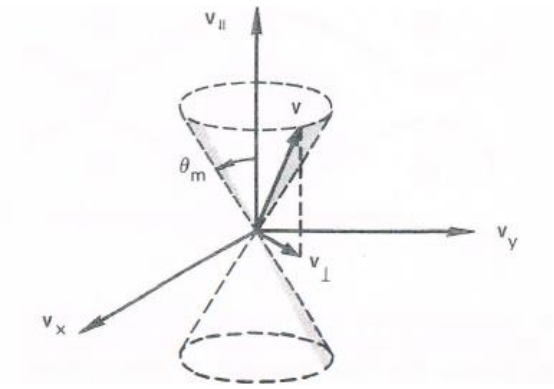

Figure 3-13: Loss Cone

Note that without collisions, both ions and electrons are equally well confined, but when collisions occur articles are lost and are scattered into the loss cone. Since electrons have higher collision frequencies they will be lost mostly than ions, so the plasma will tend to become positively charged.

Non-Uniform $\vec{E}$ Field

Consider now the case in which the Electric Field $\vec{E}$ is non-uniform.
Let's start with the case of a uniform Magnetic Field. Assume $\vec{E}$ to be in the x direction and to vary sinusoidally along it:

$$\vec{E} = E_0 \cos(kx)\,\hat{x} \tag{3-95}$$

$$\lambda = \frac{2\pi}{k} \tag{3-96}$$

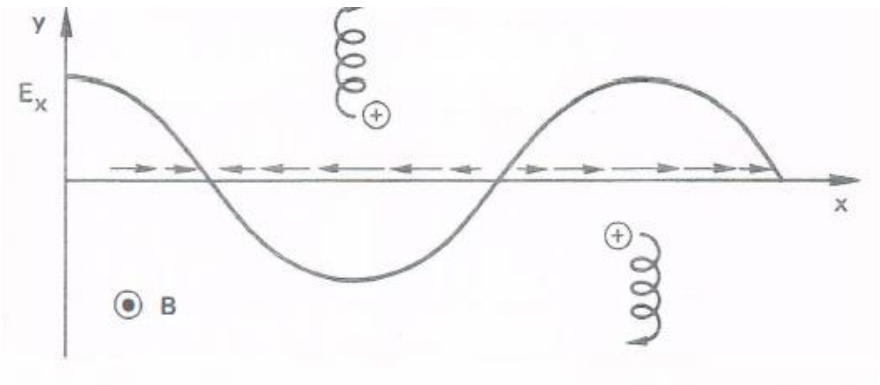

Figure 3-14: Electric Field varying sinusoidally along x

Such a charge distribution can arise in a plasma during a wave motion.
So, according to the equation of the motion, we have:

$$m\frac{d\vec{v}}{dt} = q\left[\vec{E}(x) + \vec{v} \times \vec{B}\right] \tag{3-97}$$

where:

$$\begin{cases} \dot{v}_x = \dfrac{qB}{m} v_y + \dfrac{q}{m} E_x(x) \\ \dot{v}_y = -\dfrac{qB}{m} v_x \end{cases} \tag{3-98}$$

$$\begin{cases} \ddot{v}_x = -\omega_c^2 v_x \pm \omega_c \dfrac{\dot{E}_x}{B} \\ \ddot{v}_y = -\omega_c^2 v_y - \omega_c^2 \dfrac{E_x(x)}{B} \end{cases} \tag{3-99}$$

and $E_x(x)$ is the Electric Field at the position of the particle.
As we saw in the previous analysis, the orbit of the particle in absence of Electric Field is given by:

$$x = x_0 + r_L \sin(\omega_c t) \tag{3-100}$$

$$\Longrightarrow \ddot{v}_y = -\omega_c^2 v_y - \omega_c^2 \frac{E_0}{B} \cos[k(x_0 + r_L \sin(\omega_c t))] \tag{3-101}$$

The result, as in the previous cases, will be the sum of a gyration at ω_c and a steady drift $\vec{v}_E$. What we must calculate now is $\vec{v}_E$, so we can take out the gyratory motion by averaging over a cycle, getting $\overline{v_x} = 0$.
Thus, we'll have:

$$\overline{\ddot{v}_y = 0} \tag{3-102}$$

$$\Longrightarrow -\omega_c^2 v_y - \omega_c^2 \frac{E_0}{B} \cos[k(x_0 + r_L \sin(\omega_c t))] = 0 \tag{3-103}$$

That, after some passages and considering just the small Larmor radius case- $kr_L \ll 1$, will yield to:

$$\overline{v_y} = -\frac{E_0}{B}[\cos(kx_0)]\left(1 - \frac{1}{4}k^2 r_L^2\right) = -\frac{E_x(x_0)}{B}\left(1 - \frac{1}{4}k^2 r_L^2\right) \tag{3-104}$$

$$\Longrightarrow \vec{v}_E = \frac{\vec{E} \times \vec{B}}{B^2}\left(1 - \frac{1}{4}k^2 r_L^2\right) \tag{3-105}$$

For an arbitrary variation of $\vec{E}$ we can generalize the formula above like follows:

$$\vec{v}_E = \frac{\vec{E} \times \vec{B}}{B^2}\left(1 + \frac{1}{4}r_L^2 \nabla^2\right) \tag{3-106}$$

where $\frac{1}{4}r_L^2\nabla^2$ is called "***Finite-Larmor-Radius-Effect***" and is representative of an effect called "***Drift Instability***" that makes the Electric Field $\vec{E}$ grow indefinitely causing an instability of the plasma.
Also the Grad-B Drift is a Finite-Larmor-Radius-Effect, but since in the Grad-B Drift it is proportional to kr_L while in this last case it is proportional to $k^2 r_L^2$, the non-uniformity of the Electric Field $\vec{E}$, therefore, is more important at large k or small scale lengths of inhomogeneity.
For this reason, drift instabilities belong to a general class called "***Microinstabilities***".

Time-Varying $\vec{E}$ Field

If we now consider The $\vec{E}$ Field uniform in space but varying in time, things will change.
Let's start from the case with $\vec{B}$ constant in time.
Consider $\vec{E}$ lying on the x axis, so:

$$\vec{E} = E_0 e^{i\omega t}\hat{x} \tag{3-107}$$

$$\dot{E}_x = i\omega E_x \tag{3-108}$$

$$\Longrightarrow \ddot{v}_x = -\omega_c^2\left(v_x \mp \frac{i\omega}{\omega_c}\frac{\tilde{E}_x}{B}\right) \tag{3-109}$$

We now define:

$$\tilde{v}_p = \pm \frac{i\omega}{\omega_c} \frac{\tilde{E}_x}{B} \tag{3-110}$$

$$\tilde{v}_E = -\frac{\tilde{E}_x}{B} \tag{3-111}$$

Where the tilde just remark the fact that the drift is oscillating. Thus we get:

$$\begin{cases} \ddot{v}_x = -\omega_c^2 (v_x - \tilde{v}_p) \\ \ddot{v}_y = -\omega_c^2 (v_y - \tilde{v}_E) \end{cases} \tag{3-112}$$

Like above, we're looking for a solution that is the sum of a drift and a gyratory motion:

$$\begin{cases} v_x = v_\perp e^{i\omega_c t} + \tilde{v}_p \\ v_y = \pm i v_\perp e^{i\omega_c t} + \tilde{v}_E \end{cases} \tag{3-113}$$

$$\Rightarrow \begin{cases} \ddot{v}_x = -\omega_c^2 v_x + (\omega_c^2 - \omega^2)\tilde{v}_p \\ \ddot{v}_y = -\omega_c^2 v_y + (\omega_c^2 - \omega^2)\tilde{v}_E \end{cases} \tag{3-114}$$

These last equations are those above just in case $\omega^2 \ll \omega_c^2$.
The solutions $\vec{v} = (v_x, v_y)$ tells us that the guiding center motion has two components:

- The y component, perpendicular to $\vec{E}$ and $\vec{B}$, that is the usual $\vec{E} \times \vec{B}$ Drift except for the fact that now v_E oscillates slowly with a frequency ω;
- The x component, that is a new Drift along $\vec{E}$ and called "***Polarization Drift***". Hence, we can fine the Polarization Drift as:

$$v_p = \pm \frac{1}{\omega_c B} \frac{d\vec{E}}{dt} \tag{3-115}$$

Since this Drift is in opposite direction for ions and electrons, it will provoke a ***Polarization Current***, that, for $Z = 1$, is:

$$j_p = ne\left(v_{p,i} - v_{p,e}\right) = \frac{\rho}{B^2}\frac{d\vec{E}}{dt} \tag{3-116}$$

where ρ is the mass density.

Time Varying $\vec{B}$ Field

The last case to analyze is the one where the Magnetic Field $\vec{B}$ varies in time. Since the Lorentz Force is always perpendicular to $\vec{v}$, a Magnetic Field cannot impart velocity (and, so, energy) to a charged particle, however, we can associate it an Electric Field $\vec{E}$:

$$\nabla \times \vec{E} = -\dot{\vec{B}} \tag{3-117}$$

that can accelerate particles causing the consequent no-uniformity of the fields. Let $v_\perp = \frac{d\vec{l}}{dt}$ be the transverse velocity and $\vec{l}$ the element of path along a particle trajectory (here we can neglect $v_\parallel$). We have:

$$\frac{d}{dt}\left(\frac{1}{2}mv_\perp^2\right) = q\vec{E}\cdot v_\perp = q\vec{E}\cdot\frac{d\vec{l}}{dt} \tag{3-118}$$

The change in one gyration in a field that changes slowly, is given by:

$$\delta\left(\frac{1}{2}mv_\perp^2\right)\oint q\vec{E}\cdot d\vec{l} = q\int\left(\nabla\times\vec{E}\right)\cdot d\vec{S} = -q\int\dot{\vec{B}}\cdot d\vec{S} \tag{3-119}$$

Where $\vec{S}$ is the surface enclosed by the Larmor orbit and direction given by the right-hand rule when fingers point the direction of $\vec{v}$. For ions we have $\dot{\vec{B}}\cdot d\vec{S} < 0$, and for electrons $\dot{\vec{B}}\cdot d\vec{S} > 0$, so:

$$\delta\left(\frac{1}{2}mv_\perp^2\right) = \pm q\dot{B}\pi r_L^2 = \pm q\dot{B}\pi\frac{v_\perp^2}{\omega_c}\cdot\frac{m}{\pm qB} = \frac{\frac{1}{2}mv_\perp^2}{B}\cdot\frac{2\pi B}{\omega_c} \tag{3-120}$$

Since the quantity $\frac{2\pi B}{\omega_c}$ is just the change δB during one period of gyration, we have:

$$\delta\left(\frac{1}{2}mv_{\perp}^{2}\right)=\mu\delta B \tag{3-121}$$

$$\Longrightarrow \delta\mu=0 \tag{3-122}$$

This means that ***the Magnetic Moment is invariant in slowly varying Magnetic Field*** and this characteristic allows us to prove that the ***Magnetic Flux though a Larmor orbit is constant***: given the flux ϕ by BS, with $S=\pi r_L^2$ is:

$$\phi=B\pi\frac{v_{\perp}^{2}}{\omega_c}=B\pi\frac{v_{\perp}^{2}m^{2}}{q^{2}B^{2}}=\frac{2\pi m}{q^{2}}\frac{\frac{1}{2}mv_{\perp}^{2}}{B}=\frac{2\pi m}{q^{2}}\mu \tag{3-123}$$

$$\mu=Const.\Longrightarrow\phi=Const. \tag{3-124}$$

We can now summarize the formula we found for the Guiding Centre Drift:

Table 3-1: Guiding Centre Drift main formulas

TYPE OF FORCE	DRIFT
General Force	$\vec{v}_f=\frac{1}{q}\frac{\vec{F}\times\vec{B}}{B^2}$
Electric Field	$\vec{v}_E=\frac{\vec{E}\times\vec{B}}{B^2}$
Gravitational Field	$\vec{v}_g=\frac{m}{q}\frac{\vec{g}\times\vec{B}}{B^2}$
Non-uniform $\vec{E}$ Field	$\vec{v}_E=\frac{\vec{E}\times\vec{B}}{B^2}\left(1+\frac{1}{4}r_L^2\nabla^2\right)$

Grad-B Drift

$$\vec{v}_{\nabla\vec{B}} = \pm\frac{1}{2}v_{\perp}r_L\frac{\vec{B}\times\nabla\vec{B}}{B^2}$$

Curvature Drift

$$\vec{v}_R = \frac{mv_{\parallel}^2}{qB^2}\frac{\vec{R}_c\times\vec{B}}{R_c^2}$$

Curved Vacuum Field

$$\vec{v}_R + \vec{v}_{\nabla\vec{B}} = \frac{m}{qB^2}\frac{\vec{R}_c\times\vec{B}}{R_c^2}\left(v_{\parallel}^2 + \frac{1}{2}v_{\perp}^2\right)$$

Polarization Field

$$v_p = \pm\frac{1}{\omega_c B}\frac{d\vec{E}}{dt}$$

3.1.1.6. Plasma as a Fluid

As we said at the beginning of this chapter plasma, depending on the density, sometimes behave as a fluid. However, plasma is always subjected to the Electromagnetic Laws that are represented by the Maxwell Equations, that are:

$$In\ vacuum\text{:}\begin{cases}\varepsilon_0\nabla\cdot\vec{E} = \rho\\ \nabla\times\vec{E} = -\dfrac{\partial\vec{B}}{\partial t}\\ \nabla\cdot\vec{B} = 0\\ \nabla\times\vec{B} = \mu_0\left(\vec{j} + \varepsilon_0\dfrac{\partial\vec{E}}{\partial t}\right)\end{cases} \tag{3-125}$$

$$In\ a\ medium\text{:}\begin{cases}\nabla\cdot\vec{D} = \sigma\\ \nabla\times\vec{E} = -\dfrac{\partial\vec{B}}{\partial t}\\ \nabla\cdot\vec{B} = 0\\ \nabla\times\vec{H} = \vec{j} + \dfrac{\partial\vec{D}}{\partial t}\\ \vec{D} = \varepsilon\vec{E}\\ \vec{B} = \mu\vec{H}\end{cases} \tag{3-126}$$

where σ and $\vec{j}$ stands for the "free" charge and current densities. The "bound" charge and current densities arising from polarization and magnetization of the medium are included in the definition of $\vec{D}$ and $\vec{H}$ with the constants ε and μ.
So, starting from the equation of the motion of a single particle:

$$m\frac{d\vec{v}}{dt} = q\left(\vec{E} + \vec{v} \times \vec{B}\right) \tag{3-127}$$

If we now multiply it for the density n we get the ***Fluid Equation***:

$$mn\frac{d\vec{u}}{dt} = qn\left(\vec{E} + \vec{u} \times \vec{B}\right) \tag{3-128}$$

Now, since we know that given a certain function $\vec{G}(x,t)$ we have:

$$\frac{d\vec{G}}{dt} = \frac{\partial \vec{G}}{\partial t} + (\vec{u} \cdot \nabla)\vec{G} \tag{3-129}$$

Then, for $\vec{G} = \vec{u}$, we get:

$$mn\frac{\partial \vec{u}}{\partial t} + (\vec{u} \cdot \nabla)\vec{u} = qn\left(\vec{E} + \vec{u} \times \vec{B}\right) \tag{3-130}$$

that is the ***Equation of the Fluid with a Convective Derivative*** and where $\frac{\partial \vec{u}}{\partial t}$ is the time derivative in a fixed frame.
When thermal motions are taken into account, a pressure force must be added to the right-hand side of this last equation and, in case of an isotropic distribution of the fluid with a motion in the x direction, we have:

$$mn\frac{\partial \vec{u}}{\partial t} + (\vec{u} \cdot \nabla)\vec{u} = qn\left(\vec{E} + \vec{u} \times \vec{B}\right) - \nabla\vec{p} \tag{3-131}$$

Where $\vec{p}$ is the Stress tensor whose components $p_{i,j} = mn\overline{v_i v_j}$ specify both the direction of the motion and the component of momentum involved. In the general case we replace $-\nabla\vec{p}$ with $-\nabla \cdot \vec{P}$:

$$\vec{P} = \begin{bmatrix} p & 0 & 0 \\ 0 & p & 0 \\ 0 & 0 & p \end{bmatrix} = p \tag{3-132}$$

We previously noted that a plasma could have two temperatures $T_\perp$ and $T_\parallel$ in the presence of a Magnetic Field. In that case, we'll have two different pressures $p_\perp = nK_B T_\perp$ and $p_\parallel = nK_B T_\parallel$ so, the ***Stress Tensor*** will be:

$$\vec{P} = \begin{bmatrix} p_\perp & 0 & 0 \\ 0 & p_\perp & 0 \\ 0 & 0 & p_\parallel \end{bmatrix} \tag{3-133}$$

Where the coordinate of the third column is in the direction of $\vec{B}$.
In case of a neural gas, the charged fluid will exchange moment with it through collisions, so the momentum lost for collision will be proportional to the relative velocity $\vec{u} - \vec{u}_0$, where $\vec{u}_0$ is the velocity of the neutral fluid. Calling $\tau = Const.$ the mean free time between collisions, if we don't consider collisions between charged particles, we get:

$$mn\frac{\partial \vec{u}}{\partial t} + (\vec{u}\cdot\nabla)\vec{u} = qn\left(\vec{E} + \vec{u}\times\vec{B}\right) - \nabla\cdot\vec{P} - \frac{mn(\vec{u}-\vec{u}_0)}{\tau} \tag{3-134}$$

This equation is the same of the ***Navier-Stokes Equation***:

$$\rho\left[\frac{\partial \vec{u}}{\partial t} + (\vec{u}\cdot\nabla)\vec{u}\right] = -\nabla\vec{p} + \rho\nu\nabla^2\vec{u} \tag{3-135}$$

except for the absence of electromagnetic forces and collisions between species. $\nu$is the ***Kinematic Viscosity Coefficient*** and the term $\rho\nu\nabla^2\vec{u}$ is just the collisional part $\nabla\cdot\vec{P} - \nabla\vec{p}$ in the absence of Magnetic Field. The former was derived without any explicit statement of the collision rate, while the latter describes a fluid where there are frequent collisions between particles. So, this last equation can be used to describe a plasma species, because, anyway, in the first equation we assumed implicitly the presence of collisions speaking about Maxwellian Distribution.
In general we have that, for motions perpendicular to $\vec{B}$ the ***Fluid Theory*** is a good approximation, so the two main equations are the ***Continuity Equation***:

$$\frac{\partial n}{\partial t} + \nabla\cdot(n\vec{u}) = 0 \tag{3-136}$$

And the ***State Equation***:

$$p = Cn^\gamma \tag{3-137}$$

with C a constant and defining γ as ***Ratio of Specific Heats***:

$$\gamma = \frac{c_p}{c_v} \tag{3-138}$$

$$\Longrightarrow \frac{\nabla p}{p} = \gamma \frac{\nabla n}{n} \tag{3-139}$$

For ***Isothermal Compression*** we then have:

$$\nabla p = \nabla(nK_B T) = K_B T \nabla n \tag{3-140}$$

where we obviously assumed $\gamma = 1$.
If we now consider, for simplicity, a plasma with only two species- ions and electrons- the charge and current densities will be given by:

$$\begin{cases} \sigma = n_i q_i + n_e q_e \\ \vec{J} = n_i q_i \vec{v}_i + n_e q_e \vec{v}_e \end{cases} \tag{3-141}$$

And, ignoring both the collisions and the viscosity (the Stress Tensor $\vec{P}$ coincides with Scalar Pressure p) the ***Complete Set of Fluid Equations*** will become:

$$\begin{cases} \varepsilon_0 \nabla \cdot \vec{E} = n_i q_i + n_e q_e \\ \nabla \times \vec{E} = -\dfrac{\partial \vec{B}}{\partial t} \\ \nabla \cdot \vec{B} = 0 \\ {\mu_0}^{-1} \nabla \times \vec{B} = n_i q_i \vec{v}_i + n_e q_e \vec{v}_e + \varepsilon_0 \dfrac{\partial \vec{E}}{\partial t} \\ m_j n_j \dfrac{\partial \vec{v}_j}{\partial t} + (\vec{v}_j \cdot \nabla)\vec{v}_j = q_j n_j (\vec{E} + \vec{v}_j \times \vec{B}) - \nabla p_j \qquad j = i, e \\ \dfrac{\partial n_j}{\partial t} + \nabla \cdot (n_j \vec{v}_j) = 0 \qquad j = i, e \\ p_j = C_j {n_j}^{\gamma_j} \qquad j = i, e \end{cases} \tag{3-142}$$

This group of equations is characterized by 16 independent equations in the 16 unknowns $n_i, n_e, p_i, p_e, \vec{v}_i, \vec{v}_e, \vec{E}$ and $\vec{B}$. It seems we have 18 scalar equations if we count each vector equation as three

scalar equations, however two of Maxwell's Equations are superfluous, since they can be recovered from the Divergence Equations.

3.1.1.7. Kinetic Theory

The fluid theory we've used until now is the simplest description of a plasma and fortunately it can be applied to the majority of the plasma phenomena. In this theory we neglect the collisions and we the velocity distribution is assumed to be Maxwellian everywhere and can therefore be specified by only one number: the temperature T. That's why in this case there are just four independent variables: x, y, z and t.
However, there are some phenomena, where collisions have an important role, for which this theory is inadequate. For these, we need to consider the velocity distribution $f(\vec{v})$ of each species. This treatment is called Kinetic Theory.
In this case we have seven independent variables: x, y, z, v_x, v_y, v_z and t.

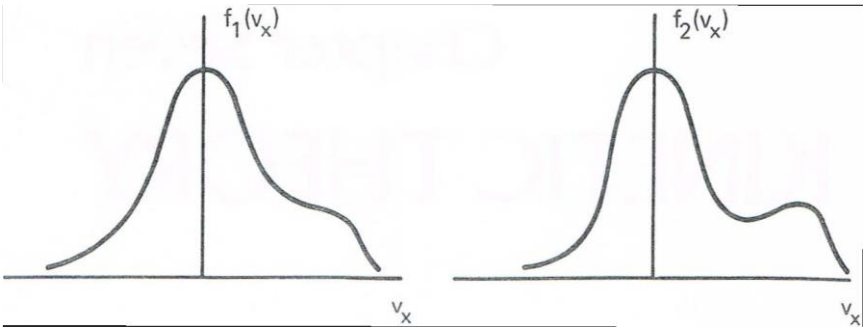

Figure 3-15: Velocity distribution of two different species

The Plasma Approximation

The procedure used to study a plasma is the following: $\vec{E}$ is calculated through the motion equations and, then, the Poisson Equation is used to calculate σ. The reason is that the plasma use to remain neutral so the Electric Field $\vec{E}$, as we saw, will adapt to preserve its neutrality. The charge distribution will adjust automatically to satisfy the Poisson Equation (but only at enough low frequencies), so we can assume $n_i = n_e$ and $\nabla \cdot \vec{E} \neq 0$ at the same time.
Hence, on time scales long enough, to let electrons and ions move we can replace the Poisson Equation with the quasi-neutrality condition- $n_i = n_e$. This is called "***Plasma Approximation***" and it's valid just for low frequency applications. For High Frequency Electronic Waves this is not suitable and $\vec{E}$ must be determined with the Maxwell's Equations.

Equations of Kinetic Theory

Now, given a multi-particle system, we can introduce the ***Distribution Function*** $f_\alpha(\vec{r}, \vec{v}, t)$ for a species α defined as:

$$f_\alpha(\vec{r},\vec{v},t)d\vec{r}d\vec{v} = dN(\vec{r},\vec{v},t) \quad (3\text{-}143)$$

Is the number of particles in the volume element $dV = d\vec{r}d\vec{v}$ in the phase space, with $d\vec{r} = dxdydz$ very little, but big enough to contain a statistically significant number of particles and $d\vec{v} = v_x v_y v_z$.
This property let us approximate the function $f_\alpha(\vec{r},\vec{v},t)$ with a continuous function.
This function will change both for the effect of the flux of particles through the element $d\vec{r}d\vec{v}$ and the collisional effect.
The flux of particles through the area S that delimits the volume element ΔV and the flux of particles generated by the collisions should be equal the time rate of the density variation of the particles in the phase space. To evaluate this flux we use the ***Divergence Theorem***:

$$\int P \cdot dS = \int \nabla \cdot P dV \quad (3\text{-}144)$$

If we define with $\vec{V} = (\vec{v},\vec{a})$ the generalized vector of the equations in the six-dimensional space $(\vec{r},\vec{v})$, we can write the Entering Flux as:

$$-\int dS \cdot [\vec{V}_f] \quad (3\text{-}145)$$

That, for the Divergence Theorem becomes:

$$-\int d\vec{r}d\vec{v} \cdot [\nabla_r \cdot (\vec{v}f) + \nabla_v \cdot (\vec{r}f)] \quad (3\text{-}146)$$

so, at the end, we'll get:

$$\frac{\partial f}{\partial t} = -\nabla_r \cdot (\vec{v}f) - \nabla_v \cdot (\vec{r}f) + \left(\frac{\partial f}{\partial t}\right)_{collisions} \quad (3\text{-}147)$$

The acceleration is always:

$$\vec{a} = \frac{\vec{F}}{m} = \frac{q\left(\vec{E} + \vec{v} \times \vec{B}\right)}{m} \quad (3\text{-}148)$$

So, simplifying and considering that $\vec{r}$ and $\vec{v}$ are independent we'll finally get the ***Boltzmann Equation***:

$$\frac{\partial f}{\partial t} + \vec{v}\nabla_r(f) + \frac{q\left(\vec{E} + \vec{v} \times \vec{B}\right)}{m}\nabla_v(f) = \left(\frac{\partial f}{\partial t}\right)_{collisions} \tag{3-149}$$

where $\frac{\partial f}{\partial t}$ is the total derivative of the Distribution Function $\frac{df}{dt}$ that, in the absence of collisions says that the Convective Derivative $\frac{df}{dt}$ is equal to zero: in this last case the equation is called "***Vlasov Equation***".
Now, considering just the electrons that are more mobile than the ions, at the equilibrium $\frac{\partial}{\partial t} = 0$ and with $\vec{B} = 0$ the Boltzmann Equation becomes:

$$\vec{v}\nabla_r f_e - \frac{e}{m}\vec{E} \cdot \nabla_v f_e = 0 \tag{3-150}$$

At the thermal equilibrium, the distribution of the electrons is different from the Maxwellian one f_M just for a factor connected to the Electric Potential ϕ:

$$f_e = f_M \mathbf{e}^{\frac{e\phi}{K_B T}} \tag{3-151}$$

where, as usual, **e** represents the exponential base and e the charge of the electron.
Integrating respect to $\vec{v}$ we get:

$$n_e = n_{e,0}\mathbf{e}^{\frac{e\phi}{K_B T}} \tag{3-152}$$

We call this last equation "***Boltzmann Relation***", and with that we admit that electrons, that are more mobile and get into thermal equilibrium more easily, can be represented by this distribution.
This is a big advantage especially in the PIC (Particle In Cell) system, solving in this way the problem of the low λ_D. However, in this case, the Poisson Equation becomes non-linear.

As we saw, the presence of a Magnetic Field tend to confine the plasma so, for the particles that leave the system, there should be a detachment from the lines of force. This happens when the ***Kinetic Pressure***- $P_k = P_e + P_i$- is stronger than the ***Magnetic Pressure***- P_m, where P_m and P_e- that is the ***Electron Pressure***- value:

$$P_m = \frac{B^2}{2\mu_0} \tag{3-153}$$

$$P_e = n_e K_B T_e \tag{3-154}$$

To compute P_i instead, assume that the p_{zz} term of the Stress Tensor is the dominant one: this can be considered true if we assume $B \to 0$ so, if μ in a constant, we'll get $v_\perp \to 0$ and the ***Ion Pressure***- P_i- will be:

$$\Longrightarrow P_i \cong n_i m_i \langle v_z^2 \rangle \tag{3-155}$$

The ***collisionality*** of the plasma tends to make the Distribution Function Maxwellian- f_M- as he following equation sais:

$$f(t) = f_M + [f(0) - f_M]\mathbf{e}^{\left(-\frac{1}{\tau}\right)} \tag{3-156}$$

To quantify it we define the ***Krook Collision Term***:

$$\left(\frac{\partial f}{\partial t}\right)_c = \frac{f - f_M}{\tau} \tag{3-157}$$

or, more in general, we use an equation called "***Fokker-Plank Equation***" that summarize the concept of Collisionality of a plasma:

$$\frac{df}{dt} = -\frac{\partial}{\partial v} \cdot (f\langle \Delta v \rangle)\frac{1}{2}\frac{\partial^2}{\partial v \partial v} : (f\langle \Delta v \Delta v \rangle) \tag{3-158}$$

3.1.1.8. Diffusion and Mobility in Weakly Ionized Gases

Any realistic plasma will have a density gradient and the plasma will tend to diffuse toward regions of low density. In this paragraph we'll analyze the problem of the diffusion of the plasma in absence of Magnetic Field and then, in the next paragraph, we'll complete the description speaking about Plasma Diffusion in presence of a Magnetic Field, introducing the MHD Equations.

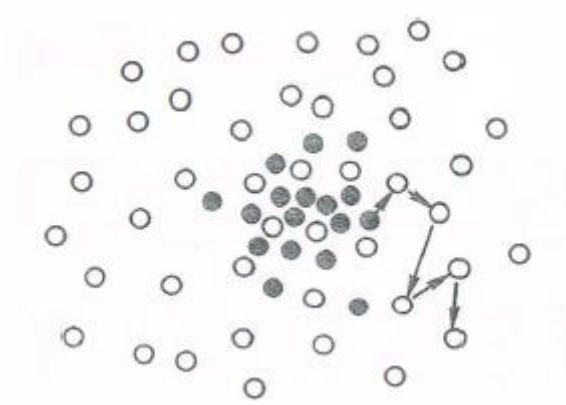

Figure 3-16: Representation of particle distribution in a plasma

Collision Parameters

The ***Mean Free Path*** is an index of the probability a collisional event to happen. Consider a gas volume with a density n_n, with cross area A and volume Adx: the cross area of the atoms will be $n_n Adx\sigma$, where σ is the atom section.

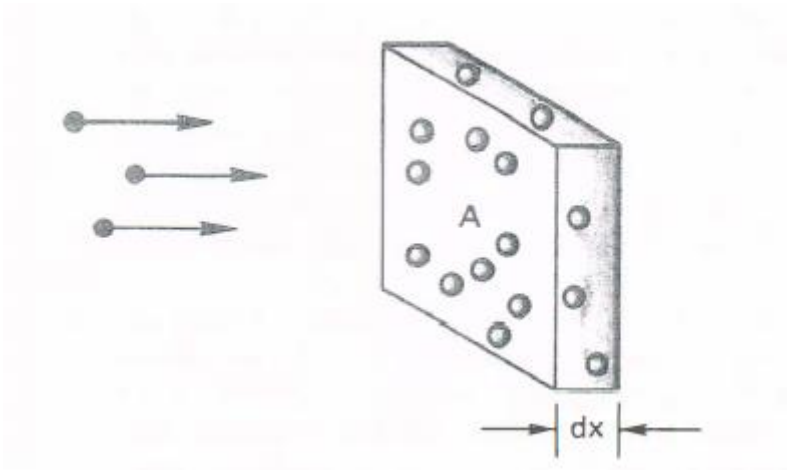

Figure 3-17: Gas control volume of density n_n,

Thus, the fraction of particles connected to a collision will be $\frac{n_n Adx\sigma}{A}$ and the exiting flux from a region with density n_n will be $\Gamma' = \Gamma(1 - n_n\sigma dx)$, so:

$$\frac{d\Gamma}{dx} = -n_n\sigma\Gamma \tag{3-159}$$

$$\Rightarrow \Gamma = \Gamma_0 \mathbf{e}^{\left(-\frac{x}{\lambda_{mpf}}\right)} \tag{3-160}$$

Having defined:

$$\lambda_{mpf} = \frac{1}{n_n \sigma} \tag{3-161}$$

Hence, the time between two collisions will be:

$$\tau = \frac{\lambda_{mpf}}{\nu} \tag{3-162}$$

and so, the Collision Frequency will be:

$$\nu = n_n \sigma v \tag{3-163}$$

In a real plasma the diffusion processes (collisions) tend to attenuate the pressure gradients if we consider a stationary process $\frac{\partial}{\partial t} = 0$ and we neglect $\vec{v} \cdot \nabla \vec{v}$. So, the equilibrium of the forces, without Magnetic Field, will be:

$$mn \frac{d\vec{v}}{dt} = mn \left[\frac{\partial \vec{v}}{\partial t} + (\vec{v} \cdot \nabla)\vec{v} \right] = \pm en\vec{E} - \nabla \vec{p} - mn\nu\vec{v} \tag{3-164}$$

$$\Longrightarrow \vec{v} = \pm \left(\frac{e}{m\nu} \right) \vec{E} - \left(\frac{K_B T}{m\nu} \right) \frac{\nabla n}{n} = \pm \mu_D \vec{E} - D \frac{\nabla n}{n} \tag{3-165}$$

being μ_D the ***Mobility Coefficient*** and D the ***Diffusion Coefficient*** (whose value is higher for the electrons). The definition of flux derives from the Diffusion one:

$$\Gamma_j = n\vec{v}_j = \pm \mu_j n\vec{E} - D_j \nabla n \tag{3-166}$$

and, if the field is zero, the diffusion is simply the classic one described by the ***Fick's Low***:

$$\Gamma = -D\nabla n \tag{3-167}$$

while, if the density is uniform $\nabla n = 0$, we get:

$$\begin{cases} \Gamma_e = n\vec{v}_e = -\mu_e n\vec{E} \\ \Gamma_i = n\vec{v}_i = \mu_i n\vec{E} \end{cases} \tag{3-168}$$

$$\Longrightarrow \vec{j} = n_i q_e \vec{v}_e + n_e q_e \vec{v}_e = e(\Gamma_i - \Gamma_e) = ne(\mu_i - \mu_e)\vec{E} \tag{3-169}$$

Decay of a Plasma by Diffusion

Consider now a plasma created in a container that decays by diffusion to the walls. Electrons and ions will reach the wall and recombine there, so the density near wall will be essentially zero. The fluid equations of motion and continuity govern the plasma behavior but if the decay is slow and the collision frequency ν is large, the time derivative in equation of motion will be negligible, getting:

$$\frac{\partial n}{\partial t} + \nabla \cdot (n\vec{v}) = 0 \tag{3-170}$$

$$\Longrightarrow \frac{\partial n}{\partial t} + \nabla \cdot \Gamma_j = 0 \tag{3-171}$$

Now, if it was $\Gamma_i \neq \Gamma_e$, we would have a serious charge imbalance: if electrons, that are faster than ions, leave the plasma, it will be created a polarity as to retard them and to accelerate ions to the equilibrium. So, by setting $\Gamma_i = \Gamma_e = \Gamma$ we'll get:

$$\Gamma = \mu_i n\vec{E} - D_i \nabla n = -\left(-\mu_e n\vec{E}\right) - D_e \nabla n \tag{3-172}$$

$$\Longrightarrow \vec{E} = \frac{D_i - D_e}{\mu_i + \mu_e}\frac{\nabla n}{n} \tag{3-173}$$

And the common flux will be:

$$\Gamma = \mu_i \frac{D_i - D_e}{\mu_i + \mu_e} \nabla n - D_i \nabla n = -\frac{\mu_i D_e + \mu_e D_i}{\mu_i + \mu_e} \nabla n \tag{3-174}$$

where we found a new coefficient called "***Ambipolar Diffusion Coefficient***":

$$D_a = \frac{\mu_i D_e + \mu_e D_i}{\mu_i + \mu_e} \tag{3-175}$$

So, if this coefficient is constant we'll have:

$$\frac{\partial n}{\partial t} = D_a \nabla^2 n \tag{3-176}$$

To compute the magnitude of D_a consider $\mu_e \gg \mu_i$, thus:

$$D_a = D_i + \frac{\mu_i}{\mu_e} D_e \propto D_i + \frac{T_i}{T_e} D_i \tag{3-177}$$

So, if $T_i = T_e \Longrightarrow D_a \cong 2D_i$.
Hence, the effect of the ambipolar electric field is to enhance the diffusion of ions by a factor of two, but the diffusion rate of the two species together is primarily controlled by the slower species.

If we now integrate the Diffusion Equation we can get the Spatial and Time Behavior of the Ambipolar Diffusion. Using the method of the separation of variables we can write:

$$n(\vec{r}, t) = T(t) S(\vec{r}) \tag{3-178}$$

$$S \frac{dT}{dt} = D_a T \nabla^2 S \tag{3-179}$$

and, after some passages, we can get the general solution:

$$T = T_0 e^{\left(-\frac{1}{\tau}\right)} \tag{3-180}$$

$$S = A\cos\left(\frac{x}{\sqrt{D_a\tau}}\right) + B\sin\left(\frac{x}{\sqrt{D_a\tau}}\right) \qquad (3\text{-}181)$$

In case of a plasma between two flat plates and we neglect the term on sine for symmetry, setting $x = \pm L$ and $S = 0$ as boundary conditions, we'll have:

$$n = n_0 e^{\left(-\frac{1}{\tau}\right)}\cos\left(\frac{\pi x}{2L}\right) \qquad (3\text{-}182)$$

This is called the ***Lowest Diffusion Mode***. The density distribution is a cosine and the peak density decays exponentially with time. The time constant τ increases with L and varies inversely with D.

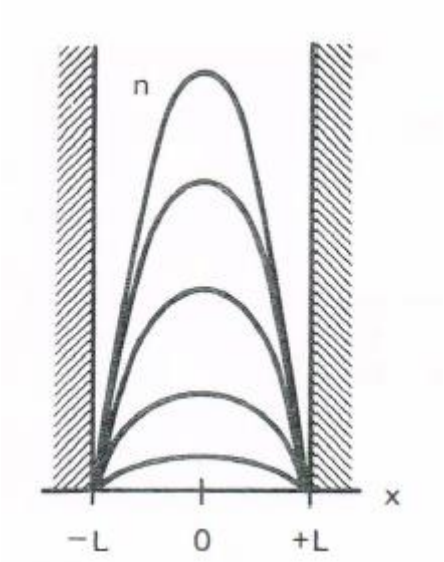

Figure 3-18: Density distribution of the plasma between two flat plates

There are, of course, higher diffusion modes with more than one peak, but we won't enter in detail of these cases.

Steady State Solutions

In many experiments, a plasma is maintained in a ***Steady State*** by continuous ionization of plasma to offset the losses. To calculate the density profile, in this case, we must add a source term to the equation of continuity:

$$\frac{\partial n}{\partial t} - D\nabla^2 n = Q(\vec{r}) \qquad (3\text{-}183)$$

When Q is positive, it represents a source and contributes to positive $\frac{\partial n}{\partial t}$. In steady state, we set $\frac{\partial n}{\partial t} = 0$ and what remains is a Poisson-type equation for $n(\vec{r})$.
If the ionization is produced by energetic electrons in the tail of the Maxwellian Distribution, like in many weakly ionized gases, then Q is proportional to the electron density n. Setting $Q = Zn$, where Z is the ***Ionization Function***, we get:

$$\nabla^2 n = -\left(\frac{Z}{D}\right) n \tag{3-184}$$

Consequently, in this particular case the density remains constant. The plasma is maintained against diffusion losses thanks to a heat source that keeps the electron temperature at its constant value and thanks of a small influx of neutral atoms that replenish those that are ionized.

Now consider a slab geometry where the source is localized on the plane $x = 0$, like a slit-collimated beam of ultraviolet light. This is called "***Plane Source***". The new steady state diffusion equation is then:

$$\frac{d^2 n}{dx^2} = -\frac{Q}{D}\delta(0) \tag{3-185}$$

Except at $x = 0$ the density should satisfy the equation:

$$\frac{d^2 n}{dx^2} = 0 \tag{3-186}$$

So, the solution will be:

$$n = n_0\left(1 - \frac{|x|}{L}\right) \tag{3-187}$$

In this case, the plasma has a linear profile.

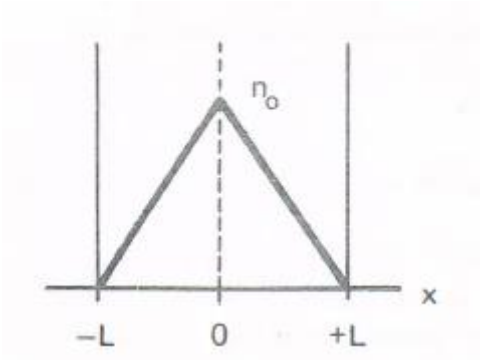

Figure 3-19: Linear profile of the plasma density for a steady state solution

Finally, let's consider a cylindrical plasma with a source located on the axis, like a beam of energetic electrons producing ionization along the axis. This is called "***Line Source***". Except at $r = 0$, the density should satisfy the following equation:

$$\frac{1}{r}\frac{\partial}{\partial r}\left(r\frac{\partial n}{\partial r}\right) = 0 \tag{3-188}$$

So, the solution that vanishes at $r = a$ will be:

$$n = n_0 \ln\left(\frac{a}{r}\right) \tag{3-189}$$

The density becomes infinite at $r = 0$.

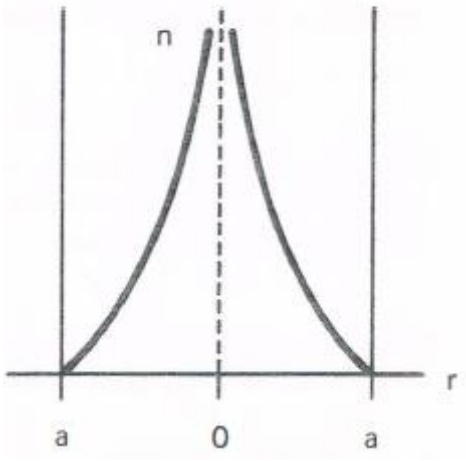

Figure 3-20: Density distribution of a cylindrical plasma with a source located on the axis

Recombination

When an ion and an electron collide, they have a finite probability of recombining into a neutral atom. To conserve momentum, a third body must be present. If the third body is an emitted photon, the process is called "***Radiative Recombination***", while if it is a particle the process is called "***Three-Body Recombination***". The loss of plasma by recombination can be represented by a negative source term in the equation of continuity that is proportional to $n_i n_e = n^2$. In absence of diffusion terms, we can re-write the equation of continuity as:

$$\frac{\partial n}{\partial t} = -\alpha n^2 \qquad \text{(3-190)}$$

where α is called "Recombination Coefficient and has unit of $[m^3/s]$.
This is a non-linear equation for n, so we cannot use the solutions superposition method to solve it.
Anyway, the solution is given by:

$$\frac{1}{n(\vec{r},t)} = \frac{1}{n_0(\vec{r})} + \alpha t \qquad \text{(3-191)}$$

where $n_0(\vec{r})$ is the initial density distribution. After the density has fallen far below its initial value, it decays reciprocally with time:

$$n \propto \frac{1}{\alpha t} \qquad \text{(3-192)}$$

In the following figure we can see the results of measurements of the density decay in the afterglow of a weakly ionized H plasma. When the density is high the recombination is dominant while, after the density has reached a low value, it's the diffusion that becomes dominant.

P

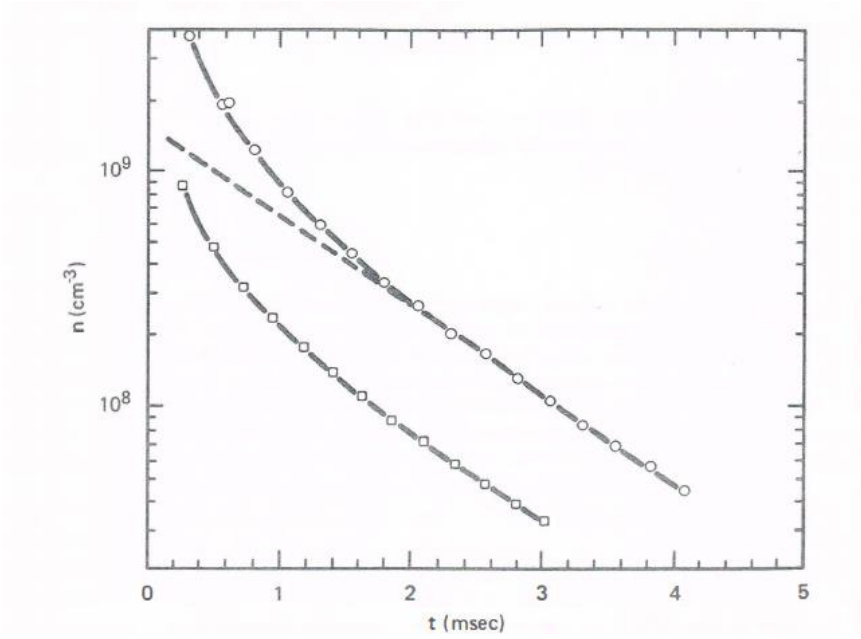

Figure 3-21: Results of the measurements of the density decay in the afterglow of a weakly ionized H plasma

Diffusion Across a Magnetic Field

The rate of plasma lost by diffusion can be decreased by a Magnetic Field. Considering always a weakly ionized plasma in a Magnetic Field, charged particles will move along $\vec{B}$ by diffusion and mobility since $\vec{B}$ does not affect the motion in parallel direction. So, we'll have for each species:

$$\Gamma_z \pm \mu n E_z - D\frac{\partial n}{\partial z} \tag{3-193}$$

If there were no collisions, particles would not diffuse in the perpendicular direction but they would continue to gyrate about the same-line force, while in presence of collisions particles migrate across $\vec{B}$ to the walls along the gradients. They do his by a random-walk process and so also the guiding centre will shift position. The particles will diffuse in the direction opposite to ∇n, the step length in the random walk is no longer λ_m, but has the magnitude of the Larmor Radius r_L.
Writing the perpendicular component of the fluid equation for each species and assuming that the plasma is isothermal and ν large enough for the $\frac{d\vec{v}_\perp}{dt}$ to be negligible:

$$mn\frac{d\vec{v}_\perp}{dt} = \pm en\left(\vec{E} + \vec{v}_\perp \times \vec{B}\right) - K_B T\nabla n - mn\nu\vec{v} = 0 \tag{3-194}$$

Where the x and y components are:

$$\begin{cases} mnvv_x = \pm enE_x - K_B T\dfrac{\partial n}{\partial x} \pm env_y B \\ mnvv_y = \pm enE_y - K_B T\dfrac{\partial n}{\partial y} \mp env_x B \end{cases} \tag{3-195}$$

Now, using the definition of μ and D we get:

$$\begin{cases} v_x = \pm\mu E_x - \dfrac{D}{n}\dfrac{\partial n}{\partial x} \pm \dfrac{\omega_c}{\nu} v_y \\ v_y = \pm\mu E_y - \dfrac{D}{n}\dfrac{\partial n}{\partial y} \mp \dfrac{\omega_c}{\nu} v_x \end{cases} \tag{3-196}$$

And substituting them for v_x we can solve for v_y first and then for v_x:

$$\begin{cases} v_y(1+\omega_c^2\tau^2) = \pm\mu E_y - \dfrac{D}{n}\dfrac{\partial n}{\partial y} - \omega_c^2\tau^2\dfrac{E_x}{B} \pm \omega_c^2\tau^2\dfrac{K_B T}{eB}\dfrac{1}{n}\dfrac{\partial n}{\partial x} \\ v_x(1+\omega_c^2\tau^2) = \pm\mu E_x - \dfrac{D}{n}\dfrac{\partial n}{\partial x} - \omega_c^2\tau^2\dfrac{E_y}{B} \mp \omega_c^2\tau^2\dfrac{K_B T}{eB}\dfrac{1}{n}\dfrac{\partial n}{\partial y} \end{cases} \tag{3-197}$$

where we can identify the $\vec{\boldsymbol{E}} \times \vec{\boldsymbol{B}}$ ***Diamagnetic Drifts***:

$$v_{E_x} = \frac{E_y}{B} \tag{3-198}$$

$$v_{E_y} = -\frac{E_x}{B} \tag{3-199}$$

$$v_{D_x} = \mp\frac{K_B T}{eB}\frac{1}{n}\frac{\partial n}{\partial y} \tag{3-200}$$

$$v_{D_y} = \pm\omega_c^2\tau^2\frac{K_B T}{eB}\frac{1}{n}\frac{\partial n}{\partial x} \tag{3-201}$$

and defining the ***Perpendicular Mobility and Diffusion Coefficients***:

$$\mu_\perp = \frac{\mu}{1 + \omega_c^2 \tau^2} \tag{3-202}$$

$$D_\perp = \frac{D}{1 + \omega_c^2 \tau^2} \tag{3-203}$$

we finally get:

$$\vec{v}_\perp = \pm \mu_\perp \vec{E} - D_\perp \frac{\nabla n}{n} + \frac{\vec{v}_E + \vec{v}_D}{1 + \left(\frac{\nu^2}{\omega_c^2}\right)} \tag{3-204}$$

So, the perpendicular velocity of either species is composed by two parts: one perpendicular to the gradients potential and density (the $\vec{v}_E + \vec{v}_D$ drift) and the one parallel to the gradients in potential and density.
The product $\omega_c \tau$ is an important quantity in magnetic confinement: when $\omega_c^2 \tau^2 \ll 1$ he Magnetic Field has little effect on diffusion while when $\omega_c^2 \tau^2 \gg 1$ the Magnetic Field significantly retards the rate of diffusion across $\vec{B}$.
Then we can see that the role of the collision frequency ν changed: in diffusion parallel to $\vec{B}$, D is proportional to ν^{-1}, since collisions retard the motion, while in diffusion perpendicular to $\vec{B}$, $D_\perp$ is proportional to ν, since collisions are needed for the cross-field migration.
The same consideration can be made for the role of m because $\nu \propto \frac{1}{\sqrt{m}}$, so we can see that $D \propto \frac{1}{\sqrt{m}}$ and $D_\perp \propto \sqrt{m}$.
Finally, we can conclude saying that in parallel diffusion electrons move faster than ions because of their higher thermal velocity, while in perpendicular diffusion electron escape more slowly because of their smaller Larmor radius.

Since the Diffusion and Mobility Coefficients are anisotropic in the presence of a magnetic field, the problem of the Ambipolar Diffusion is not intuitive as in the case with $\vec{B} = 0$.
Anyway, in general, the problem requires to solve simultaneously the equation of continuity for ions and electrons: in this case it's not the fluxes Γ_j, but the divergences of the flux that should match, so:

$$\nabla \cdot \Gamma_j = \nabla \cdot \Gamma_i = \nabla \cdot \Gamma_e \tag{3-205}$$

with:

$$\begin{cases} \nabla \cdot \Gamma_i = \nabla_\perp \cdot \left(\mu_{i,\perp} n \vec{E}_\perp - D_{i,\perp} \nabla n\right) + \dfrac{\partial}{\partial z}\left(\mu_i n E_z - D_i \dfrac{\partial n}{\partial z}\right) \\ \nabla \cdot \Gamma_e = \nabla_\perp \cdot \left(-\mu_{e,\perp} n \vec{E}_\perp - D_{e,\perp} \nabla n\right) + \dfrac{\partial}{\partial z}\left(-\mu_e n E_z - D_e \dfrac{\partial n}{\partial z}\right) \end{cases} \quad (3\text{-}206)$$

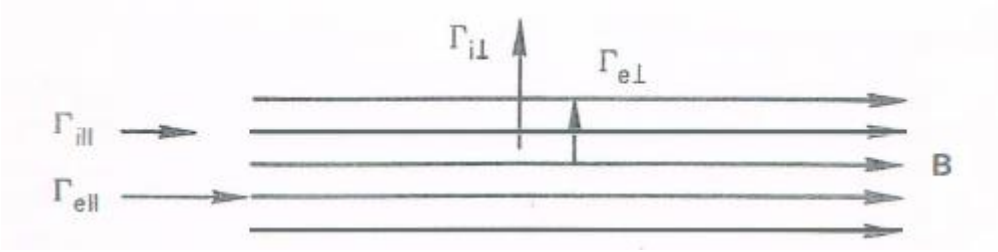

Figure 3-22: Representation of the fluxes components for the Ambipolar Diffusion

3.1.1.9. Fully Ionized Plasma

When the plasma is composed of ions and electrons alone, all collisions are ***Coulomb Collisions*** between charged particles. However, there's a big difference between collisions between like particles (ion-ion or electron-electron collisions) and unlike particles (ion-electron collisions).
If we consider a head-on collision between two identical particles, the particles will emerge with their velocity reversed: they simply interchange their orbits and the two guiding centers remain in the same places.
The worst that can happen is a $90°$collision in which the velocities will be changed $90°$ in direction and the guiding centers will be shifted but the "center of mass" of the two guiding centers remains stationary.
So, ***collisions between like particles give rise to very little diffusion***.

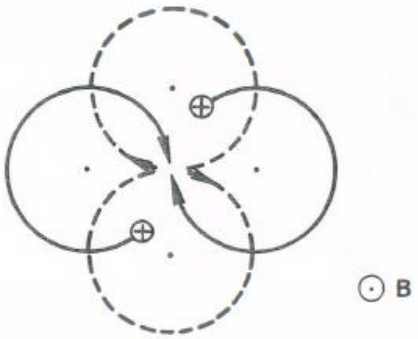

Figure 3-23: Representation of a head-on collision between two identical particles

Instead, when two particles of opposite charge collide the situation is totally different. The worst case is the $180°$ collision in which the particles emerge with their velocities reversed. Since they must continue to gyrate about the lines of force in the proper sense both guiding centers will move in the same direction. So, ***unlike particle collision give rise to diffusion***.

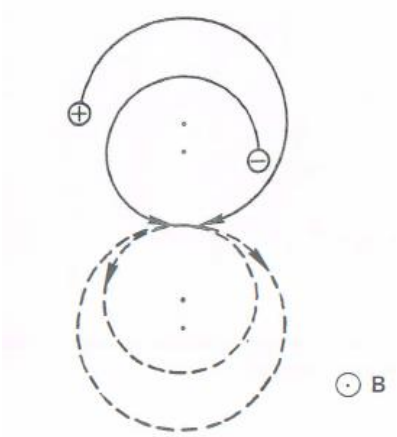

Figure 3-24: Representation of a head-on collision between two particles with opposite charge

Plasma Resistivity

The fluid equations of motion may be written as follows:

$$\begin{cases} m_i n \dfrac{d\vec{v}_i}{dt} = en\left(\vec{E} + \vec{v}_i \times \vec{B}\right) - \nabla p_i - \nabla \cdot \vec{\pi}_i + P_{i,e} \\ m_e n \dfrac{d\vec{v}_e}{dt} = en\left(\vec{E} + \vec{v}_e \times \vec{B}\right) - \nabla p_e - \nabla \cdot \vec{\pi}_e + P_{e,i} \end{cases} \tag{3-207}$$

where $P_{i,e}$ and $P_{e,i}$ represents, respectively, the momentum gain of the ion fluid caused by collisions with electrons, and vice versa, and $\vec{\pi}_i$ and $\vec{\pi}_e$ represents the stress tensor.
Since the collision don't give rise to much diffusion we can neglect the terms $\nabla \cdot \vec{\pi}_j$ and, because of the conservation of momentum, we have:

$$P_{i,e} = -P_{e,i} \tag{3-208}$$

with:

$$P_{e,i} = mn(\vec{v}_i - \vec{v}_e)\nu_{ei} = \eta e^2 n^2 (\vec{v}_i - \vec{v}_e) \tag{3-209}$$

where η is a constant of proportionality and is called "***Specific Resistivity***". Thus, we get:

$$\nu_{ei} = \frac{ne^2}{m}\eta \tag{3-210}$$

Now, just to understand the meaning of η suppose a plasma in an Electric Field- $\vec{E}$- and that the current that it derives is all carried by the electrons (which are more mobile than the ions). Supposing $\vec{B} = 0$ and $K_B T_e = 0$ so that $\nabla \cdot P_e = 0$, than in steady state the equation we wrote above reduces to:

$$en\vec{E} = P_{e,i} \tag{3-211}$$

And, since $\vec{j} = en(\vec{v}_i - \vec{v}_e)$, we get:

$$P_{e,i} = \eta en\vec{j} \tag{3-212}$$

$$\Longrightarrow \vec{E} = \eta\vec{j} \tag{3-213}$$

that is a simply Ohm's law and η represents just the Specific Resistivity.
Again, to understand it better, think of a medium where we have an Electric Field- $\vec{E}$. Just using the well known Ohm's Law, we get:

$$\vec{E} = \frac{V}{L} = \frac{R\vec{\imath}}{L} \tag{3-214}$$

$$R = \eta\frac{L}{A} \tag{3-215}$$

$$\Longrightarrow \vec{E} = \frac{\eta\vec{\imath}}{A} = \eta\vec{j} \tag{3-216}$$

Now, considering again that the electron mobility is higher than those of the ions, in a mono-dimensional case we can write:

$$\vec{j} = \frac{ne^2}{m_e\nu}\vec{E} \tag{3-217}$$

$$\Longrightarrow \eta = \frac{m_e \nu}{n e^2} \tag{3-218}$$

Some values of η are listed below:

Table 3-2: Values of the specific resistivity η for different materials

Element or Material	**Specific Resistivity**
Hydrogen-H	$\eta = 5 \times 10^{-7} [\Omega \times m]$
Copper- Cu	$\eta = 2 \times 10^{-8} [\Omega \times m]$
Stainless Steel	$\eta = 7 \times 10^{-7} [\Omega \times m]$
Mercury- Hg	$\eta = 10^{-6} [\Omega \times m]$

The value found for Hydrogen is often called the "***Spritzer Resistivity***" thanks to the scientist that first compute it.
Taking into account the complete formula:

$$\begin{cases} \eta_{\parallel} = 5.2 \times 10^{-5} \dfrac{Z \ln \Lambda}{T^{3/2}[eV]} \\ \eta_{\perp} = 2.0 \eta_{\parallel} \end{cases} \tag{3-219}$$

And counting it for $K_B T_e = 100\ eV$ we then get the value in the table.

THE SINGLE FLUID MHD MODEL

Now we can start with the analysis of diffusion in fully ionized plasma.
In the previous paragraph we derived the kinetic equations of a plasma, that describe the way the Distribution Function evolve in the phase space and, then, we reduced the number of variables of the equation from seven to four, using equations with physical and dynamic parameters (like particle density, momentum, kinetic energy, etc.) that describe the plasma as a mix of different fluids, composed by particles with different masses and charges, but all subjected to the same electromagnetic forces and that evolves in time and space respecting the conservation laws and that interact between each other and with other species through collisions.
Every species is described by the same set of equation that differs just for the different masses, charges and collision terms.

From now we'll describe the plasma as a single fluid with a mass density ρ and an electrical conductivity $1/\eta$. These are the equation of the ***Magneto-Hydro-Dynamics***- ***MHD Equations***.
In this model, the plasma evolves in space and time with a velocity $\vec{v}$:

$$\vec{v} = \frac{\sum_j n_j m_j \vec{u}_j}{\sum_j n_j m_j} \tag{3-220}$$

that represents the ***Average Macroscopic Velocity*** of the plasma.
Of course, this velocity has an appreciable meaning when the components of the plasma move in solidarity: if the motion of the components is much different its meaning is not so clear.
So, the ***MHD Model*** is particularly suitable for the overall motion of the plasma, in particular in situation of macroscopic equilibrium and not in case of a phenomena where we need to analyze the relative motion between electron and ions or the motion of one particular species; in these last cases we should come back to the ***Double-Fluid Model***.

So, let's start with the description of the ***MHD Model***.

3.1.1.10. The MHD Equations

The following equation will be calculated supposing that the transport coefficients (like resistivity, viscosity and thermal conductivity) are simple scalar and are constant. Even if it's not always true, it's not a strange hypothesis if the collision frequency is high: in that case the plasma is maintained in condition of isotropy.
We can start from the ***Continuity Equation***:

$$\frac{\partial n_j}{\partial t} + \nabla \cdot \left(n_j \vec{u}_j\right) = 0 \tag{3-221}$$

This, multiplied for m and added over all the particles species, leads to:

$$\frac{\partial \rho}{\partial t} + \nabla \cdot (\rho \vec{v}) = 0 \tag{3-222}$$

where the ***Total Mass Density*** of the plasma ρ is given by:

$$\rho = \sum_j n_j m_j \tag{3-223}$$

Then, to get the ***Equation of the Motion*** we must add the Electromagnetic Forces to the Navier-Stokes Equation, that in absence of charge separation are reduced just to the Hall Force $\vec{j} \times \vec{B}$, so we have:

$$\frac{\partial \vec{v}}{\partial t} + (\vec{v} \cdot \nabla)\vec{v} = \vec{f} - \frac{1}{\rho}\nabla p + \frac{1}{\rho c}\vec{j} \times \vec{B} + \nu \nabla^2 \vec{v} \qquad (3\text{-}224)$$

We can now express the current $\vec{j}$ through the Maxwell Equations:

$$\nabla \times \vec{B} = \frac{4\pi}{c}\vec{j} + \frac{1}{c}\frac{\partial \vec{E}}{\partial t} \qquad (3\text{-}225)$$

Now, neglecting the processes that happen in very short times and with typical velocities $v \ll c$, so $\left|\frac{E}{B}\right| \sim \frac{v}{c} \ll 1$, we have:

$$\left|\frac{1}{c}\frac{\partial \vec{E}}{\partial t}\right| : \left|\nabla \times \vec{B}\right| \sim \frac{\frac{E}{ct}}{\frac{B}{L}} \sim \frac{v}{c}\frac{E}{B} \sim \left(\frac{v}{c}\right)^2 \qquad (3\text{-}226)$$

So, we can neglect the diffusion current and get:

$$\vec{j} = \frac{c}{4\pi}\nabla \times \vec{B} \qquad (3\text{-}227)$$

That leads us to write the Equation of the Motion just with the Magnetic Field:

$$\frac{\partial \vec{v}}{\partial t} + (\vec{v} \cdot \nabla)\vec{v} = \vec{f} - \frac{1}{\rho}\nabla p + \frac{1}{4\pi\rho}\left(\nabla \times \vec{B}\right) \times \vec{B} + \nu \nabla^2 \vec{v} \qquad (3\text{-}228)$$

Then, knowing that:

$$\left(\nabla \times \vec{B}\right) \times \vec{B} = \left(\vec{B} \cdot \nabla\right)\vec{B} - \nabla^2\left(\frac{B^2}{2}\right) \qquad (3\text{-}229)$$

We finally get:

$$\frac{\partial \vec{v}}{\partial t} + (\vec{v} \cdot \nabla)\vec{v} = \vec{f} - \frac{1}{\rho}\nabla\left(p + \frac{B^2}{8\pi}\right) + \frac{(\vec{B} \cdot \nabla)\vec{B}}{4\pi\rho} + \nu\nabla^2\vec{v} \tag{3-230}$$

So, the effect of the Magnetic Field is to introduce an isotropic pressure and a tension along the lines of force.

For the ***Energy Equation*** we have:

$$\begin{aligned} \rho\left(\frac{\partial \varepsilon}{\partial t} + \vec{v} \cdot \nabla\varepsilon\right) &= \nabla \cdot (K_B \nabla T) - p\nabla \cdot \vec{v} + \frac{j^2}{\sigma} \\ &= \nabla \cdot (K_B \nabla T) - p\nabla \cdot \vec{v} + \frac{1}{\sigma}\left[\frac{c}{4\pi}(\nabla \times \vec{B})\right]^2 \end{aligned} \tag{3-231}$$

Now, we can write the Induction Maxwell Equation:

$$\frac{\partial \vec{B}}{\partial t} = -c\nabla \times \vec{E} \tag{3-232}$$

that can be combined with the following equations:

$$\vec{j} = \sigma\left(\vec{E} + \frac{\vec{v}}{c} \times \vec{B}\right) = \frac{c}{4\pi}(\nabla \times \vec{B}) \tag{3-233}$$

$$\Longrightarrow \vec{E} = \frac{c}{4\pi\sigma}\nabla \times \vec{B} - \frac{\vec{v}}{c} \times \vec{B} \tag{3-234}$$

$$\Longrightarrow \frac{\partial \vec{B}}{\partial t} = \frac{c^2}{4\pi\sigma}\nabla^2\vec{B} + \nabla \times (\vec{v} \times \vec{B}) \tag{3-235}$$

that is called "***Magneto-Hydro-Dynamic Equation***" and:

$$\eta = \frac{c^2}{4\pi\sigma} \tag{3-236}$$

is the ***Electric Resistivity***.

The first term of this last equation represents the Diffusion of the Magnetic Field, while the second term represents the Convection of the Magnetic Field by the plasma in motion.

The relative importance of these last two terms is measured by their ratio, that is a pure number called "***Reynolds Magnetic Number***":

$$R_M = \frac{\frac{vB}{L}}{\frac{\eta B}{L^2}} = \frac{vL}{\eta} \tag{3-237}$$

Now we can analyze the MHD Equation in different situations.

Plasma at rest: $\vec{v} = \mathbf{0}$

In this case the Magneto-Hydro-Dynamic Equation becomes:

$$\frac{\partial \vec{B}}{\partial t} = \eta \nabla^2 \vec{B} \tag{3-238}$$

that indicates how the field changes in a scale time:

$$\tau_{Diff} = \frac{L^2}{\eta} = \frac{4\pi\sigma L^2}{c^2} \tag{3-239}$$

because the Flux Lines diffuse into the plasma when the resistivity is not exactely equal to zero. The reason for the Magnetic Field Decay is that the Magnetic Field is generated by Electric Currents and these currents are dissipated for Joule Effect.

Plasma in motion with no resistivity: $\vec{v} \neq \mathbf{0}, \boldsymbol{\eta} = \mathbf{0}$

The MHD Equation now is:

$$\frac{\partial \vec{B}}{\partial t} = \nabla \times \left(\vec{v} \times \vec{B}\right) \tag{3-240}$$

and for a given $\vec{B}$ at $t = 0$ let us calculate how it changes in time.

This equation shows that the Concatenate Magnetic Flux should conserve in the dynamic of a plasma with no resistivity. About that we should introduce two theorems that ***Alfvén*** theorized in ***1942*** about it:

a) The Magnetic Flux though a circuit concatenated with plasma is constant. So, the flux through a circuit γ with area S is given by:

$$\phi = \int \vec{B} \cdot dS \tag{3-241}$$

When the circuit moves with the plasma the flux will vary for two different effects: the local variation of $\vec{B}$ with time and the variation of the deformed area of the motion (lateral flux loss):

$$\frac{d\phi}{dt} = \int \frac{\partial \vec{B}}{\partial t} \cdot dS + \oint \vec{B}(\vec{v} \times d\vec{r}) = -\int \left\{ -\frac{\partial \vec{B}}{\partial t} + \nabla \times \left(\vec{v} \times \vec{B}\right) \right\} \cdot dS \tag{3-242}$$

The argument of the integral gets zero if $\vec{v}$ is the plasma velocity. So, if the circuit moves with the Plasma, ϕ results constant, that means that the flux is transported without variations: the field is frozen.

b) Fluid elements that are initially associated to a certain flux line keep on be solidal with those lines. So, writing the MHD Equation in the following form:

$$\frac{\partial \vec{B}}{\partial t} = \left(\vec{B} \cdot \nabla\right)\vec{V} - \left(\vec{V} \cdot \nabla\right)\vec{B} - \vec{B}\left(\vec{V} \cdot \nabla\right) \tag{3-243}$$

and using the Continuity Equation we get:

$$\frac{d\vec{B}}{dt} = \left(\vec{B} \cdot \nabla\right)\vec{v} + \frac{\vec{B}}{\rho}\frac{d\rho}{dt} \tag{3-244}$$

$$\Longrightarrow \frac{d}{dt}\left(\frac{\vec{B}}{\rho}\right) = \left(\frac{\vec{B}}{\rho} \cdot \nabla\right)\vec{v} \tag{3-245}$$

If we now consider a linear fluid element defined from the $d\vec{r}$ vector with initial extremes 1 and 2 that moves for a time dt to the positions $1'$ and $2'$, we have that the variation of the $d\vec{r}$ vector is:

$$d\vec{r}(t+dt) - d\vec{r}(dt) = (\vec{v}_2 - \vec{v}_1)dt = (d\vec{r}\cdot\nabla)\vec{v}dt \quad (3\text{-}246)$$

$$\Longrightarrow \frac{d}{dt}d\vec{r} = (d\vec{r}\cdot\nabla)\vec{v} \quad (3\text{-}247)$$

$$\Longrightarrow d\vec{r} \propto \frac{\vec{B}}{\rho} \quad (3\text{-}248)$$

So, if $d\vec{r}$ is initially along $\vec{B}$ the proportionality is conserved. This situation happens only when the velocities of the fluid element and the Magnetic Field are the same, so when the plasma and the magnetic field are solidal: if the density of the plasma increase also the intensity of the Magnetic Field will increase, and vice-versa.

In this chapter, we just gave an idea of which are the main plasma equations used to describe electric thruster, in particular, the Magneto Hydro Dynamic Equations.
In the next chapter, we will describe some basic and simplified equations of the operations of an MPD Thruster.

CHAPTER 4: PHYSICS OF AN MPD THRUSTER

The most powerful type of Electromagnetic Thruster is the ***MPD Thruster***, in particular the ***Self-Induced Magnetic Fields*** version that operates in ***Steady*** (or ***Quasi-Steady***) ***fashion***, which can generate multi-Newton Thrust levels with a few cm of diameter.
Let's see its working principle.

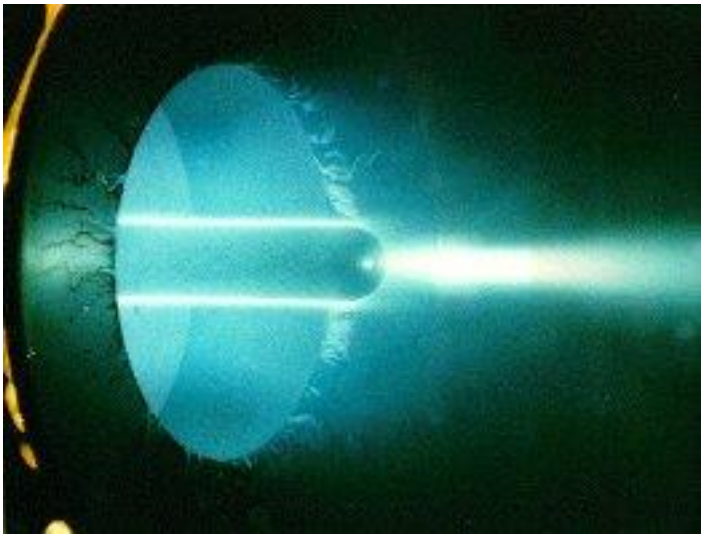

Figure 4-1: An MPD Thruster

ELECTROMAGNETIC FORCES ON PLASMAS-MPD THRUSTERS

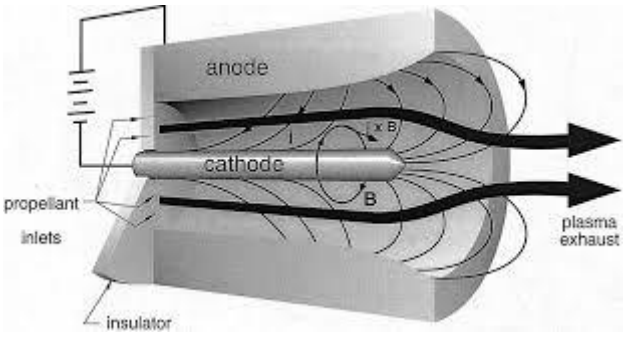

Figure 4-2: An MPD Thruster Scheme

4.1.1.2. General Plasma Physics of an MPD Thruster

Given a charge q moving at velocity $\vec{v}$ in an Electric Field $\vec{E}$ and in a Magnetic Field $\vec{B}$ the ***Lorentz Force***, as we said multiple times, is given by:

$$\vec{F}_{Lorentz} = q\left(\vec{E} + \vec{v} \times \vec{B}\right) \tag{4-2}$$

We know that $\vec{F}$ cannot depend on the rectilinear motion of the observer and so it's also for q and $\vec{B}$ for non-relativistic velocities. So it's the Electric Field- $\vec{E}$- that must be different in different reference frames. Let $\vec{E}$ the Electric Field in laboratory frame and $\overrightarrow{E'}$ the Electric Field in another frame moving at a velocity $\vec{u}$ relative to the first one.
Thus we have:

$$\vec{E} + \vec{v} \times \vec{B} = \overrightarrow{E'} + (\vec{v} - \vec{u}) \times \vec{B} \tag{4-3}$$

$$\Longrightarrow \overrightarrow{E'} = \vec{E} + \vec{u} \times \vec{B} \tag{4-4}$$

In particular, if $\vec{u} = \vec{v}$ the Lorentz Force is seen to be purely electrostatic, getting $\vec{F}_{Lorentz} = q\overrightarrow{E'}$.
The frame that moves at the $\vec{u}$ velocity is often chosen to be the one moving at the mean mass velocity of the plasma.
Now consider a plasma where there's a number density n_j of the j^{th} type of charged particles, which have a charge q_j and move with a velocity $\vec{v}_j$. The net Lorentz Force per unit volume is:

$$\vec{f} = \sum\nolimits_j n_j q_j \left(\vec{E} + \vec{v}_j \times \vec{B}\right) \tag{4-5}$$

and, since the plasma is neutral, we have that:

$$\sum\nolimits_j n_j q_j = 0 \tag{4-6}$$

so:

$$\vec{f} = \sum\nolimits_j \left(n_j q_j \vec{v}_j\right) \times \vec{B} \tag{4-7}$$

But we also know that:

$$\sum_j n_j q_j \vec{v}_j = \vec{J} \tag{4-8}$$

being $\vec{J}$ the ***Current Density Vector***, that is measured in $[A/m^2]$. So, finally we get:

$$\vec{f} = \vec{J} \times \vec{B} \tag{4-9}$$

Notice that the $\vec{v}_j$ used in the previous formulas could be the velocity of any frame, including the ***Plasma Frame***.

As already said multiple times, the dominant contribution to $\vec{J}$ is given by the electrons because of the higher mobility so, in the plasma frame we have that:

$$\vec{J} = \vec{J}_e = -en_e\vec{v}_e \tag{4-10}$$

being $\vec{v}_e$ the electron mean mass velocity vector (that is not the thermal velocity $\vec{c}_e$).
These electrons have a very rapid and chaotic motion, except for the whole swarm slowly drift $\vec{v}_e$ and, typically, we have that:

$$|\vec{v}_e| \ll \vec{c}_e \tag{4-11}$$

Now, to understand this swarm consider the net Lorentz force on it per unit volume:

$$\vec{f}_e = -n_e m_e \vec{v}_e \nu_e = \frac{m_e \nu_e}{e}\vec{J} \tag{4-12}$$

$$\Longrightarrow \vec{J} = \frac{e^2 n_e}{m_e \nu_e}\left(\overrightarrow{E'} + \vec{v}_e \times \vec{B}\right) \tag{4-13}$$

or, since:

$$\vec{v}_e = -\frac{\vec{J}}{n_e e} \tag{4-14}$$

$$\Longrightarrow \vec{j} = \frac{e^2 n_e}{m_e \nu_e} \overrightarrow{E'} - \frac{e}{m_e \nu_e} \vec{j} \times \vec{B} \tag{4-15}$$

Now, defining the ***Scalar Conductivity***- σ- and the ***Hall Parameter***- β- as:

$$\sigma = \frac{e^2 n_e}{m_e \nu_e} \tag{4-16}$$

$$\beta = \frac{eB}{m_e \nu_e} \tag{4-17}$$

$$\vec{\beta} = \beta \left(\frac{\vec{B}}{B} \right) \tag{4-18}$$

we can finally write the ***Generalized Ohm's Law***:

$$\sigma \overrightarrow{E'} = \vec{j} + \vec{j} \times \vec{\beta} \tag{4-19}$$

where, as written above:

$$\overrightarrow{E'} = \vec{E} + \vec{u} \times \vec{B} \tag{4-20}$$

Now, remembering the definition of Gyro Frequency:

$$\omega = \frac{eB}{m_e} \tag{4-21}$$

we can write:

$$\vec{\beta} = \frac{\omega}{\nu_e} \tag{4-22}$$

That represents the ratio between gyro frequency and collision frequency. It should be high for low pressures and densities, where collisions are rare and for high magnetic field, where the gyro frequency is high. Normally, in MPD Thrusters we have $\vec{\beta} \sim 1$.

We now want to calculate the ***Electromagnetic Work***.
The rate at which the external fields work on the charged particles is:

$$W = \sum_j n_j q_j \left(\vec{E} + \vec{v}_j \times \vec{B}\right) \cdot \vec{v}_j = \vec{E} \cdot \sum_j n_j q_j \vec{v}_j \tag{4-23}$$

$$W = \vec{E} \cdot \vec{j} \tag{4-24}$$

It's evident that the Magnetic Field doesn't directly contribute to the total work, but it does by modifying the Electric Field- $\vec{E}$- or the Current Density Vector- $\vec{j}$.
This total work goes, partly, into heating the plasma (***Dissipation***) and, partly, into bodily pushing it (***Mechanical Work***), in fact:

$$W = \vec{E} \cdot \vec{j} = \left(\overrightarrow{E'} - \vec{u} \times \vec{B}\right) \cdot \vec{j} = \overrightarrow{E'} \cdot \vec{j} + \left(\vec{j} \times \vec{B}\right) \cdot \vec{u} \tag{4-25}$$

being:

$$\left(\vec{u} \times \vec{B}\right) \cdot \vec{j} = -\left(\vec{j} \times \vec{B}\right) \cdot \vec{u} \tag{4-26}$$

Now, using also Ohm's Law, we have that:

$$\overrightarrow{E'} \cdot \vec{j} = \frac{1}{\sigma}\left(\vec{j} + \vec{j} \times \vec{\beta}\right) \cdot \vec{j} = \frac{j^2}{\sigma} \tag{4-27}$$

$$\Longrightarrow W = \frac{j^2}{\sigma} + \left(\vec{j} \times \vec{B}\right) \cdot \vec{u} \tag{4-28}$$

As we can see easily, the first term is the well known ***Joule Heating Effect***, while the second one is simply the rate at which the ***Lorentz Force*** -$\vec{j} \times \vec{B}$- ***does Mechanical Work*** on plasma moving at the velocity $\vec{u}$.

This second term shows that it is possible to accelerate a plasma with a Magnetic Field. Thus, in an efficient accelerator, we should try to maximize $\left(\vec{j} \times \vec{B}\right) \cdot \vec{u}$ at the expense of $\frac{j^2}{\sigma}$.

As we said in the previous chapter, the Magnetic Field in an MPD Thruster can be self-induced or provided by external coils.
Now, we know that the general relationship between $\vec{B}$ and $\vec{j}$ (in a Steady State and without magnetic materials) is given by the ***Ampere's Law***:

$$\vec{j} = \nabla \times \frac{\vec{B}}{\mu_0} \tag{4-29}$$

being $\mu_0 = 4\pi \cdot 10^{-7}\ \frac{H}{m}$ the ***Magnetic Permeability of Vacuum***.
In the integral form we have:

$$\iint \vec{j} \cdot d\vec{A} = \oint \frac{\vec{B}}{\mu_0} \cdot d\vec{l} \tag{4-30}$$

which states that the circulation of $\frac{\vec{B}}{\mu_0}$ around a closed line equals the total current linked by the loop.
Just to make an example, inside a long solenoid carrying a current $\vec{\imath}$ the field $\vec{B}$ is nearly constant and we get:

$$\vec{\imath} n = \frac{\vec{B}}{\mu_0} l \tag{4-31}$$

where n is the number of turns, so:

$$\vec{B} = \mu_0 \frac{n}{l} \vec{\imath} \tag{4-32}$$

But we also know that the Magnetic Field has the essential property of being solenoidal, so:

$$\nabla \cdot \vec{B} = 0 \tag{4-33}$$

So, in regions where no current is flowing we also have that $\nabla \times \vec{B} = 0$ so, by $\vec{B} = -\nabla\psi$,
we can define the ***Magnetic Potential***- ψ- that obeys the ***Laplace's Equation***:

$$\nabla^2\psi = 0 \qquad (4\text{-}34)$$

However, such a potential cannot exist in a current-carrying plasma, so the vector $\vec{B}$ must be found by simultaneous solution of Ampere's Law (according to which we can write $\nabla \cdot \vec{j} = 0$) and the Ohm's Law (with the additional condition $\nabla \cdot \vec{B} = 0$).

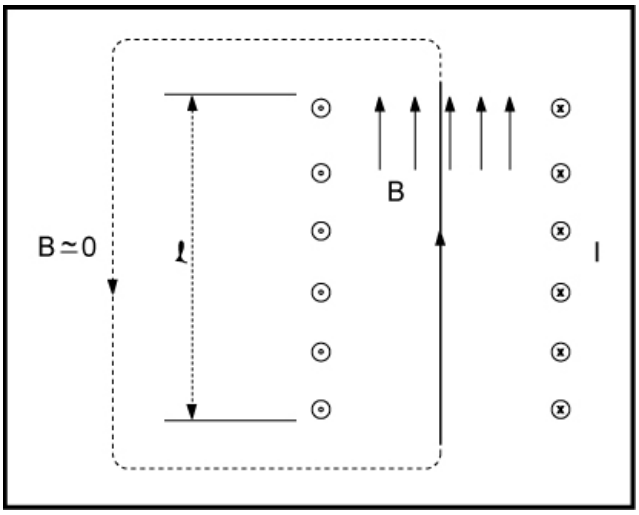

Figure 4-3: Scheme of a conductive plasma inside a solenoid.

Considering now a conductive plasma inside a solenoid, so that an external $\vec{B}$ field- $\vec{B}_{ext}$- and a self induced $\vec{B}$ field- $\vec{B}_{ind}$- coexist. The first one is due to the coil currents, while the second one is due to currents in the plasma itself. Suppose the plasma currents are due to the flow at the velocity $\vec{u}$ in the total magnetic field $\vec{B}$, while any external electrodes are shot-circuited, so that $\vec{E} = 0$ in the laboratory frame. Then, we have that:

$$\overrightarrow{E'} = \vec{E} + \vec{u} \times \vec{B} = \vec{u} \times \vec{B} \qquad (4\text{-}35)$$

with $E' \cong uB$. Now, neglecting the Hall Effect, we have that $j \sim \sigma u B$ and that the induced field obeys separately its own Ampere's Law:

$$\vec{j} = \nabla \times \frac{\vec{B}_{ind}}{\mu_0} \qquad (4\text{-}36)$$

with $B_{ind} \cong \mu_0 j l$, being l the characteristic distance for variation B_{ind} and $\vec{j}$ the Plasma Current Density. This happens because $\nabla \times \vec{B}_{ext} = 0$ in the plasma (outside the coil wires).

$$\Longrightarrow B_{ind} \cong \mu_0 luB\sigma \tag{4-37}$$

Now, we have that:

$$\vec{B} = \vec{B}_0 + \vec{B}_{ind} \tag{4-38}$$

$$\Longrightarrow \frac{\vec{B}_{ind}}{\vec{B}_0 + \vec{B}_{ind}} \sim \mu_0 lu\sigma \tag{4-39}$$

This last formula shows that the field created by the plasma currents becomes comparable to the external field when the ***Magnetic Reynolds Number***- $R_{em} = \mu_0 lu\sigma$ is of the order of the unit.

For a high power MPD accelerator, for example, we have these values:

- $\sigma = 1000\ s/mH$
- $u = 10000\ m/s$
- $l = 0.1\ m$

getting:

$$R_{em} \sim 10^{-6} \cdot 10^{-1} \cdot 10^{3} \cdot 10^{4} = 1 \tag{4-40}$$

So, the operation with self-induced magnetic field becomes possible. This simplifies a lot the design, since no heavy and power-consuming external coils are needed.
However, in some case external field may be preferable.

4.1.1.3. A Simple Plasma Accelerator

Now consider a rectangular channel with two conducting and two insulating walls with a plasma flowing in the channel at the velocity $\vec{u}$ and an external Electric Field $\vec{E}$ applied to it:

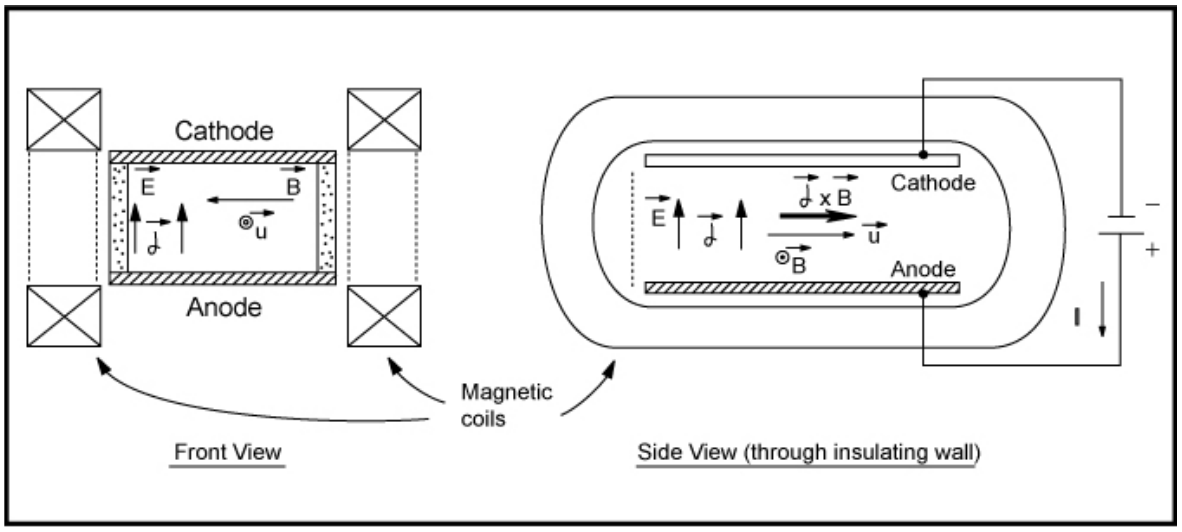

Figure 4-4: Scheme of a plasma flowing in a rectangular channel with two insulating and two conducting walls.

If we ignore the Hall Effect and the magnitude of $\left|\vec{E}\right| > \left|\vec{u}\vec{B}\right|$ (the ***Induced Faraday Field***), a current $\vec{j} = \sigma\overrightarrow{E'} = \sigma\left(\vec{E} + \vec{u} \times \vec{B}\right)$ will flow in the direction of $\vec{E}$.

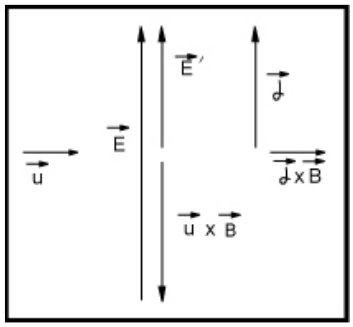

Figure 4-5: Scheme of current direction.

The Lorentz Force $\vec{f} = \vec{j} \times \vec{B}$ is then in the forward direction and so we have an accelerator. On the other hand, instead, if $\left|\vec{E}\right| < \left|\vec{u}\vec{B}\right|$, the current $\vec{j}$ flows in the direction opposite to $\vec{E}$. Externally, a positive current flows into the positive pole of the "battery" and could be used to re-charge it.
This is thus an MHD generator and the battery would probably be replaced by a passive load. The Lorentz Force points backwards, so the fluid is forced to flow by an external pressure gradient (like in a turbine).

In a moderate pressure, plasma β can easily exceed the unit.
To understand better the Ohm's Law consider the following images:

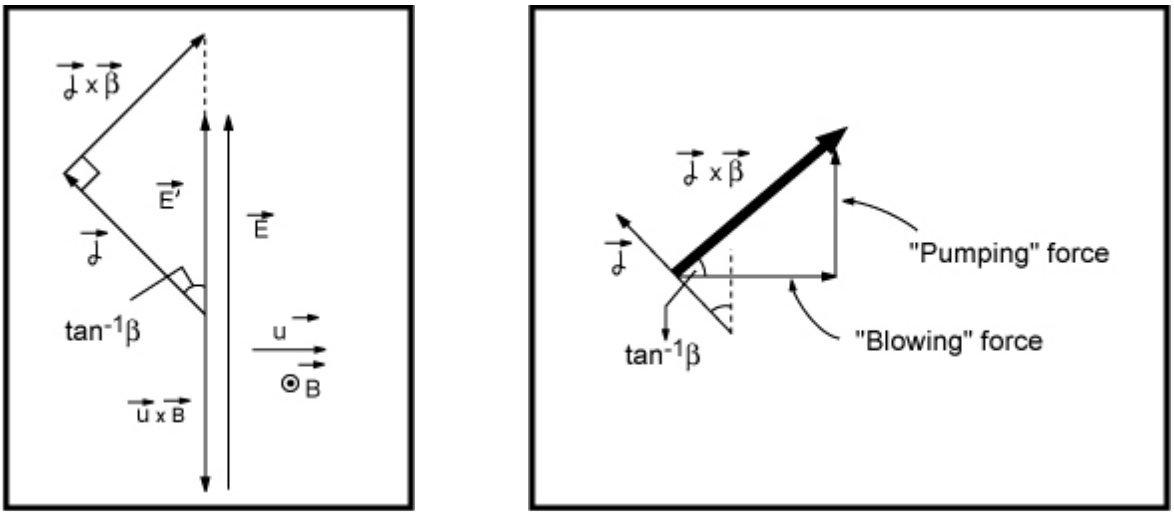

Figure 4-6: Scheme of electromagnetic forces acting on a plasma.

We can see that the effect is to turn the current and the Lorentz Force counter-clockwise by a $\tan^{-1}(\beta)$. There's still a ***forward force***- called "***Blowing Force***"-, but also a ***transverse force***- called "***Pumping Force***" that pumps the fluid towards the cathode wall, creating a transverse pressure gradient.
As we said before, the Hall Effect doesn't contribute directly to the work, but it contributes to the Joule Dissipation $\frac{j^2}{\sigma}$, so we can turn the whole diagram by $\tan^{-1}(\beta)$ clockwise and have the $\vec{j}$ flow only transversally and $\vec{f} = \vec{j} \times \vec{B}$ axially. However, that implies a forward component of the external field $\vec{E}$:

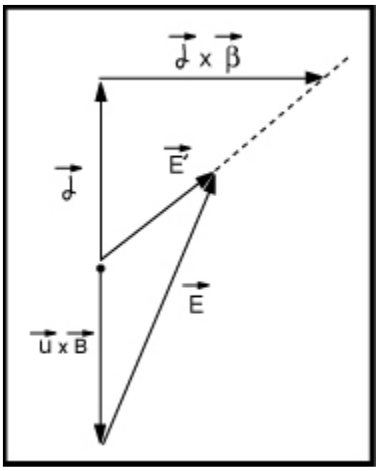

Figure 4-7: Scheme of electromagnetic forces acting on a plasma.

So, we should build the electrode wall in such a way that an axial voltage can be sustained.

4.1.1.4. Basics Design of an MPD Thruster

Consider now the possibility to wrap the continuous electrode accelerator into an annulus, eliminating the insulating walls:

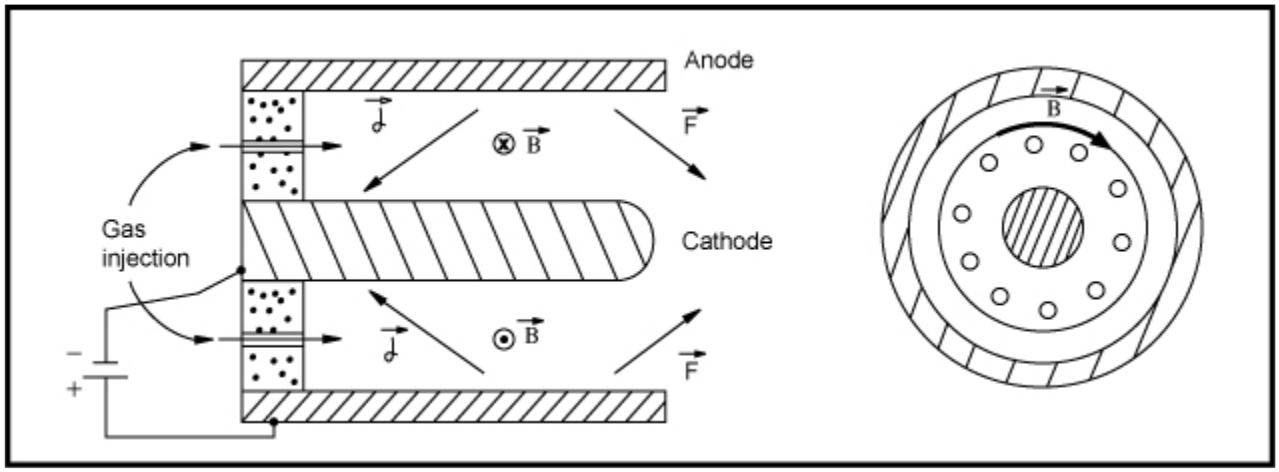

Figure 4-8: Continuous electrode accelerator wrapped into an annulus.

The Magnetic Field is now azimuthal, which circular lines of force and the insulating sidewalls have been replaced by the annular plasma itself. Anyway, an insulating backwall is still required.
The current tends to concentrate near the edge of the downstream anode and near the cathode root. Then, the pumping force will now tend to produce a highly concentrated jet of plasma: in fact a highly luminous central core is usually observed on MPD plumes, extending from the downstream part of the cathode to several cathode lengths.

Now, speaking about the Magnetic Field, notice that the azimuthal $\vec{B}$ can be provided by the plasma current flowing in the meridional plane. This can be seen from Ampere's Law, written in cylindrical coordinates:

$$\begin{cases} \mu_0 j_r = \dfrac{1}{r}\dfrac{\partial B_x}{\partial \phi} - \dfrac{\partial B_\phi}{\partial x} = \dfrac{\partial B_\phi}{\partial x} \quad for\ B_x = 0 \\ \mu_0 j_x = \dfrac{1}{r}\dfrac{\partial (rB_\phi)}{\partial r} - \dfrac{1}{r}\dfrac{\partial B_r}{\partial \phi} = \dfrac{1}{r}\dfrac{\partial (rB_\phi)}{\partial r} \quad for\ B_r = 0 \end{cases} \tag{4-41}$$

The direction of $\vec{B}$ is the one required for the acceleration and his magnitude, in a point P can be simply related to the amount of current i' that crosses the surface S: this surface leans on the ring that contains P and extends around the cathode tip.
Thus, from the ***Integral Ampere's Law*** we have:

$$B(P) = \mu_0 \frac{i'}{2\pi r} \tag{4-42}$$

where r is the radial coordinate of P. In particular, $i' = i$ (where i is the Total Current) for any point on the insulating backplate, and it's $i' = 0$ for point outside the cylinder, like the point Q in the figure below.

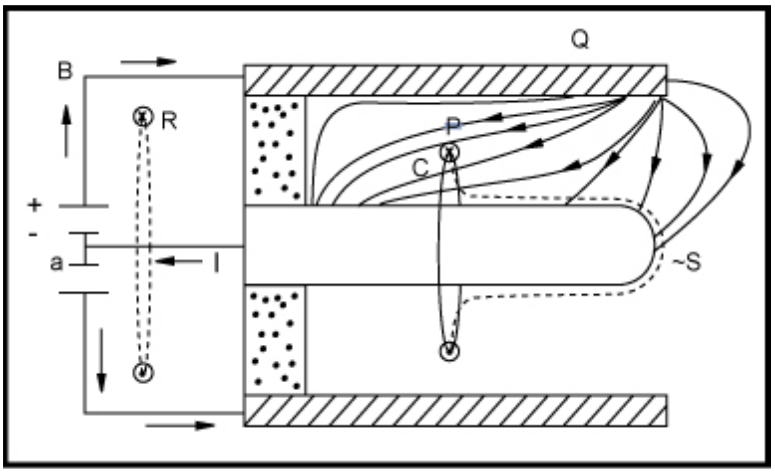

Figure 4-9: Representation of the current flow in a MPD Thruster.

4.1.1.5. Approximate Calculation of the Thrust

There are two contributes to the trust of our accelerator:

- The integral of the gas pressure over the back-facing surfaces, that is called "***Electrothermal/Aerodynamic Thrust***" and it would be the only one acting in a device where the Joule Heating Effect- $\frac{j^2}{\sigma}$- dominates over the Lorentz Work- $\left(\vec{j} \times \vec{B}\right) \cdot \vec{u}$.
- The reaction to the Lorentz Forces exerted on the plasma

At high efficiencies, the Electromagnetic Thrust dominates over the Electrothermal. Let's calculate it:

$$\vec{F}_{EM} = \iint \int \vec{j} \times \vec{B} dV = \frac{1}{\mu_0} \iint \int \left(\nabla \times \vec{B}\right) \times \vec{B} dV \qquad (4\text{-}43)$$

For the ***BAC-CAB Rule*** we have:

$$\left(\nabla \times \vec{B}\right) \times \vec{B} = \left(\vec{B}\nabla\right)\vec{B} - \nabla\left(\frac{B^2}{2}\right) \qquad (4\text{-}44)$$

but since $\left|\vec{B}\right|$ doesn't vary along its own direction in our case, we have:

$$(\vec{B}\nabla)\vec{B} = -\frac{B^2}{r}\vec{l}_r \tag{4-45}$$

$$\Longrightarrow \vec{F}_{EM} = -\frac{1}{\mu_0}\iint\int \nabla\left(\frac{B^2}{2}\right)dV \tag{4-46}$$

and, applying the ***Gauss Theorem***:

$$\vec{F}_{EM} = -\frac{1}{\mu_0}\iint \frac{B^2}{2}d\vec{A} \tag{4-47}$$

where the integral extends to the surface surrounding the plasma and $d\vec{A}$ points outwards from the surface. Since we are interested only on the axial force we can write:

$$\vec{F}_{EM} = -\frac{1}{\mu_0}\iint \frac{B^2}{2}dA_x \tag{4-48}$$

where $d\vec{A}_x$ is the projection of each area element to the axial direction.
For any cylindrical surface, $dA_x = 0$. The only surface surrounding the plasma which face backwards (or forward) are the back-plate, the cathode tip and the anode rim.
Now, for the back-plate, using $i' = i$ we have:

$$(F_{EM})_{Back-Plate} = +\frac{1}{\mu_0}\int_{R_c}^{R_a}\left(\frac{\mu_0 i}{2\pi r}\right)^2 2\pi r\, dr = \frac{\mu_0 i^2}{4\pi}\ln\frac{R_a}{R_c} \tag{4-49}$$

Where R_a and R_c are the anode and the cathode radii and the positive sign is because the normal $d\vec{A}$ to the surface points backwards (out of the plasma).
The calculation of the cathode tip and anode rim contributions is more complicated, since we would need to know the distribution of the current on these surfaces. However, for conventional built thrusters, these contributions have been estimated experimentally to amount at most $10\ \%$ of the total and they're counted with the ***Maecker's Formula*** (that arises the same formula we wrote above):

$$F = \frac{\mu_0 i^2}{4\pi}\ln\frac{R_a}{R_c} \tag{4-50}$$

This formula is the results of many experimental calculus and it is object of many studies.
From Maecker's Law we can notice that F is independent of the size and it scales as the square of the total current.
Thus, the magnitude of the ***Exit Velocity***- u_e- is:

$$u_e = \frac{F}{\dot{m}} = \frac{\mu_0}{4\pi} \ln \frac{R_a}{R_c} \frac{i^2}{\dot{m}} \tag{4-51}$$

In the diagrams below, we can see the trend of the Thrust and the Thrust Efficiency respect to the Current and the Thrust Efficiency respect to the Specific Impulse.

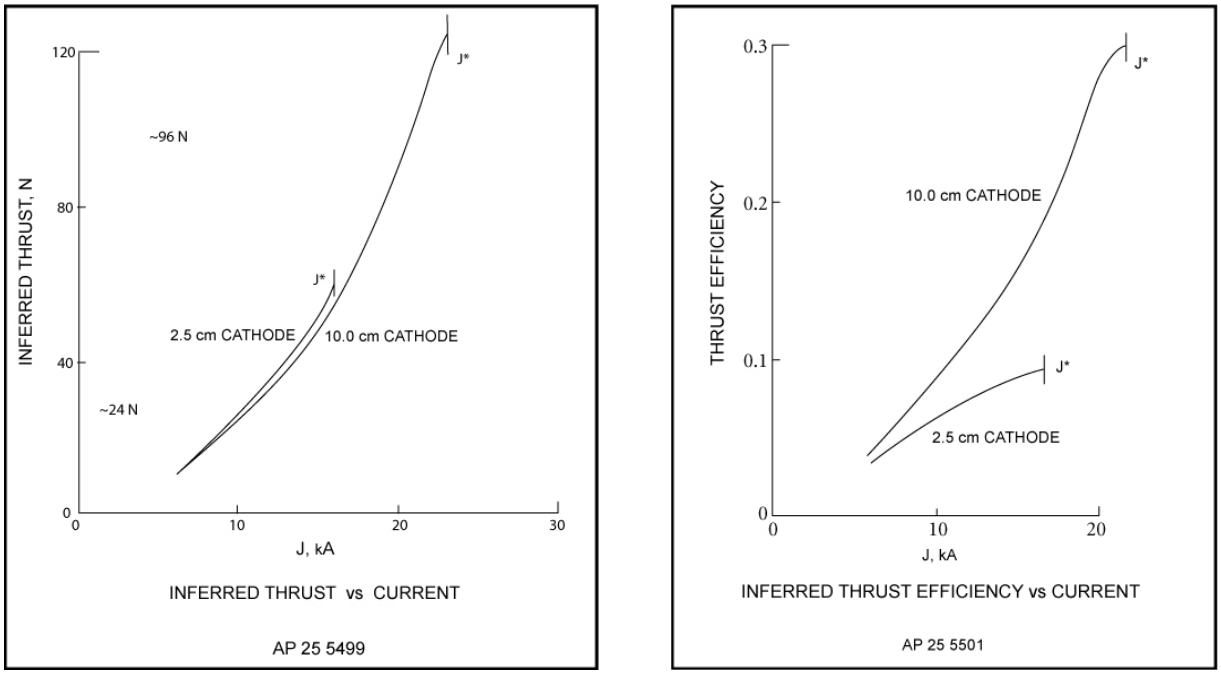

Figure 4-10: Trend of the Thrust (on the left) and the Thrust Efficiency (on the right) respect to the Current.

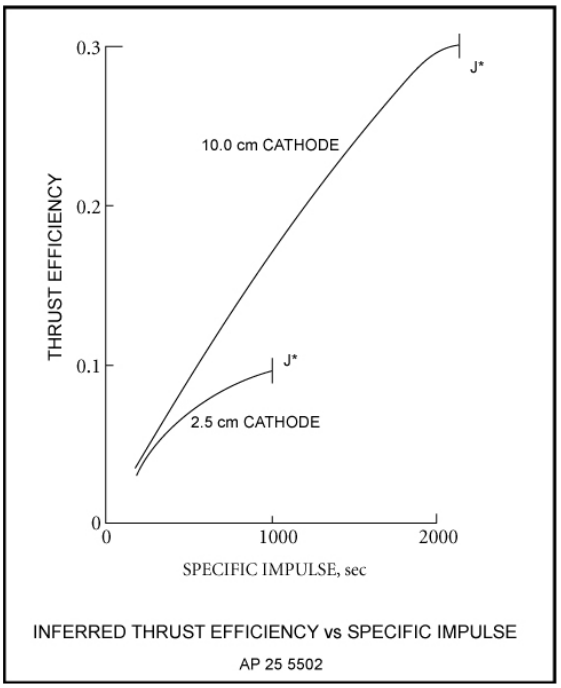

Figure 4-11: Trend of theThrust Efficiency respect to the Specific Impulse.

It has been found that the speed of sound at representative points in the flow scales like $\frac{1}{\sqrt{M}}$, being M the Molecular Mass of the gas and, from the formula of the exit velocity, we can see that the Mach Number at the exit varies like the quantity:

$$\frac{i^2\sqrt{M}}{\dot{m}} \tag{4-52}$$

This parameter is the most important scaling parameter for an MPD Thruster. It has been found that, for each geometrical arrangement, there's a limiting value of $\frac{i^2\sqrt{M}}{\dot{m}}$ beyond which the operation becomes highly unsteady and erosion of the electrodes increases a lot.
Experimentally a rough value of the current- i- has been found for any combination of propellant and mass rate- $\dot{m}$. For a mass rate of $\dot{m} = 6\ g/s$ of ***Argon***, for instance, we have that:

$$i^* = 23\ kA \tag{4-53}$$

$$\Longrightarrow \left(\frac{i^2\sqrt{M}}{\dot{m}}\right)^* = 560 \tag{4-54}$$

Anyway, this value is going to be pushed to highest possible values, because with its increasing also the Specific Impulse and the Ratio of Magnetic Pressure to Dynamic Pressure increase.

Now, if the Thrust Efficiency is:

$$\eta = \frac{\frac{1}{2}\dot{m}u_e^2}{iV} = \frac{1}{2}\frac{F^2}{\dot{m}\,iV} \tag{4-55}$$

we obtain:

$$\Longrightarrow V = \frac{1}{2\eta}\left(\frac{\mu_0}{4\pi}\ln\frac{R_a}{R_c}\right)^2 \frac{i^3}{\dot{m}} \tag{4-56}$$

Thus, while η varies little with current- i-, V varies as its cube.
At lower currents, η goes down, the Electrothermal Component of the Thrust predominates, and the near-electrode voltage drops become comparable to the voltage needed for acceleration.

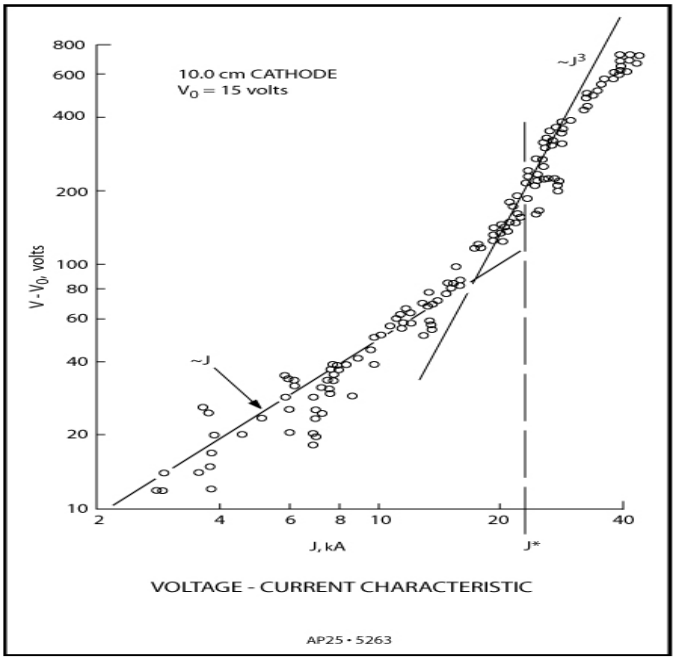

Figure 4-12: Electrode voltage drops vs voltage needed for the acceleration.

4.1.1.6. Power Requirements

Considering the example above and assuming $R_c = 1\ cm$ and $R_a = 5\ cm$ the Thrust is:

$$F = 10^{-7} \cdot 23000^2 \ln\left(\frac{5}{1}\right) = 85.1\ N \qquad (4\text{-}57)$$

And the Jet-Power- P_{Jet}- results being:

$$P_{Jet} = \frac{F^2}{2\dot{m}} = \frac{85.1^2}{2 \cdot 0.006} = 6.04 \cdot 10^5\ W \qquad (4\text{-}58)$$

Consider that the best efficiencies obtained so far are of the order of 50%: the actual power required for an MPD is about $1.2\ MW$, a very difficult requirement to meet in space except for nuclear reactors.

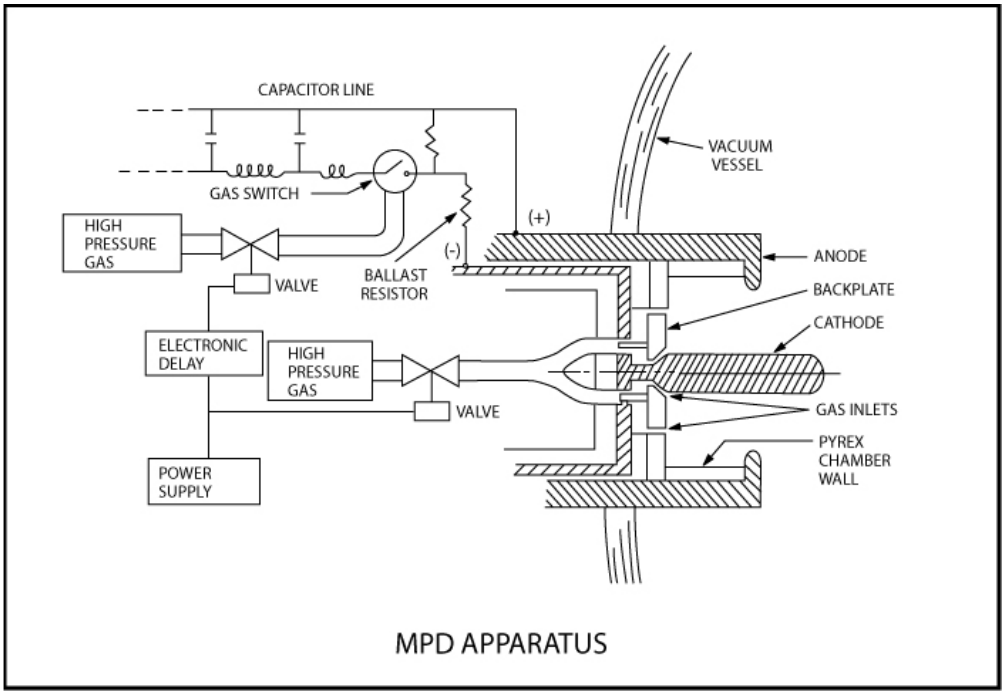

Figure 4-13: Scheme on an MPD Apparatus.

MODEL FOR MPD PERFORMANCE-ONSET

When current flows through a highly conductive and rapidly moving plasma the current tends to concentrate near the entrance and exit of the channel because of a strong Electromagnetic Field which tends to block current over most of the channel length.
Just to understand it, considering the annular chamber of an MPD Thruster let's suppose to unwrap it into a rectangular 1-D channel, as in the figure above:

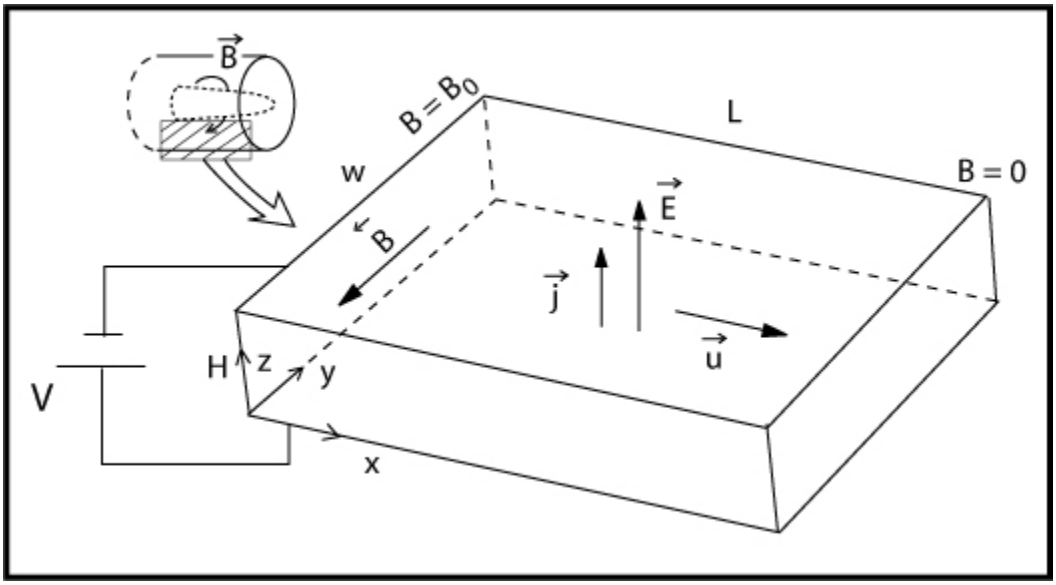

Figure 4-14: Representation of an MPD Channel unwrapped into a rectangular 1-D channel.

According to the ***Ampere's Law*** we have:

$$\vec{j} = \frac{1}{\mu_0} \nabla \times \vec{B} \tag{4-59}$$

being, in this case:

$$\nabla = \frac{\partial}{\partial x} \vec{\imath}_x \tag{4-60}$$

$$\Longrightarrow j_z = j = \frac{1}{\mu_0} \frac{dB_y}{dx} \tag{4-61}$$

and defining $B = -B_y$ we get:

$$j = -\frac{1}{\mu_0} \frac{dB}{dx} \tag{4-62}$$

If we then ignore Hall Effects, ***Ohm's Law*** gives us:

$$\vec{j} = \sigma\left(\vec{E} + \vec{u} \times \vec{B}\right) \tag{4-63}$$

or, using:

$$\begin{cases} E = E_z = \dfrac{V}{H} \\ B = -B_y \\ u = u_x \end{cases} \tag{4-64}$$

$$\Longrightarrow j = \sigma(E - uB) = \sigma\left(\frac{V}{H} - uB\right) \tag{4-65}$$

$$\frac{dB}{dx} = -\mu_0 j \tag{4-66}$$

Now, the flow velocity- $\vec{u}$- evolves along x according to the ***Momentum Equation*** and ignoring the pressure forces:

$$\dot{m}\frac{du}{dx} + A\frac{dP}{dx} = A\left(\vec{j} \times \vec{B}\right)_x = jBwH \tag{4-67}$$

$$\Longrightarrow \dot{m}\frac{du}{dx} = -\frac{1}{\mu_0}\frac{dB}{dx}BwH = -\frac{wH}{\mu_0}\frac{d}{dx}\left(\frac{B^2}{2}\right) \tag{4-68}$$

$$\dot{m}\frac{du}{dx} + \frac{wH}{\mu_0}\frac{d}{dx}\left(\frac{B^2}{2}\right) = 0 \tag{4-69}$$

$$\frac{d}{dx}\left[\dot{m}u + \frac{wH}{\mu_0}\left(\frac{B^2}{2}\right)\right] = 0 \tag{4-70}$$

$$\dot{m}u + \frac{wH}{\mu_0}\left(\frac{B^2}{2}\right) = Const. \tag{4-71}$$

$$\Longrightarrow \dot{m}u + wH\frac{B^2}{2\mu_0} = \dot{m}u_0 + wH\frac{B_0^2}{2\mu_0} \tag{4-72}$$

$$\Longrightarrow u = \frac{wH}{2\mu_0}\left(\frac{B_0^2 - B^2}{\dot{m}}\right) \tag{4-73}$$

$$\Longrightarrow \frac{dB}{dx} = -\sigma\mu_0\left[E - \frac{wH}{2\mu_0\dot{m}}B(B_0^2 - B^2)\right] \tag{4-74}$$

$$\Longrightarrow \frac{dB}{E - \frac{wH}{2\mu_0\dot{m}}B(B_0^2 - B^2)} = -\sigma\mu_0 dx \tag{4-75}$$

$$\int_0^x -\sigma\mu_0 dx = \int_{B_0}^{B} \frac{dB}{E - \frac{wH}{2\mu_0\dot{m}}B(B_0^2 - B^2)} \tag{4-76}$$

and approximating the conductivity σ as a constant, we get:

$$\Longrightarrow \sigma\mu_0 x = \int_{B}^{B_0} \frac{dB}{E - \frac{wH}{2\mu_0\dot{m}}B(B_0^2 - B^2)} \tag{4-77}$$

The denominator of this last equation represents the Driving Field.
The field B_0 at $x = 0$ is a measure of the current i, in fact integrating between $x = 0$ and $x = L$ we get:

$$\int_0^L j dx = \frac{i}{w} = \frac{B_0}{\mu_0} \tag{4-78}$$

$$\Longrightarrow B_0 = \frac{\mu_0 i}{w} \tag{4-79}$$

$$\Longrightarrow \sigma\mu_0 L = \int_0^{B_0} \frac{dB}{E - \frac{wH}{2\mu_0 \dot{m}} B(B_0^2 - B^2)} \tag{4-80}$$

Where once i and $\dot{m}$ are specified, only E remains as unknown, but we use the equation $V = EH$.
Consider now the case where the maximum value of the back Electromagnetic Field reaches almost the level E: in this case the integrand will be very large as long as this condition prevails, and it indicates a large value of $\sigma\mu_0 L$.
Then, we know that B remains flat when $E - uB \ll E$ and there will be little current in this region, as you can see in the figure below:

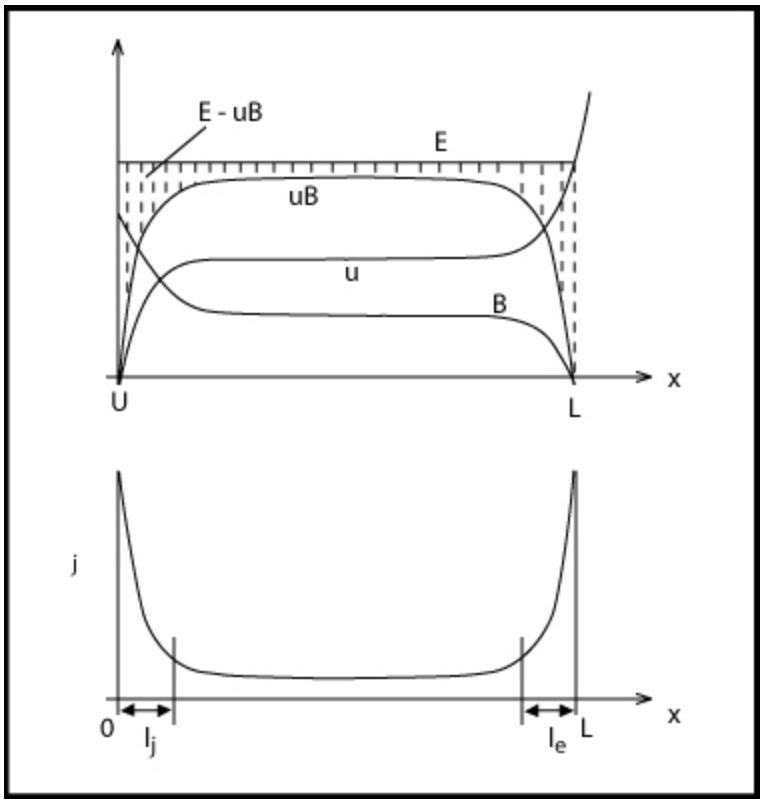

Figure 4-15: Current density vs position along the channel.

We can see that two strong current concentrations develop, near $x = 0$ and $x = L$.
The denominator is minimum when B has a value such that to maximizes $B_0^2 - B^2$, so when $B_0^2 - 3B^2 = 0$.

$$\Longrightarrow B_1 = B_{(uB)max} = \frac{B_0}{\sqrt{3}} \tag{4-81}$$

$$\Longrightarrow (E - uB)_{max} = E - \frac{wH}{2\mu_0 \dot{m}} \frac{2B_0^3}{3\sqrt{3}} \tag{4-82}$$

And, since we assumed this difference to be much less than E, we get:

$$\Longrightarrow E \cong \frac{wH}{\mu_0 \dot{m}} \frac{B_0^3}{3\sqrt{3}} \tag{4-83}$$

$$\Longrightarrow V \cong \frac{1}{3\sqrt{3}} \left(\frac{H}{w}\right) \mu_0^2 \frac{i^3}{\dot{m}} \tag{4-84}$$

We notice that near $x = 0$ and $x = L$, for $uB \ll E$ we get:

$$\frac{dB}{dx} = -\sigma \mu_0 E \tag{4-85}$$

So, the thickness l of the thin current layer (where B varies substantially) can be estimated as follow:

$$l_0 = \frac{B_0 - B_1}{\sigma \mu_0 E} \tag{4-86}$$

$$l_e = \frac{B_1}{\sigma \mu_0 E} \tag{4-87}$$

where B_1 was defined above.

$$l_0 = \frac{3\left(\sqrt{3} - 1\right)\dot{m}}{\sigma w H B_0^2} \tag{4-88}$$

$$l_e = \frac{3\dot{m}}{\sigma w H B_0^2} \tag{4-89}$$

So, after some passages, we get:

$$\sigma u_e \mu_0 l_0 \cong \frac{3}{2}\left(\sqrt{3} - 1\right) \tag{4-90}$$

$$\sigma u_e \mu_0 l_e \cong \frac{3}{2} \tag{4-91}$$

being $\sigma u \mu_0 l$ the ***Magnetic Reynolds Number***- R_m- based on length l.
Since we assumed these layers to be thin, we can now say that this happens when:

$$R_m(L) \gg 1 \tag{4-92}$$

The high current inlet and exit layer, however, are very dissipative and their resistance can be estimated as:

$$R_0 = \frac{\frac{4}{3}H}{\sigma w l_0} \tag{4-93}$$

$$R_e = \frac{\frac{4}{3}H}{\sigma w l_e} \tag{4-94}$$

so, the Ohmically Dissipated Power- P_D- is:

$$P_D = i_0^2 R_0 + i_e^2 R_e \tag{4-95}$$

being:

$$i_0 = \frac{w}{\mu_0}(B_0 - B_1) = \frac{w B_0}{\mu_0}\left(1 - \frac{1}{\sqrt{3}}\right) = i\left(1 - \frac{1}{\sqrt{3}}\right) \tag{4-96}$$

$$i_e = i - i_0 = \frac{i}{\sqrt{3}} \tag{4-97}$$

Substituting we get:

$$P_D = \frac{4}{9\sqrt{3}}\left(\frac{H}{w}\right)^2 \frac{{\mu_0}^2 i^4}{\dot{m}} \tag{4-98}$$

Most of this dissipation is used to ionize and excite the gas atoms.

INSTABILITY ONSET

For a given thruster, as $\frac{i^2}{\dot{m}}$ increases, also the ionization fraction α_e increases rapidly:

$$\alpha_e = \frac{m_i}{eV_i}\frac{4}{9\sqrt{3}}\left(\frac{H}{w}\frac{\mu_0 i^2}{\dot{m}}\right)^2 \tag{4-99}$$

being eV_i the effective ionization energy per atom.
When it reaches the unit, the behavior of the plasma changes drastically because any extra dissipation cannot be absorbed into ionization anymore and goes directly into heating of the plasma. This causes the increasing of conductivity with current concentrations leading to further current concentrations.

We can write:

$$\frac{H}{w}\frac{\mu_0 i^2}{\dot{m}} = \sqrt{\frac{9\sqrt{3}}{4}\frac{eV_i}{m_i}} \tag{4-100}$$

and finally:

$$u_e = \frac{1}{2}\sqrt{\frac{9\sqrt{3}}{4}\frac{eV_i}{m_i}} = 0.981\sqrt{\frac{eV_i}{m_i}} \tag{4-101}$$

The velocity $\sqrt{\frac{2eV_i}{m_i}}$ at which the particle Kinetic Energy would be capable of ionizing is called "***Alfvèn Critical Speed***".
In the following table we can see some values of parameters with different gases:

Table 4-1: Properties of different gases.

GAS	Hydrogen- H	Nitrogen- Na	Argon- Ar	Lithium- Li
$\boldsymbol{M_i\ (g/mol)}$	1	14	40	7
$\boldsymbol{V_i\ (Volts)}$	13.6	14.6	15.8	5.4
$\boldsymbol{(I_{sp})_{max}\ (s)}$	5120	1420	870	1220

Finally, let's see the Efficiency of an MPD Thruster.
If we consider just the power lost for Ohmic Dissipation and of near-electrode voltage drops, we have:

$$\Delta V = \Delta V_{Cathode} + \Delta V_{Anode} \tag{4-102}$$

$$\eta = \frac{\frac{1}{2}\dot{m}u_e^2}{\frac{1}{2}\dot{m}u_e^2 + P_D + i\Delta V} \tag{4-103}$$

Substituting the formulas we found above we finally get:

$$\eta = \frac{1}{3.05 + \frac{8\Delta V\dot{m}}{\mu_0^2 i^3}\left(\frac{H}{w}\right)^2} \tag{4-104}$$

Even if the voltage Drops could be eliminated, this efficiency can reach a maximum of:

$$\eta_{max} = \frac{1}{3.05} = 0.328 \tag{4-105}$$

So, the best that can be done when there's a voltage drop is to approach the "onset" at a point we get:

$$\eta = \frac{1}{3.05 + 2.88\Delta V \sqrt{\left(\frac{\frac{w}{H}}{\mu_0 \dot{m}}\right)} \sqrt[4]{\left(\frac{m_i}{eV_i}\right)^3}} \qquad (4\text{-}106)$$

For argon, for example, having values of:

- $\dot{m} = 6\ g/s$;
- $\frac{w}{H} = 4$;
- $\Delta V = 10\ V$

we get:

$$\eta^* = 0.259 \qquad (4\text{-}107)$$

.

Values of this order are very typical and most of the inefficiency are due to the strong dissipation in the inlet and exit layers, that is intrinsic to the constant area. One solution that has been developed is to use a ***Convergent-Divergent Geometry*** that has the effect of weakening these dissipative layers, retarding the onset and increasing the Efficiency.

In this chapter we just described the main equations which rule the operations of an MPD Thruster, deriving important parameters such as the Thrust, the efficiency and the exhaust velocity of this engine.
In the next chapters we'll make a rapid description of the method used to solve the MHD equations previously described and then we will post the analysis with a 1-D code written specifically for this analysis.

CHAPTER 5: MAGNETOGASDYNAMICS AND PLASMA ACCELERATORS

As it was pointed out previously, plasma is a gas containing charged particles (ions and electrons) that may give rise to, and/or interact with, electric and magnetic fields. On the other hand, obviously, the equations of gas dynamics are applicable to plasmas, provided that the contributions of the magnetic and electric fields are taken into account. Thus, Maxwell's equations will also be needed.
In the context of plasma physics, ***Magnetogasdynamics*** (***MGD***), often also referred to as ***Magnetohydrodynamics*** (***MHD***), arises from the ***combination of Maxwell equations and gas dynamics equations***.

FUNDAMENTALS OF MAGNETOGASDYNAMICS

Assuming an isotropic medium, in the absence of electric polarization and magnetic polarization, and calling σ the charge density, $\vec{J}$ the current density, and $\vec{E}$ and $\vec{B}$ the electric and magnetic fields, respectively, Maxwell's equations read:

$$\nabla \cdot \vec{E} = \frac{\sigma}{\varepsilon_0} \tag{5-2}$$

$$\nabla \cdot \vec{B} = 0 \tag{5-3}$$

$$\nabla \times \vec{E} = -\frac{\partial \vec{B}}{\partial t} \tag{5-4}$$

$$\nabla \times \vec{B} = \mu_0 \vec{J} + \frac{1}{c^2}\frac{\partial \vec{E}}{\partial t} \tag{5-5}$$

Here ε_0 and μ_0 are, respectively, the dielectric constant and the magnetic permeability of vacuum, and $c = 1/\varepsilon_0\mu_0$ is the ***speed of propagation of electromagnetic waves in vacuum***.
The gas dynamics equations, if dissipative effects (i.e., viscosity and heat transfer) are neglected and accounting for electric and magnetic forces, read:

Continuity Equation:

$$\frac{\partial \rho}{\partial t} + \nabla \cdot \left(\rho \vec{V}\right) = 0 \tag{5-6}$$

Momentum Equation:

$$\frac{\partial(\rho\vec{V})}{\partial t} + \nabla \cdot (\rho\vec{V}\vec{V}) = -\nabla P + \sigma\vec{E} + \vec{J} \times \vec{B} \tag{5-7}$$

For a great number of practical applications, at any point of the plasma domain, the density of positive charges (ions) is almost balanced by the density of negative charges (electrons), giving rise to the so-called ***charge quasi-neutrality***.

$$\sigma_{ions} \cong \sigma_{elec} \rightarrow \ \sigma = \sigma_{ions} - \sigma_{elec} \cong 0 \tag{5-8}$$

Under the hypothesis of charge neutrality, the term of the electrical field can be dropped in the momentum equation. In addition, upon substitution of $\nabla \times \vec{B} = \mu_0\vec{J}$ into the momentum equation, and after some manipulation, one finally gets:

$$\frac{\partial(\rho\vec{V})}{\partial t} + \nabla \cdot \left[\rho\vec{V}\vec{V} + \left(P + \frac{1}{2\mu_0}\vec{B} \cdot \vec{B}\right)\vec{I} - \frac{1}{\mu_0}\vec{B}\vec{B}\right] = 0 \tag{5-9}$$

Energy Equation:

$$\frac{\partial(\rho e_t)}{\partial t} + \nabla \cdot \left[\left(\frac{P}{\gamma - 1} + \frac{1}{2}\rho\vec{V} \cdot \vec{V}\right)\vec{V}\right] = -\nabla \cdot (P\vec{V}) + \vec{E} \cdot \vec{J} \tag{5-10}$$

where:

$$\rho e_t = \frac{P}{\gamma - 1} + \frac{1}{2}\rho\vec{V} \cdot \vec{V} \tag{5-11}$$

The term $\vec{E} \cdot \vec{J}$ arises from averaging the Lorentz force on the particles, and neglecting the contribution of the ions compared to that of the electrons, and realizing that the magnetic field doesn't produce work.
According to the ***Poynting's Theorem***:

$$\nabla \cdot \left(\vec{E} \times \frac{\vec{B}}{\mu_0}\right) + \vec{E} \cdot \vec{J} = -\frac{\partial}{\partial t}\left(\frac{\varepsilon_0}{2}\vec{E} \cdot \vec{E} + \frac{1}{2\mu_0}\vec{B} \cdot \vec{B}\right) \tag{5-12}$$

It can be shown that the electric energy is negligible compared to the magnetic energy. Then energy equation yields:

$$\frac{\partial}{\partial t}\left(\rho e_t + \frac{1}{2\mu_0}\vec{B}\cdot\vec{B}\right) + \nabla\cdot\left[\left(\frac{\gamma}{\gamma-1}P + \frac{1}{2}\rho\vec{V}\cdot\vec{V}\right)\vec{V} + \left(\vec{E}\times\frac{\vec{B}}{\mu_0}\right)\right] = 0 \qquad (5\text{-}13)$$

Taking into account ***Ohm's Law***:

$$\vec{J} = \sigma_e\left(\vec{E} + \vec{V}\times\vec{B}\right) \quad \rightarrow \quad \vec{E} = \frac{\vec{J}}{\sigma_e} - \vec{V}\times\vec{B} \qquad (5\text{-}14)$$

σ_e being the ***plasma conductivity***, after some manipulation, the energy equation finally reads:

$$\frac{\partial}{\partial t}\left(\rho e_t + \frac{1}{2\mu_0}\vec{B}\cdot\vec{B}\right) + \nabla\cdot\left[\left(\rho e_t + P + \frac{\vec{B}\cdot\vec{B}}{\mu_0}\right)\vec{V} - \frac{1}{\mu_0}(\vec{B}\cdot\vec{V})\vec{B}\right] = \frac{\vec{J}\cdot\vec{J}}{\sigma_e} \qquad (5\text{-}15)$$

In virtue of the hypothesis of neutrality, the electric field needn't be considered explicitly, although it does exist, and the expression for $\partial\vec{B}/\partial t$ can be conveniently manipulated to give:

$$\frac{\partial\vec{B}}{\partial t} = -\nabla\times\left(\frac{\nabla\times\vec{B}}{\sigma_e\mu_0} - \vec{V}\times\vec{B}\right) = \frac{1}{\sigma_e\mu_0}\left[\nabla^2\vec{B} - \nabla\left(\nabla\cdot\vec{B}\right)\right] + \nabla\times\left(\vec{V}\times\vec{B}\right) = \qquad (5\text{-}16)$$

$$= \nu_e\nabla^2\vec{B} + \nabla\cdot\left(\vec{B}\vec{V} - \vec{V}\vec{B}\right) \qquad (5\text{-}17)$$

$\nu_e = 1/\sigma_e\mu_0$ being the magnetic diffusivity.
The continuity, momentum and energy equations, together the equation for the magnetic field may be written in the form:

$$\frac{\partial}{\partial t}\begin{bmatrix}\rho\\ \rho\vec{V}\\ \vec{B}\\ \rho e_t+\dfrac{\left|\vec{B}\right|^2}{2\mu_0}\end{bmatrix}+\nabla\cdot\begin{bmatrix}\rho\vec{V}\\ \rho\vec{V}\vec{V}+\left(P+\dfrac{\left|\vec{B}\right|^2}{2\mu_0}\right)\vec{I}-\dfrac{1}{\mu_0}\vec{B}\vec{B}\\ \left(\vec{V}\vec{B}-\vec{B}\vec{V}\right)\\ \left(\rho e_t+P+\dfrac{\left|\vec{B}\right|^2}{\mu_0}\right)\vec{V}-\left(\vec{B}\cdot\vec{V}\right)\vec{B}\end{bmatrix}=\begin{bmatrix}0\\ 0\\ \nu_e\nabla^2\vec{B}\\ \nu_e\dfrac{\left|\vec{V}\times\vec{B}\right|^2}{\mu_0}\end{bmatrix} \tag{5-18}$$

This is a ***system of 8 O.D.E***. expressed in ***conservative form***, with sources terms (arising as a consequence of the space gradients of the magnetic field).

QUASI-ONE-DIMENSIONAL MODEL OF A PLASMA ACCELERATOR

Let us consider now that the plasma flows within a straight duct centered along the x coordinate, so that the physical properties at each section are averaged over the cross-sectional area $A(x)$, that in turn is assumed to change smoothly, this is:

$$\frac{d}{dx}\left(\sqrt{A}\right)\ll 1 \tag{5-19}$$

In that case the physical variables become a function of only x and t. In addition, consistently with this simplified ***quasi-one-dimensional model***, the magnetic field will be assumed to be transversal to x, this is, B_z for a duct with planar walls or B_ϕ for a duct with symmetry of revolution, and the only component of the electrical field is E_y (or E_r).

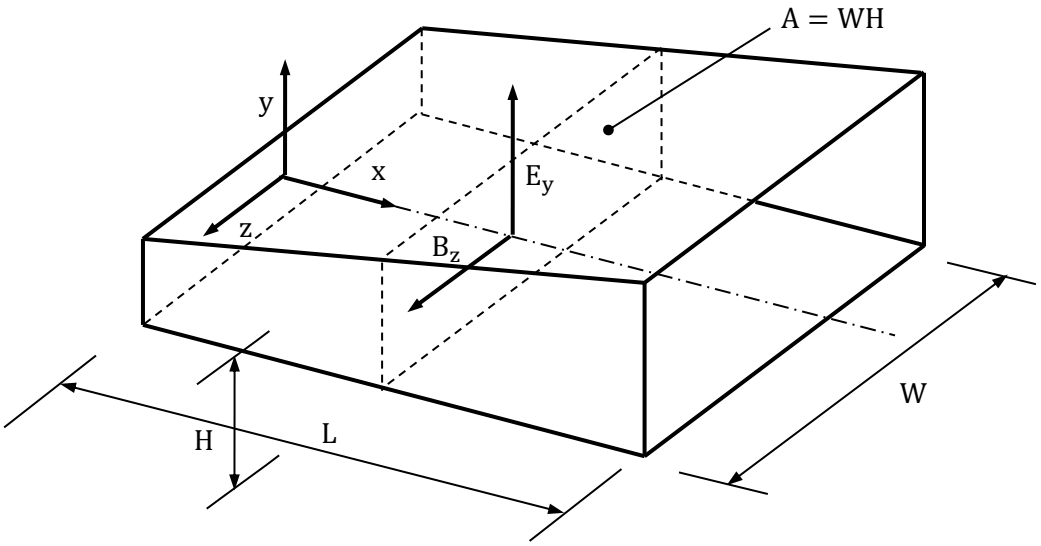

Figure 5-1: Duct with planar walls.

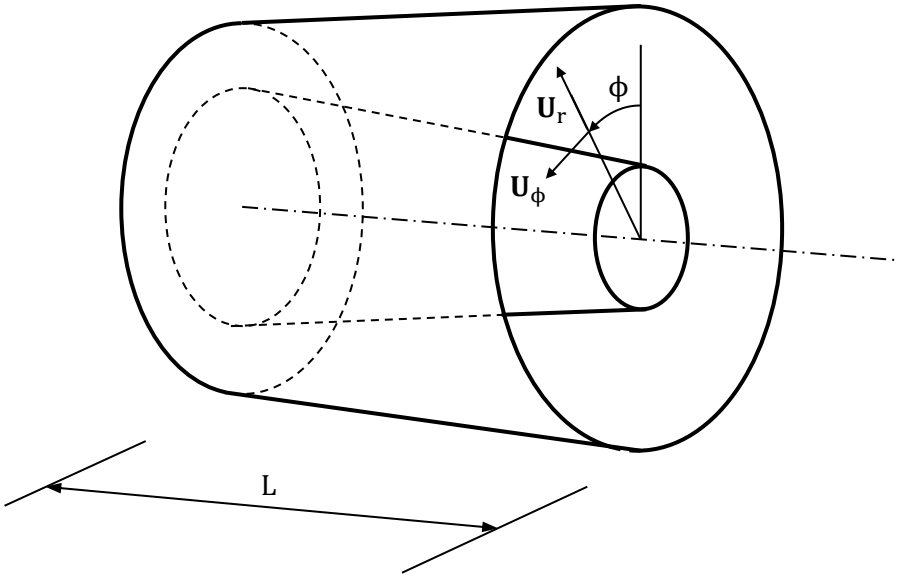

Figure 5-2: Duct with symmetry of revolution (mean radius is assumed constant).

However, some equations must now be reviewed, since additional source terms on the right side arise now as a consequence of conservation balances.

Continuity Equation:

$$\frac{\partial(\rho A)}{\partial t}+\frac{\partial}{\partial x}(\rho A u)=0 \tag{5-20}$$

or:

$$\frac{\partial \rho}{\partial t}+\frac{\partial}{\partial x}(\rho u)=-\rho u\frac{1}{A}\frac{dA}{dx} \tag{5-21}$$

Momentum Equation:

$$\frac{\partial(\rho A u)}{\partial t}+\frac{\partial}{\partial x}(\rho A u^2)=-\frac{\partial}{\partial x}(PA)+P\frac{dA}{dx}-JB_y A \tag{5-22}$$

or:

$$\frac{\partial(\rho A u)}{\partial t}+\frac{\partial}{\partial x}(\rho A u^2+PA)=P\frac{dA}{dx}-\frac{B_y}{\mu_0}\frac{\partial B_y}{\partial x}A \tag{5-23}$$

or:

$$\frac{\partial(\rho u)}{\partial t}+\frac{\partial}{\partial x}\left[\rho u^2+\left(P+\frac{1}{2\mu_0}B_y^2\right)\right]=-\rho u^2\frac{1}{A}\frac{dA}{dx} \tag{5-24}$$

or:

$$\rho\frac{\partial u}{\partial t}+\rho u\frac{\partial u}{\partial x}+\frac{\partial}{\partial x}\left(P+\frac{1}{2\mu_0}B_z^2\right)=0 \tag{5-25}$$

Energy Equation:

$$A\frac{\partial}{\partial t}\left(\rho e_t+\frac{B_y^2}{2\mu_0}\right)+\frac{\partial}{\partial x}\left(\rho h_t u A+\frac{B_z^2}{\mu_0}uA\right)=\frac{1}{\sigma_e}J_y^2 A \tag{5-26}$$

or:

$$\frac{\partial}{\partial t}\left(\rho e_t + \frac{B_y^2}{2\mu_0}\right) + \frac{\partial}{\partial x}\left(\rho h_t u + \frac{B_z^2}{\mu_0}u\right) = \frac{1}{\sigma_e}J_y^2 - \left(\rho h_t u + \frac{B_z^2}{\mu_0}u\right)\frac{1}{A}\frac{dA}{dx} \tag{5-27}$$

The system can be written in conservative form:

$$\frac{\partial}{\partial t}\begin{bmatrix}\rho\\ \rho u\\ B_y\\ \rho e_t + \frac{1}{2\mu_0}B_y^2\end{bmatrix} + \frac{\partial}{\partial x}\begin{bmatrix}\rho u\\ \rho u^2 + \left(P + \frac{1}{2\mu_0}B_y^2\right)\\ B_y u\\ \rho h_t u + \frac{1}{\mu_0}B_z^2 u\end{bmatrix} = \begin{bmatrix}-\rho u\frac{1}{A}\frac{dA}{dx}\\ -\rho u^2\frac{1}{A}\frac{dA}{dx}\\ \nu_e\frac{\partial^2 B_y}{\partial x^2}\\ \frac{1}{\sigma_e}J_y^2 - \rho h_t u\frac{1}{A}\frac{dA}{dx}\end{bmatrix} \tag{5-28}$$

Taking into account:

$$\rho e_t + \frac{1}{2\mu_0}B_y^2 u = \frac{P}{\gamma-1} + \frac{1}{2}\rho u^2 + \frac{1}{2\mu_0}B_y^2 u \qquad \rho h_t u + \frac{1}{\mu_0}B_y^2 u = \frac{\gamma}{\gamma-1}Pu + \frac{1}{2}\rho u^3 + \frac{1}{\mu_0}B_y^2 u \tag{5-29}$$

In primitive variables $\vec{V}^T = [\rho \quad u \quad B_y \quad P]$:

$$\frac{\partial}{\partial t}\begin{bmatrix}\rho\\ \rho u\\ B_y\\ \rho e_t + \frac{1}{2\mu_0}B_y^2\end{bmatrix} = \begin{bmatrix}1 & 0 & 0 & 0\\ u & \rho & 0 & 0\\ 0 & 0 & 1 & 0\\ \frac{1}{2}u^2 & \rho u & \frac{B_y}{\mu_0} & \frac{1}{\gamma-1}\end{bmatrix}\frac{\partial}{\partial t}\begin{bmatrix}\rho\\ u\\ B_y\\ P\end{bmatrix} = [L]\frac{\partial}{\partial t}\begin{bmatrix}\rho\\ u\\ B_y\\ P\end{bmatrix} \tag{5-30}$$

It can be shown that the above system is equivalent to:

$$\frac{\partial}{\partial t}\begin{bmatrix}\rho\\ u\\ B_y\\ P\end{bmatrix}+\begin{bmatrix}u & \rho & 0 & 0\\ 0 & u & \frac{1}{\rho}\frac{B_y}{\mu_0} & \frac{1}{\rho}\\ 0 & B_y & u & 0\\ 0 & \gamma P & 0 & u\end{bmatrix}\frac{\partial}{\partial x}\begin{bmatrix}\rho\\ u\\ B_y\\ P\end{bmatrix} \tag{5-31}$$

Eigenvalues of the system are:

$$det\begin{bmatrix}u-\lambda & \rho & 0 & 0\\ 0 & u-\lambda & \frac{1}{\rho}\frac{B_y}{\mu_0} & \frac{1}{\rho}\\ 0 & B_y & u-\lambda & 0\\ 0 & \gamma P & 0 & u-\lambda\end{bmatrix}= \tag{5-32}$$

$$=(u-\lambda)\left[(u-\lambda)^3-(u-\lambda)\frac{1}{\rho}\frac{B_y^2}{\mu_0}-(u-\lambda)\frac{\gamma P}{\rho}\right]= \tag{5-33}$$

$$\begin{aligned}(u-\lambda)\left[(u-\lambda)^3-(u-\lambda)\left(\frac{\gamma P}{\rho}+\frac{1}{\rho}\frac{B_y^2}{\mu_0}\right)\right]\\ =(u-\lambda)^2\left[(u-\lambda)^2-\left(\frac{\gamma P}{\rho}+\frac{1}{\rho}\frac{B_y^2}{\mu_0}\right)\right]=0\end{aligned} \tag{5-34}$$

$$\lambda_1=\lambda_2=u \qquad \lambda_3=u-\sqrt{\frac{\gamma P}{\rho}+\frac{1}{\rho}\frac{B_y^2}{\mu_0}} \qquad \lambda_4=u+\sqrt{\frac{\gamma P}{\rho}+\frac{1}{\rho}\frac{B_y^2}{\mu_0}} \tag{5-35}$$

The quantity $c_s=\sqrt{\gamma P/\rho}$ is the ***Acoustic Wave Speed***, accounting for the velocity of propagation of pressure perturbations, while $c_a=\sqrt{B_y^2/\rho\mu_0}$ is the so-called ***Alfven Wave Speed***, i.e., the velocity of propagation of magnetic perturbations. For this reason, the term $\sqrt{c_s^2+c_a^2}$ gives rise to the ***Magneto-Acoustic Wave Speed***.

RIGHT EIGENVECTORS

Let's consider the ***Right Eigenvectors***. For $\lambda_{1,2}=u$:

$$\begin{bmatrix} 0 & \rho & 0 & 0 \\ 0 & 0 & \frac{1}{\rho}\frac{B_y}{\mu_0} & \frac{1}{\rho} \\ 0 & B_y & 0 & 0 \\ 0 & \gamma P & 0 & 0 \end{bmatrix} \begin{bmatrix} \delta\rho \\ \delta u \\ \delta B_y \\ \delta P \end{bmatrix} = \begin{bmatrix} 0 \\ 0 \\ 0 \\ 0 \end{bmatrix} \tag{5-36}$$

giving:

$$\begin{aligned} &\delta u = 0 \quad \delta P \\ &= -\frac{B_y}{\mu_0}\delta B_y \quad for\ any\ \delta\rho, \delta B_y, or\ equivalently \begin{bmatrix} \delta\rho \\ 0 \\ \delta B_y \\ -\frac{B_y}{\mu_0}\delta B_y \end{bmatrix} \end{aligned} \tag{5-37}$$

For $\lambda_{3,4} = u \mp \sqrt{\gamma P/\rho + B_y^2/\rho\mu_0}$:

$$\begin{bmatrix} \pm\sqrt{\frac{\gamma P}{\rho} + \frac{1}{\rho}\frac{B_y^2}{\mu_0}} & \rho & 0 & 0 \\ 0 & \pm\sqrt{\frac{\gamma P}{\rho} + \frac{1}{\rho}\frac{B_y^2}{\mu_0}} & \frac{1}{\rho}\frac{B_y}{\mu_0} & \frac{1}{\rho} \\ 0 & B_y & \pm\sqrt{\frac{\gamma P}{\rho} + \frac{1}{\rho}\frac{B_y^2}{\mu_0}} & 0 \\ 0 & \gamma P & 0 & \pm\sqrt{\frac{\gamma P}{\rho} + \frac{1}{\rho}\frac{B_y^2}{\mu_0}} \end{bmatrix} \begin{bmatrix} \delta\rho \\ \delta u \\ \delta B_y \\ \delta P \end{bmatrix} = \begin{bmatrix} 0 \\ 0 \\ 0 \\ 0 \end{bmatrix} \tag{5-38}$$

giving:

$$\begin{aligned} &\delta u = \mp\sqrt{\frac{\gamma P}{\rho} + \frac{1}{\rho}\frac{B_y^2}{\mu_0}}\frac{\delta\rho}{\rho} \quad \delta P = \mp\frac{\gamma P}{\sqrt{\frac{\gamma P}{\rho} + \frac{1}{\rho}\frac{B_y^2}{\mu_0}}}\delta u = \frac{\gamma P}{\rho}\delta\rho \quad \delta B_y \\ &= \pm\frac{B_y}{\rho}\delta\rho \quad for\ any\ \delta\rho \end{aligned} \tag{5-39}$$

A STEADY PLASMA ACCELERATOR

A ***Steady Solution***, provided boundary conditions are steady as well, arises from dropping the time derivatives. In the next development, it will be assumed that the voltage is constant along the channel, this is, $HE_y = V = const$, so:

$$\frac{d}{dx}(\rho u A) = \frac{d\dot{m}}{dx} = 0 \quad \rightarrow \quad \dot{m} = \rho u A = const. \tag{5-40}$$

$$\frac{d}{dx}\left[\rho u^2 + \left(P + \frac{1}{2\mu_0}B_z^2\right)\right] = -\rho u^2 \frac{1}{A}\frac{dA}{dx} \tag{5-41}$$

$$\rightarrow \ \rho u \frac{du}{dx} + u\frac{d}{dx}(\rho u) + \rho u^2 \frac{1}{A}\frac{dA}{dx} + \frac{d}{\partial x}\left(P + \frac{1}{2\mu_0}B_z^2\right) = 0 \tag{5-42}$$

$$\rightarrow \ \rho u \frac{du}{dx} + \frac{d}{dx}\left(P + \frac{1}{2\mu_0}B_z^2\right) = 0 \tag{5-43}$$

$$\frac{d}{dx}(\rho h_t u) = \frac{E_y}{\mu_0}\frac{dB_z}{dx} - \rho h_t u \frac{1}{A}\frac{dA}{dx} \ \rightarrow \ \frac{d}{dx}(\dot{m} h_t) = \frac{E_y}{\mu_0}\frac{dB_z}{dx}A$$
$$\rightarrow \ \rho u \frac{dh_t}{dx} = \frac{E_y}{\mu_0}\frac{dB_z}{dx} \tag{5-44}$$

It is convenient to ***consider a non-dimensional system***, using the following reference quantities:

$$B_{ref} = B_0 \qquad u_{ref} = \frac{B_0^2 A^*}{2\mu_0 \dot{m}} \qquad h_{ref} = u_{ref}^2$$

(5-45)

$$P_{ref} = \frac{B_0^2}{2\mu_0} \qquad \rho_{ref} = \frac{P_{ref}}{h_{ref}} = \frac{2\mu_0}{B_0^2}\left(\frac{\dot{m}}{A^*}\right)^2$$

$$E_{ref} = B_{ref} u_{ref} = \frac{B_0^3 A^*}{2\mu_0 \dot{m}} \qquad J_{ref} = \frac{B_{ref}}{\mu_0 L} \qquad A_{ref} = A^*$$
$$x_{ref} = L \qquad V_{ref} = E_{ref} H^* \tag{5-46}$$

The 'star' superscript stands for the axial section where the flow is critical (i.e., the so-called ***Magneto-Sonic Conditions***, as it will be seen later).
The non-dimensional variables are defined as follows:

$$\tilde{B} = \frac{B_z}{B_0} \qquad \tilde{u} = \frac{u}{u_{ref}} \qquad \tilde{P} = \frac{P}{P_{ref}} \qquad \tilde{\rho} = \frac{\rho}{\rho_{ref}}$$
$$\tilde{h} = \frac{h}{h_{ref}} \qquad \tilde{E} = \frac{E_y}{E_{ref}} \tag{5-47}$$

$$\tilde{J} = \frac{J_y}{J_{ref}} \qquad a = \frac{A}{A^*} = \frac{H}{H^*} \qquad \tilde{x} = \frac{x}{L} \qquad \tilde{V} = \frac{V_y}{V_{ref}} \tag{5-48}$$

The above general equations in non-dimensional form read:

Continuity Equation:

$$\dot{m} = \rho u A = \tilde{\rho} \frac{2\mu_0}{B_0^2} \left(\frac{\dot{m}}{A^*}\right)^2 \tilde{u} \frac{B_0^2 A^*}{2\mu_0 \dot{m}} a A^* = \tilde{\rho}\tilde{u} a \dot{m} \quad \rightarrow \quad \tilde{\rho}\tilde{u} a = 1 \tag{5-49}$$

Momentum Equation:

$$\rho u \frac{du}{dx} + \frac{d}{dx}\left(P + \frac{1}{2\mu_0} B_z^2\right) = 0$$
$$\rightarrow \quad \tilde{\rho}\tilde{u} a \frac{\dot{m}}{A} \frac{d\tilde{u}}{d\tilde{x}} \frac{B_0^2 A^*}{2\mu_0 \dot{m}} \frac{1}{L} + \frac{1}{L} \frac{B_0^2}{2\mu_0} \frac{d}{d\tilde{x}} \left(\tilde{P} + \tilde{B}^2\right) = 0 \tag{5-50}$$

$$\rightarrow \quad \tilde{\rho}\tilde{u} \frac{d\tilde{u}}{d\tilde{x}} + \frac{d}{d\tilde{x}} \left(\tilde{P} + \tilde{B}^2\right) = 0 \tag{5-51}$$

Energy Equation:

$$\rho u \frac{d}{dx}\left(h + \frac{u^2}{2}\right) = \frac{E_y}{\mu_0}\frac{dB_z}{dx} \quad \rightarrow \quad \tilde{\rho}\tilde{u}\frac{P_{ref}}{h_{ref}}\frac{u_{ref}}{L}\frac{d}{d\tilde{x}}\left(\tilde{h} + \frac{\tilde{u}^2}{2}\right) = \tilde{E}B_{ref}u_{ref}\frac{B_{ref}}{\mu_0 L}\frac{d\tilde{B}}{d\tilde{x}} \tag{5-52}$$

$$\rightarrow \quad \tilde{\rho}\tilde{u}\frac{d}{d\tilde{x}}\left(\tilde{h} + \frac{\tilde{u}^2}{2}\right) = 2\tilde{E}\frac{d\tilde{B}}{d\tilde{x}} \tag{5-53}$$

If one multiply both sides by a, since $\bar{E}a = \bar{V} = const.$, one gets the integral (calling $\mathbf{0} \equiv \boldsymbol{inlet}$):

$$\tilde{h} + \frac{\tilde{u}^2}{2} - 2\tilde{V}\tilde{B} = \tilde{h}_0 + \frac{\tilde{u}_0^2}{2} - 2\tilde{V} \tag{5-54}$$

Alternatively, the internal energy equation is obtained subtracting the momentum equation by $\bar{u}$, yielding:

$$\tilde{\rho}\tilde{u}\frac{d\tilde{h}}{d\tilde{x}} - \tilde{u}\frac{d\tilde{P}}{d\tilde{x}} - 2\tilde{u}\tilde{B}\frac{d\tilde{B}}{d\tilde{x}} = -2\tilde{E}\frac{d\tilde{B}}{d\tilde{x}} \tag{5-55}$$

Ohm's Law:

$$J_y = \sigma_e\left(E_y - uB_z\right) \quad \rightarrow \quad \tilde{J}\frac{B_{ref}}{\mu_0 L} = \sigma_e B_{ref}u_{ref}\left(\tilde{E} - \tilde{u}\tilde{B}\right) \tag{5-56}$$

The ***Magnetic Reynolds Number*** and its inverse are defined as:

$$R_m = \sigma_e\mu_0 u_{ref}L = \frac{B_0^2 A^*\sigma_e L}{2\dot{m}} \qquad \varepsilon = \frac{2\dot{m}}{B_0^2 A^*\sigma_e L} \tag{5-57}$$

Then ***Non-Dimensional Ohm's Law*** then yields:

$$\varepsilon\tilde{J} = \tilde{E} - \tilde{u}\tilde{B} \tag{5-58}$$

Also:

$$J_y = -\mu_0 \frac{dB_z}{dx} = -\mu_0 \tilde{J} \frac{B_{ref}}{\mu_0 L} = \frac{d\tilde{B}}{d\tilde{x}} \frac{B_{ref}}{L} \quad \rightarrow \quad \tilde{J} = -\frac{d\tilde{B}}{d\tilde{x}} \tag{5-59}$$

And the ***Energy Equation*** becomes:

$$\tilde{\rho}\tilde{u}\frac{d\tilde{h}}{d\tilde{x}} - \tilde{u}\frac{d\tilde{P}}{d\tilde{x}} = 2\bar{u}\bar{B}\frac{d\tilde{B}}{d\tilde{x}} - 2\tilde{E}\frac{d\tilde{B}}{d\tilde{x}} = 2\varepsilon\tilde{J}^2 \tag{5-60}$$

The voltage changes according to:

$$V_y = E_y H \quad \rightarrow \quad \tilde{V}V_{ref} = \tilde{E}E_{ref}H^* a \quad \rightarrow \quad \widetilde{\tilde{V}} = \tilde{E}a \tag{5-61}$$

For realistic MPD thrusters, ε is of the order of 0.1 – 0.3.

In plasma accelerators, the magnetic contribution is dominant over the pressure contribution. Then, for the sake of simplicity, aiming easy computations that will give some light into the behavior of a plasma accelerator, let us neglect by now the pressure contribution and assume the case of constant area, i.e., $a = 1$.

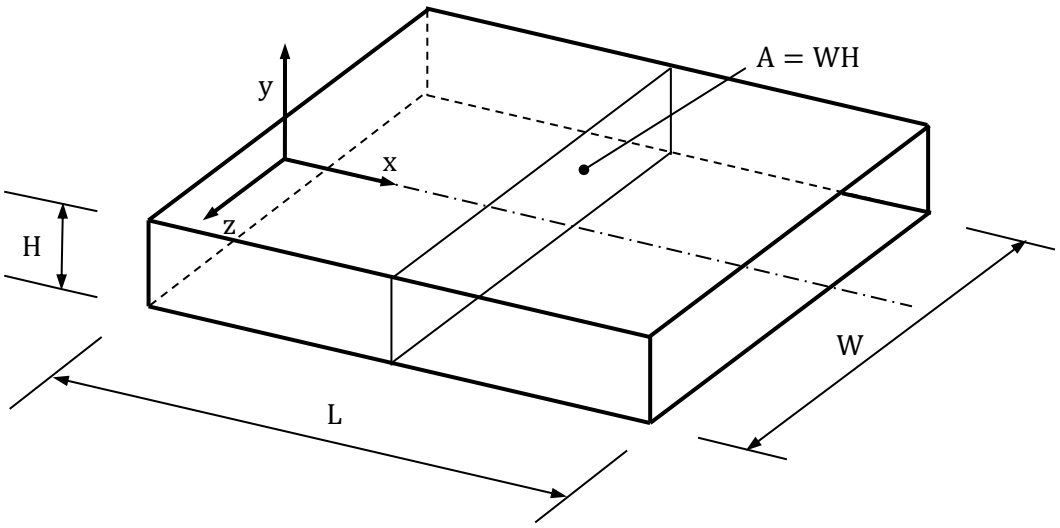

Figure 5-3: Duct with constant area.

The ***Momentum Equation*** is then easily integrated, giving:

$$\tilde{u} = \tilde{u}_0 + 1 - \tilde{B}^2 \tag{5-62}$$

As it will be shown in next chapters, $\tilde{u}_0 \ll 1$, so it can be dropped. ***Ohm's Law*** becomes:

$$\tilde{J} = -\frac{d\tilde{B}}{d\tilde{x}} = \frac{1}{\varepsilon}\left(\tilde{E} - \tilde{u}\tilde{B}\right) = \frac{1}{\varepsilon}\left[\tilde{E} - \tilde{B}\left(1 - \tilde{B}^2\right)\right] \tag{5-63}$$

Since:

$$\tilde{E} = \frac{2\mu_0 \dot{m}}{B_0^3 A} E_y = \frac{2\dot{m}}{B_0^2 A \sigma_e L} \frac{\mu_0 \sigma_e L}{B_0} E = \varepsilon \frac{\mu_0 \sigma_e L}{B_0} E \tag{5-64}$$

The axial position is related to the Magnetic Field through:

$$\tilde{x} = \varepsilon \int_{\hat{B}}^{1} \frac{d\tilde{B}}{\tilde{E} - \tilde{B}\left(1 - \tilde{B}^2\right)} \tag{5-65}$$

Assuming the values:

$$\sigma = 1000\, S/m \qquad V = 32\, V \quad H = 0.04\, m \quad W = 0.16\, m \quad B_0 = 0.12\, T \tag{5-66}$$

$$\tilde{E} = \frac{2\mu_0 \dot{m}}{B_0^3 A} E_y = 1.09083 \tag{5-67}$$

Aiming for a total magnetic expansion, up to $\tilde{B} = 0$, one gets a ***Total Length***:

$$L = \frac{2\dot{m}}{\sigma w H B_0^2} \int_0^1 \frac{d\tilde{B}}{\tilde{E} - \tilde{B}\left(1 - \tilde{B}^2\right)} = \frac{2\dot{m}}{\sigma w H B_0^2} 1.21131 = 1.5772 \cdot 10^{-1} m = 15.77\, cm \tag{5-68}$$

The Current Density is:

$$\tilde{J} = \frac{1}{\varepsilon}\left[\tilde{E} - \tilde{B}\left(1 - \tilde{B}^2\right)\right] \qquad (5\text{-}69)$$

This expression reveals a maximum of $\bar{J}$ close to the inlet and outlet of the channel, since the factor $\tilde{B}\left(1 - \tilde{B}^2\right)$ decays to zero there.

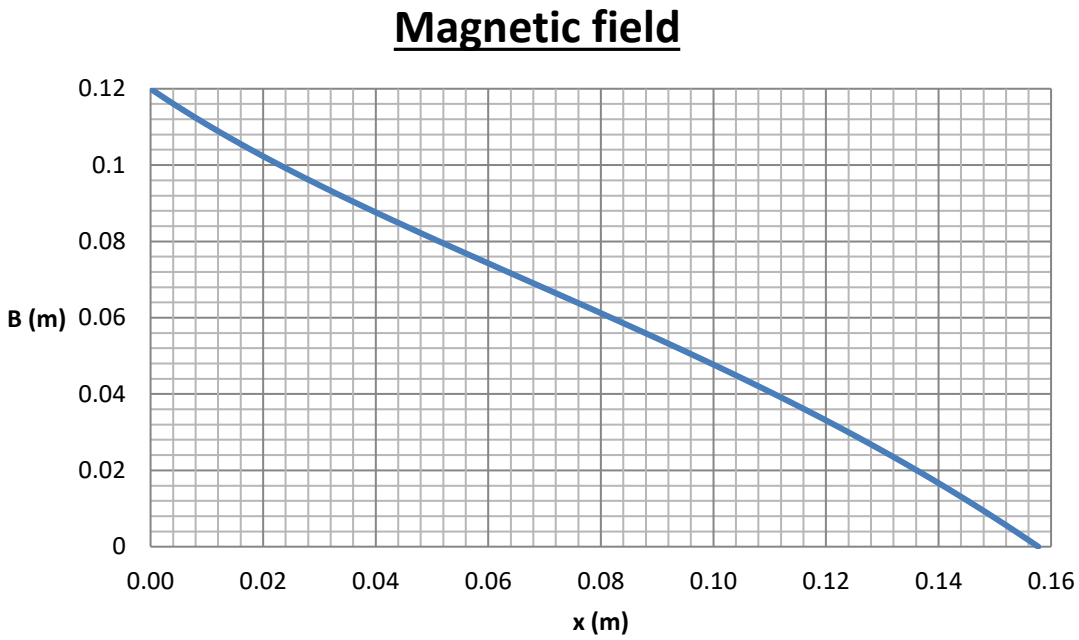

Figure 5-4: Magnetic field vs positioon along the channel.

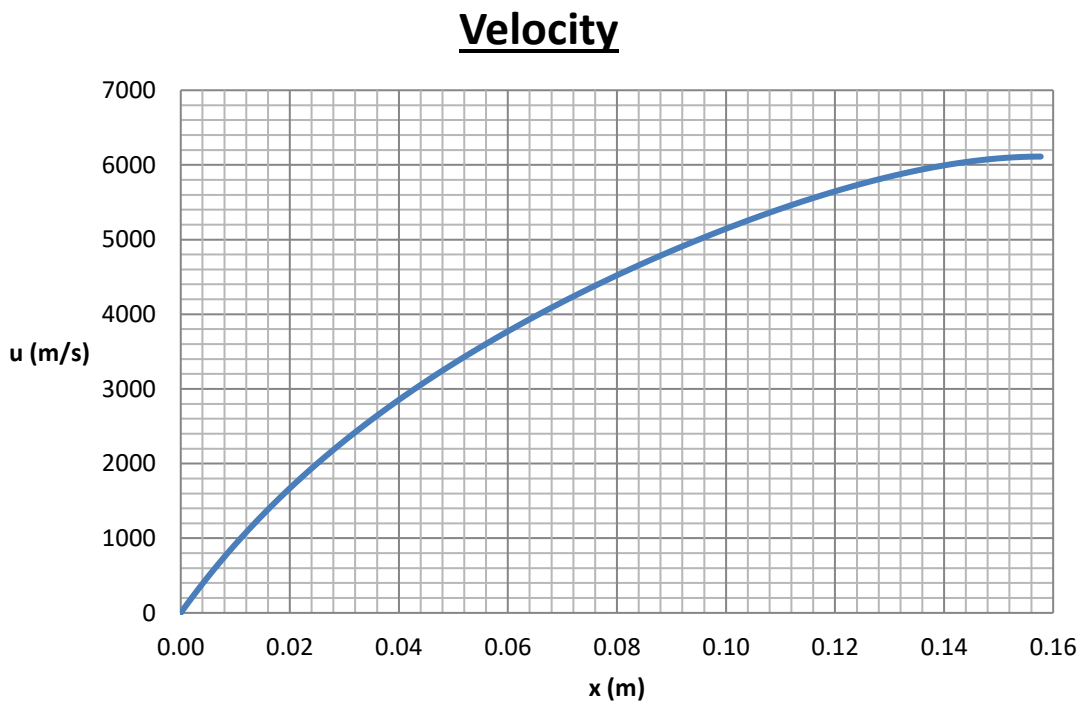

Figure 5-5: Velocity vs position along the channel.

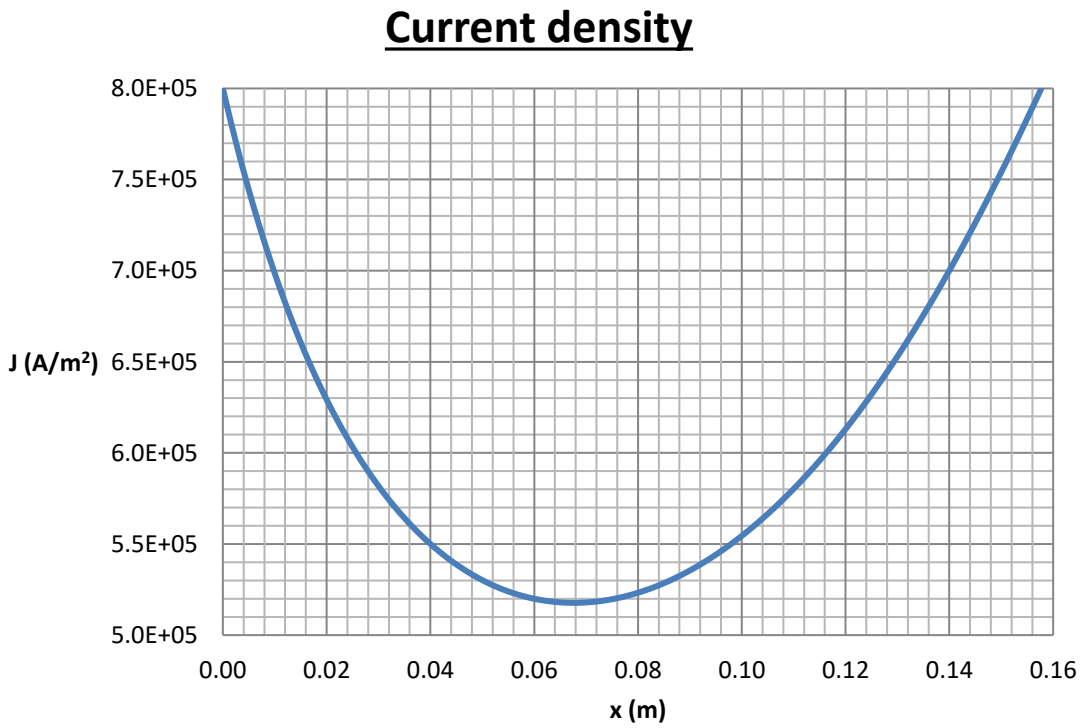

Figure 5-6: Current Density vs position along the channel.

THE ZEROTH ORDER SOLUTION

In the limit for $\varepsilon \to 0$, the above system becomes singular. Indeed, the above expressions for planar duct yield:

$$\left[\tilde{E} - \tilde{B}\left(1 - \tilde{B}^2\right)\right] = 0 \qquad (5\text{-}70)$$

This algebraic equation gives $\bar{B} = const.$, and $\bar{J} = 0$. However, since really $\neq 0$, neither of these two asymptotic results occur. But what physically does occur is that, as a consequence of the imposed boundary conditions, properties change rapidly across two (thin) layers at the inlet and outlet. So, one can distinguish three zones: the so-called ***Outer Zone***, where ε is assumed zero, and the ***Two Thin Layers***.

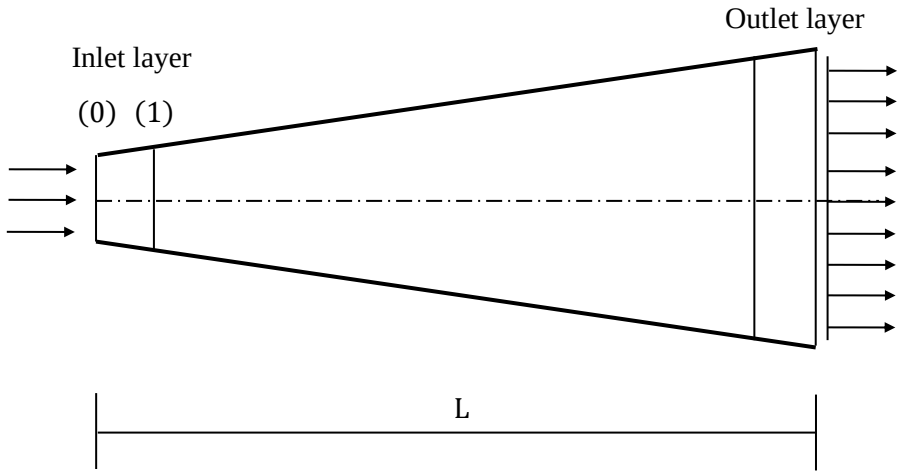

Figure 5-7: Representation of the Outer Zone and the Two Thin Layers.

For the ***Outer Zone*** (with superscript "o") the ***Energy Equation*** reduces to the expression of isentropic flow, since:

$$\tilde{\rho}^o \tilde{u}^o \frac{d\tilde{h}^o}{d\tilde{x}} - \tilde{u}^o \frac{d\tilde{P}^o}{d\tilde{x}} = 0 \quad \to \quad \frac{d\tilde{h}^o}{d\tilde{x}} = \frac{1}{\tilde{\rho}^o} \frac{d\tilde{P}^o}{d\tilde{x}} \qquad (5\text{-}71)$$

The ***Ohm's Law*** turns into:

$$\tilde{E}^o = \tilde{u}^o \tilde{B}^o \quad \to \quad \tilde{u}^o = \frac{\tilde{E}^o}{\tilde{B}^o} \qquad (5\text{-}72)$$

Using the ***Continuity Equation*** $\tilde{\rho}^o \tilde{u}^o a = 1$, combined with $\tilde{V}^o = \tilde{E}^o a$, one gets:

$$\frac{\tilde{B}^o}{\tilde{\rho}^o} = \tilde{E}^o a = \tilde{V} = const. \tag{5-73}$$

One may define the equivalent pressure as a quantity that accounts for both the ***Gas Pressure*** and the ***Magnetic Pressure*** (i.e., magnetic energy per unit volume) as they appear in the momentum equation:

$$\tilde{P}^o_{eq} = \tilde{P}^o + \left(\tilde{B}^o\right)^2 \tag{5-74}$$

This pressure is a function of density, then, the ***Magneto-Sonic Speed*** will be:

$$\tilde{c}^o = \sqrt{\frac{d\tilde{P}^o_{eq}}{d\tilde{\rho}^o}} = \sqrt{\frac{d\tilde{P}^o}{d\tilde{\rho}^o} + 2\tilde{\rho}^o \tilde{V}^2} = \sqrt{(\tilde{c}^o_s)^2 + (\tilde{c}^o_a)^2} \tag{5-75}$$

With $\tilde{c}^o_s$ and $\tilde{c}^o_a$ being, respectively, the (***non-dimensional) speed of sound*** and the ***Alfven Speed***:

$$(\tilde{c}^o_s)^2 = \frac{d\tilde{P}^o}{d\tilde{\rho}^o} = \frac{dP^o}{d\rho^o}\frac{\rho_{ref}}{P_{ref}} = \gamma \frac{P^o}{\rho^o}\left(\frac{2\mu_0}{B_0^2}\rho^* u^*\right)^2 \tag{5-76}$$

$$(\tilde{c}^o_a)^2 = \frac{1}{\rho^o}\frac{(B^o_z)^2}{\mu_0}\left(\frac{2\mu_0}{B_0^2}\rho^* u^*\right)^2 \tag{5-77}$$

Recovering dimensional units:

$$\begin{aligned} c^o = \tilde{c}^o \frac{B_0^2 \rho^* u^*}{2\mu_0} &= \sqrt{\left(\tilde{c}^o_s \frac{B_0^2 \rho^* u^*}{2\mu_0}\right)^2 + 2\tilde{B}^o \tilde{E}^o a \left(\frac{B_0^2 \rho^* u^*}{2\mu_0}\right)^2} \\ &= \sqrt{\gamma \frac{P^o}{\rho^o} + \frac{1}{\rho^o}\frac{(B^o_z)^2}{\mu_0}} \end{aligned} \tag{5-78}$$

It is well known that for conventional nozzles, the flow can only reach sonic conditions at the nozzle throat, provided the downstream pressure at the divergent section is low enough.

In a similar way, now in plasmas, assuming subcritical inlet flow, for a given flow rate and throat area, the existence of ***Magneto-Sonic Chocked Flow*** will depend on the upstream conditions, i.e., the conditions immediately past the thin inlet layer.

At the sections (0) and (1) of the ***Inlet Layer*** the flow conditions are, respectively, $\tilde{\rho}_0^i$, $\tilde{u}_0^i$, $\tilde{B}_0^i$, $\tilde{P}_0^i$, and $\tilde{\rho}_1^i$, $\tilde{u}_1^i$, $\tilde{B}_1^i$, $\tilde{P}_1^i$. Since the layer is assumed very thin (of the order of ε), the area within it changes very little, so it can be taken roughly constant. For the ***Inner Zone*** it is convenient to rescale distances with ε, i.e., $\xi_i = \tilde{x}/\varepsilon$. The equations in the inner zone are then:

$$\tilde{\rho}^i \tilde{u}^i = \bar{\rho}_0 \bar{u}_0 \tag{5-79}$$

$$\frac{1}{a_0}\frac{d\tilde{u}^i}{d\xi_i} + \frac{d}{d\xi_i}\left[\tilde{P}^i + \left(\tilde{B}^i\right)^2\right] = 0 \tag{5-80}$$

$$\tilde{h}^i + \frac{\left(\tilde{u}^i\right)^2}{2} - 2\tilde{V}\tilde{B}^i = \tilde{h}_0 + \frac{\tilde{u}_0^2}{2} - 2\tilde{V} \tag{5-81}$$

$$\frac{d\tilde{B}^i}{d\xi_i} = \tilde{E}^i - \tilde{u}^i\tilde{B}^i \qquad \tilde{E}^i = \frac{\tilde{V}}{a_0} \tag{5-82}$$

The ***Momentum Equation*** is easily integrated:

$$\tilde{u}^i = \tilde{u}_0 + a_0\left(\tilde{P}_0 - \tilde{P}^i\right) + a_0\left[\left(\tilde{B}_0\right)^2 - \left(\tilde{B}^i\right)^2\right] \tag{5-83}$$

The ***Matching Conditions for the Inner and Outer Zone*** are:

$$\tilde{\rho}_1^i \tilde{u}_1^i = \tilde{\rho}_1^o \tilde{u}_1^o \tag{5-84}$$

$$\tilde{u}_1^o = \tilde{u}_1^i = \tilde{u}_0 + a_0\left(\tilde{P}_0 - \tilde{P}_1^o\right) + a_0\left[\left(\tilde{B}_0\right)^2 - \left(\tilde{B}_1^o\right)^2\right] \tag{5-85}$$

$$\tilde{h}_1^o + \frac{\left(\tilde{u}_1^o\right)^2}{2} - 2\tilde{V}\tilde{B}_1^o = \tilde{h}_{t0} - 2\tilde{V} \tag{5-86}$$

Since the $\tilde{B}^i$ must tend smoothly to the value of the outer zone, the derivative $d\tilde{B}^i/d\xi_i$ must necessarily tend to zero, yielding:

$$\tilde{V} = a_0 \tilde{u}_1^o \tilde{B}_1^o \tag{5-87}$$

Assuming known $\tilde{u}_0$, one computes $\tilde{\rho}_0$, from continuity, and then $\tilde{P}_0$, from $\tilde{h}_{t0}$.

NUMERICAL SCHEME TO SOLVE THE COMPLETE SET OF EQUATIONS

For the numerical integration of the complete set of equations, the equations must be solved for each individual derivative:

$$\frac{1}{\tilde{\rho}}\frac{d\tilde{\rho}}{d\tilde{x}} + \frac{1}{\tilde{u}}\frac{d\tilde{u}}{d\tilde{x}} = -\frac{1}{a}\frac{da}{d\tilde{x}} \tag{5-88}$$

$$\tilde{\rho}\tilde{u}\frac{d\tilde{u}}{d\tilde{x}} + \frac{d\tilde{P}}{d\tilde{x}} + 2\tilde{B}\frac{d\tilde{B}}{d\tilde{x}} = 0 \tag{5-89}$$

$$\tilde{\rho}\tilde{u}\frac{d\tilde{h}}{d\tilde{\rho}}\frac{d\tilde{\rho}}{d\tilde{x}} + \tilde{\rho}\tilde{u}\frac{d\tilde{h}}{d\tilde{P}}\frac{d\tilde{P}}{d\tilde{x}} + \tilde{\rho}\tilde{u}^2\frac{d\tilde{u}}{d\tilde{x}} + 2\frac{\tilde{V}}{a}\frac{d\tilde{B}}{d\tilde{x}} = 0 \tag{5-90}$$

Being $\tilde{h} = \tilde{h}(\tilde{\rho}, \tilde{P})$

$$\frac{d\tilde{B}}{d\tilde{x}} = -\frac{1}{\varepsilon}\left(\tilde{E} - \tilde{u}\tilde{B}\right) \tag{5-91}$$

If one solves for the individual derivatives, this system can also be expressed as:

$$\frac{d\tilde{\rho}}{d\tilde{x}} = \frac{1}{\tilde{u}^2 - \tilde{c}_s^2}\left\{-\tilde{\rho}\tilde{u}^2\frac{1}{a}\frac{da}{d\tilde{x}} + \frac{2}{\varepsilon\tilde{u}}[(\gamma-1)\tilde{E} - \gamma\tilde{u}\tilde{B}]\left(\tilde{E} - \tilde{u}\tilde{B}\right)\right\} \tag{5-92}$$

$$\frac{d\tilde{u}}{d\tilde{x}} = \frac{1}{\tilde{u}^2 - \tilde{c}_s^2}\left\{\tilde{c}_s^2\tilde{u}\frac{1}{a}\frac{da}{d\tilde{x}} - \frac{2}{\varepsilon\tilde{\rho}}[(\gamma-1)\tilde{E} - \gamma\tilde{u}\tilde{B}]\left(\tilde{E} - \tilde{u}\tilde{B}\right)\right\} \tag{5-93}$$

$$\frac{d\tilde{B}}{d\tilde{x}} = -\frac{1}{\varepsilon}\left(\tilde{E} - \tilde{u}\tilde{B}\right) \tag{5-94}$$

$$\begin{aligned}\frac{d\tilde{P}}{d\tilde{x}} = \frac{1}{\tilde{u}^2 - \tilde{c}_s^2}\Big\{&-\gamma\tilde{P}\tilde{u}^2\frac{1}{a}\frac{da}{d\tilde{x}} \\ &+ \frac{2}{\varepsilon}[(\gamma-1)\tilde{E}\tilde{u} - \tilde{B}(\gamma-1)\tilde{u}^2 - \tilde{B}\tilde{c}_s^2]\left(\tilde{E} - \tilde{u}\tilde{B}\right)\Big\}\end{aligned} \tag{5-95}$$

A singularity arises for $\tilde{u} = \tilde{c}_s$. But, since the numerators of $\frac{d\tilde{\rho}}{d\tilde{x}}$ and $\frac{d\tilde{u}}{d\tilde{x}}$ are:

$$\begin{aligned}-\tilde{u}^2\frac{\tilde{\rho}}{a}\frac{da}{d\tilde{x}} + \frac{2}{\varepsilon\tilde{u}}[(\gamma-1)\tilde{E} - \gamma\tilde{u}\tilde{B}]\left(\tilde{E} - \tilde{u}\tilde{B}\right) \\ = \frac{1}{\tilde{u}}\left[-\tilde{u}^2\frac{\tilde{\rho}\tilde{u}}{a}\frac{da}{d\tilde{x}} + \frac{2}{\varepsilon}[(\gamma-1)\tilde{E} - \gamma\tilde{u}\tilde{B}]\left(\tilde{E} - \tilde{u}\tilde{B}\right)\right]\end{aligned} \tag{5-96}$$

$$\begin{aligned}\tilde{c}_s^2\tilde{u}\frac{1}{a}\frac{da}{d\tilde{x}} - \frac{2}{\varepsilon\tilde{\rho}}[(\gamma-1)\tilde{E} - \gamma\tilde{u}\tilde{B}]\left(\tilde{E} - \tilde{u}\tilde{B}\right) \\ = \frac{1}{\tilde{\rho}}\left[\tilde{c}_s^2\frac{\tilde{\rho}\tilde{u}}{a}\frac{da}{d\tilde{x}} - \frac{2}{\varepsilon}[(\gamma-1)\tilde{E} - \gamma\tilde{u}\tilde{B}]\left(\tilde{E} - \tilde{u}\tilde{B}\right)\right]\end{aligned} \tag{5-97}$$

A necessary condition to null both expressions simultaneously is certainly $\tilde{u} = \tilde{c}_s$. Under this hypothesis, the numerator of $d\tilde{P}/d\tilde{x}$ is also zero and the derivatives become indeterminate of the type $0/0$. However, the smoothness of the sonic passage implies a constrain for $\tilde{E}$, in the sense that the indeterminations yield finite values in the limit $\tilde{u} \to \tilde{c}_s$. The development gives rise to a quadratic expression in terms of $d\tilde{u}/d\tilde{x}$. Care must be taken, however, so as to ensure that the positive value for $d\tilde{u}/d\tilde{x}$ is chosen, consistently with the continuous acceleration of the plasma.

CONSTANT AREA DUCT

Let's consider now a particular case: a ***constant area duct***. In this case $a \equiv 1$, so we get $\tilde{E} = \tilde{V}$, and the expression for the velocity derivative becomes:

$$\frac{d\tilde{u}}{d\tilde{x}} = -\frac{1}{\tilde{u}^2 - \tilde{c}_s^2}\left\{\frac{2}{\varepsilon\tilde{\rho}}[(\gamma-1)\tilde{E} - \gamma\tilde{u}\tilde{B}]\left(\tilde{E} - \tilde{u}\tilde{B}\right)\right\} \tag{5-98}$$

The smoothness through the sonic passage implies that the numerator is zero too. Thus, we get two roots:

$$\tilde{u} = \frac{\gamma - 1}{\gamma}\frac{\tilde{E}}{\tilde{B}} \tag{5-99}$$

$$\tilde{u} = \frac{\tilde{E}}{\tilde{B}} \tag{5-100}$$

Since the product $\tilde{u}\tilde{B}$ increases through the channel, the first root is expected to be associated to the sonic passage, while the second one to a supersonic flow.
Hence, the set of ordinary differential equation becomes:

$$\frac{1}{\tilde{\rho}}\frac{d\tilde{\rho}}{d\tilde{x}} + \frac{1}{\bar{u}}\frac{d\tilde{u}}{d\tilde{x}} = 0 \Longrightarrow \tilde{\rho}\tilde{u} = \tilde{\rho}_0\tilde{u}_0 = 1 \tag{5-101}$$

$$\tilde{\rho}\tilde{u}\frac{d\tilde{u}}{d\tilde{x}} + \frac{d\tilde{P}}{d\tilde{x}} + 2\tilde{B}\frac{d\tilde{B}}{d\tilde{x}} = 0 \Longrightarrow \tilde{u} + \tilde{P} + \tilde{B}^2 = \tilde{u}_0 + \tilde{P}_0 + \tilde{B}_0 = \tilde{u}_0 + \tilde{P}_0 + 1 \tag{5-102}$$

$$\tilde{\rho}\tilde{u}\frac{d\tilde{h}}{d\tilde{\rho}}\frac{d\tilde{\rho}}{d\tilde{x}} + \tilde{\rho}\tilde{u}\frac{d\tilde{h}}{d\tilde{P}}\frac{d\tilde{P}}{d\tilde{x}} + \tilde{\rho}\tilde{u}^2\frac{d\tilde{u}}{d\tilde{x}} + 2\frac{\tilde{V}}{a}\frac{d\tilde{B}}{d\tilde{x}} = 0 \tag{5-103}$$

and, remembering that $\tilde{\rho}\tilde{u} = 1,\ \tilde{B}_0 = 1$ and also $a = 1$ and being:

$$\int \frac{d\tilde{h}}{d\tilde{\rho}}\frac{d\tilde{\rho}}{d\tilde{x}} + \frac{d\tilde{h}}{d\tilde{P}}\frac{d\tilde{P}}{d\tilde{x}} + \int \tilde{u}\frac{d\tilde{u}}{d\tilde{x}} = \left(\tilde{h} + \frac{\tilde{u}^2}{2}\right) - \left(\tilde{h}_0 + \frac{\tilde{u}_0^2}{2}\right) \tag{5-104}$$

we get:

$$\Longrightarrow \left(\tilde{h} + \frac{\tilde{u}^2}{2}\right) - \left(\tilde{h}_0 + \frac{\tilde{u}_0^2}{2}\right) + 2\tilde{V}\left(\tilde{B} - 1\right) = 0 \tag{5-105}$$

Now, for a calorically perfect gas we can write:

$$\frac{\gamma}{\gamma - 1}\frac{\tilde{P}}{\tilde{\rho}} + \frac{\tilde{u}^2}{2} - \tilde{h}_{t0} + 2\tilde{V}\left(\tilde{B} - 1\right) = 0 \tag{5-106}$$

being:

$$\tilde{h}_{t0} = \tilde{h}_0 + \frac{\tilde{u}_0^2}{2} \tag{5-107}$$

and, remembering that $\gamma \frac{\tilde{P}}{\tilde{\rho}} = \tilde{u}_s^2$ using the first root:

$$\tilde{u}_s = \frac{\gamma - 1}{\gamma}\frac{\tilde{E}}{\tilde{B}_s} \tag{5-108}$$

$$\frac{1}{\gamma - 1}\tilde{u}_s^2 + \frac{\tilde{u}_s^2}{2} - \tilde{h}_{t0} + 2\tilde{V}\left(\tilde{B}_s - 1\right) = 0 \tag{5-109}$$

$$\frac{\gamma + 1}{2(\gamma - 1)}\left(\frac{\gamma - 1}{\gamma}\frac{\tilde{V}}{\tilde{B}_s}\right)^2 - \tilde{h}_{t0} + 2\tilde{V}\left(\tilde{B}_s - 1\right) = 0 \tag{5-110}$$

Being $\tilde{E} = \tilde{V}$, since $a = 1$. Thus, we can write:

$$\frac{\gamma - 1}{\gamma}\frac{\tilde{E}}{\tilde{B}_s} + \tilde{P}_s + \tilde{B}_s = \tilde{u}_0 + \tilde{P}_0 + 1 \tag{5-111}$$

$$\Longrightarrow \tilde{P}_s = \frac{\tilde{\rho}_s}{\gamma}\gamma\frac{\tilde{P}_s}{\tilde{\rho}_s} = \frac{1}{\gamma\tilde{u}_s}\tilde{u}_s^2 = \frac{\tilde{u}_s}{\gamma} = \frac{\gamma - 1}{\gamma^2}\frac{\tilde{E}}{\tilde{B}_s} \tag{5-112}$$

$$\Longrightarrow \frac{\gamma-1}{\gamma}\frac{\tilde{V}}{\tilde{B}_s}+\frac{\gamma-1}{\gamma^2}\frac{\tilde{V}}{\tilde{B}_s}+\tilde{B}_s^2=\tilde{u}_0+\tilde{P}_0+1 \tag{5-113}$$

$$\Longrightarrow \frac{\gamma^2-1}{\gamma^2}\frac{\tilde{V}}{\tilde{B}_s}+\tilde{B}_s^2=\tilde{u}_0+\tilde{P}_0+1 \tag{5-114}$$

so, after some passages:

$$\Longrightarrow \tilde{u}^2-\frac{2\gamma}{\gamma+1}\left(\tilde{u}_0+\tilde{P}_0+1-\tilde{B}^2\right)\tilde{u}+\frac{2(\gamma-1)}{\gamma+1}\left[\tilde{h}_{t0}+2\tilde{V}\left(1-\tilde{B}\right)\right]=0 \tag{5-115}$$

that certainly gives $\tilde{u}\left(\tilde{B}\right)$. For a given value of $\bar{B}$, two possible solutions for $\tilde{u}$ exist, one supersonic and the other subsonic:

$$\tilde{u}=\frac{\gamma}{\gamma+1}\left(\tilde{u}_0+\tilde{P}_0+1-\tilde{B}^2\right)\pm\sqrt{\left[\frac{\gamma}{\gamma+1}\left(\tilde{u}_0+\tilde{P}_0+1-\tilde{B}^2\right)\right]^2-\frac{2(\gamma-1)}{\gamma+1}\left[\tilde{h}_{t0}+2\tilde{V}\left(1-\tilde{B}\right)\right]} \tag{5-116}$$

A smooth sonic passage is obtained by forcing the determinant to be zero, yielding:

$$\left[\left(\tilde{u}_0+\tilde{P}_0+1\right)-\tilde{B}^2\right]^2=\frac{2(\gamma^2-1)}{\gamma^2}\tilde{h}_{t0}+\frac{2(\gamma^2-1)}{\gamma^2}2\tilde{V}\left(1-\tilde{B}\right) \tag{5-117}$$

Together with the condition $\tilde{u}=\tilde{c}_s$:

$$\tilde{u}=\tilde{c}_s=\sqrt{\gamma\frac{\tilde{P}}{\tilde{\rho}}}=\sqrt{\gamma\tilde{h}}\quad\rightarrow\quad\tilde{u}^2=\frac{2\gamma}{2+\gamma}\left[\tilde{h}_{t0}-2\tilde{V}\left(\tilde{B}-1\right)\right] \tag{5-118}$$

$$\frac{\gamma}{\gamma+1}\left(\tilde{u}_0+\tilde{P}_0+1-\tilde{B}^2\right)=\sqrt{\frac{2\gamma}{2+\gamma}\left[\tilde{h}_{t0}-2\tilde{V}\left(\tilde{B}-1\right)\right]} \tag{5-119}$$

As an alternative procedure, we can use the first root for the sonic point $\tilde{u}_s = (\gamma-1)\tilde{V}/(\gamma\tilde{B}_s)$ and also $\tilde{u}_s^2 = \gamma\,\tilde{P}_s/\tilde{\rho}_s = \gamma\tilde{P}_s\tilde{u}_s$. The energy equation then gives:

$$\frac{1}{\gamma-1}\tilde{u}_s^2 + \frac{\tilde{u}_s^2}{2} - \tilde{h}_{t0} + 2\tilde{V}\left(\tilde{B}_s - 1\right) = 0 \tag{5-120}$$

$$\frac{\gamma+1}{2(\gamma-1)}\left(\frac{\gamma-1}{\gamma}\frac{\tilde{V}}{\tilde{B}_s}\right)^2 - \tilde{h}_{t0} + 2\tilde{V}\left(\tilde{B}_s - 1\right) = 0 \tag{5-121}$$

$$\frac{\gamma^2-1}{2\gamma^2}\left(\frac{\tilde{V}}{\tilde{B}_s}\right)^2 - \tilde{h}_{t0} + 2\tilde{V}\left(\tilde{B}_s - 1\right) = 0 \tag{5-122}$$

From the momentum equation one gets $\tilde{u}_0 + \tilde{P}_0$:

$$\begin{aligned}\frac{\gamma-1}{\gamma}\frac{\tilde{V}}{\tilde{B}_s} + \frac{\gamma-1}{\gamma^2}\frac{\tilde{V}}{\tilde{B}_s} + \tilde{B}_s^2 = \tilde{u}_0 + \tilde{P}_0 + 1 \quad \Longrightarrow \quad \tilde{u}_0 + \tilde{P}_0 \\ = \frac{\gamma^2-1}{\gamma^2}\frac{\tilde{V}}{\tilde{B}_s} + \tilde{B}_s^2 - 1\end{aligned} \tag{5-123}$$

and also:

$$\tilde{P}_s = \frac{\tilde{\rho}_s}{\gamma}\gamma\frac{\tilde{P}_s}{\tilde{\rho}_s} = \frac{1}{\gamma\tilde{u}_s}\tilde{u}_s^2 = \frac{\tilde{u}_s}{\gamma} = \frac{\gamma-1}{\gamma^2}\frac{\tilde{E}}{\tilde{B}_s} \tag{5-124}$$

Given $\tilde{h}_{t0}$, and assuming known $\tilde{V}$, the two equations above give $\tilde{u}_0 + \tilde{P}_0$ and $\tilde{B}_s$ (magnetic field at the sonic point), in terms of $\tilde{h}_{t0}$ and $\tilde{V}$.
Finally, by integration of Ohm's law, one gets:

$$\frac{d\tilde{B}}{d\tilde{x}} = -\frac{1}{\varepsilon}\left(\tilde{V} - \tilde{u}\tilde{B}\right) \quad \Longrightarrow \quad \tilde{x} = \varepsilon\int_{\hat{B}}^{1}\frac{d\tilde{B}}{\tilde{V} - \tilde{u}\left(\tilde{B}\right)\tilde{B}} \tag{5-125}$$

and assuming zero magnetic field at the end of the channel, we get:

$$1 = \varepsilon \int_0^1 \frac{d\tilde{B}}{\tilde{V} - \tilde{u}(\tilde{B})\tilde{B}} \qquad (5\text{-}126)$$

In this chapter, we have presented a mathematical analysis of a self-field quasi-one-dimensional plasma flows, with the hypothesis of zero axial current.
In the next chapter we will present some results obtained with a MATLAB® code whose main object is to reproduce the mathematical analysis presented before and, in the last chapter, some conclusions about this thesis will be drawn.

CHAPTER 6: RESULTS

In the last chapter, we performed a mathematical analysis of a **self-field accelerated quasi-one-dimensional plasma flows with zero axial current**, in particular in the case of a **constant area duct**.
These equations are the basics to understand the behavior of self-induced MPD thruster.
In this chapter we're going to show and analyze some results obtained with a ***Matlab Code*** created specifically to develop this Algorithm which are in agreement with the paper "***The Structure of Self-Field Accelerated Plasma Flows***" of ***Prof. Martinez-Sanchez***.

The procedure used to create the algorithm describing the behavior of the plasma flow is summarized below:

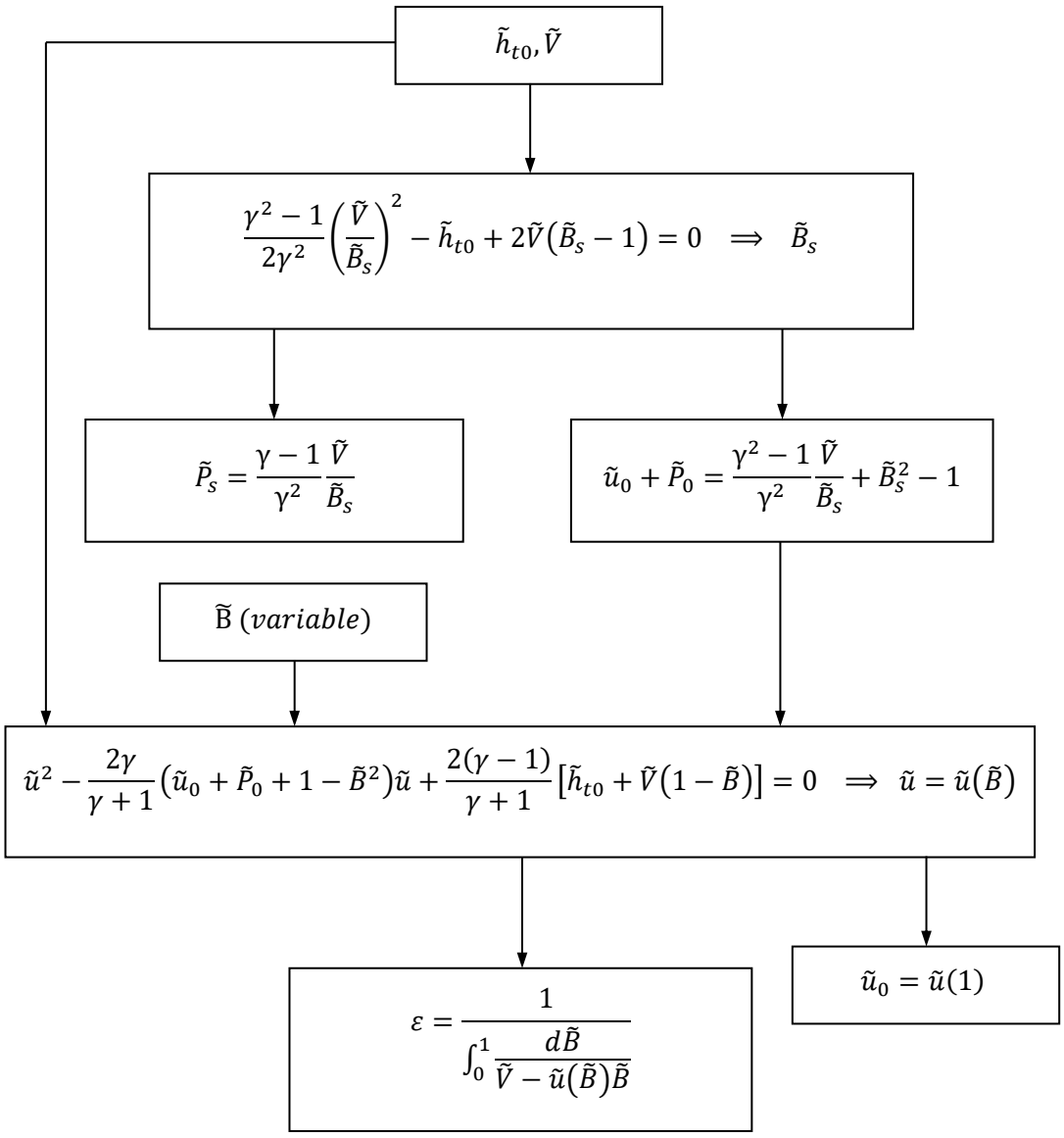

Figure 6-1: Block scheme of the matlab code procedure.

RESULTS OF THE ANALYSIS OF A SELF-FIELD PLASMA FLOW IN A CONSTANT AREA CHANNEL WITH ZERO AXIAL CURRENT

In our analysis, we assumed the following values:

- $B_0 = 0.1\ Tesla$
- $\dot{m}/A^* = 0.5\ kg/s$
- $u_{ref} = 7960\ m/s$
- $P_{ref} = 3980\ N/m^2$
- $\rho_{ref} = 6.28 * 10^{-5}\ kg/m^3$
- $E_{ref} = 796\ V/m$

Below, you can see some graphs obtained with this Matlab Code, varying a couple of non-dimensional parameters calculated before: $\tilde{E}$, which we saw being equal to $\tilde{V}$ in case of Constant Area Channel, and $\tilde{T}_0$, from which, of course, $\tilde{h}_0$ depends.

As you we can see from the block diagram above, these are the two initial data which, throughout the mathematical analysis previously described, will let us find all the other variables.

The graphs are in agreement with those reproduced by Prof. Martinez Sanchez and they are an interesting point of analysis for the behavior of the flow inside the thruster.

The two solutions of the equation:

$$\tilde{u}^2 - \frac{2\gamma}{\gamma+1}\left(\tilde{u}_0 + \tilde{P}_0 + 1 - \tilde{B}^2\right)\tilde{u} + \frac{2(\gamma-1)}{\gamma+1}\left[\tilde{h}_{t0} + \tilde{V}\left(1-\tilde{B}\right)\right] = 0 \quad \Longrightarrow \quad \tilde{u} = \tilde{u}\left(\tilde{B}\right) \tag{6-2}$$

are the subsonic and supersonic velocities, for a given $\tilde{B}$ and the sonic passage can be found finding the minimum of this equation for a certain $\tilde{B} = \tilde{B}_S$.

Considering the final equation:

$$\varepsilon = \frac{1}{\int_0^1 \frac{d\tilde{B}}{\tilde{V} - \tilde{u}\left(\tilde{B}\right)\tilde{B}}} \tag{6-3}$$

We can easily see that the smallest $\tilde{E}$ possible corresponds to the maximum of the quantity $\tilde{u}\tilde{B}$, since otherwise the equation would become singular.

This conclusion, can be easily seen also from the graphs: substituting different values of E, into the code, we can clearly see that, for $\tilde{E}$ smaller than this value, the Magnetic Reynolds Number goes to infinite and the product $\tilde{u}\tilde{B}$ as well, leading to a singularity in the graph.

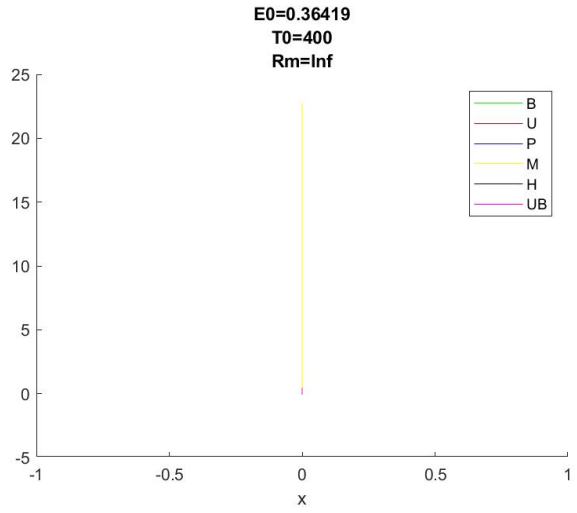

Figure 6-2: Trend of different parameters for $\tilde{E} = 0.36419$ and $T = 400\ K$.

If we now increase $\tilde{E}$ up to his minimum value, we can see that the Magnetic Reynolds Number, even though still very large, is quietly reduced and that the flow accelerates and that there is the formation of strong inlet and exit current concentrations.

Moreover, we can also see that, as expected, P is very small and there is a predominance of the back electromagnetic field $\tilde{u}\tilde{B}$ over the ohmic drop $\tilde{E}$-$\tilde{u}\tilde{B}$ for almost all the channel. However, despite the smallness of P, we can see that its gradient is strongly positive near the exit. This is due to the ohmic heating in that region with negligible magnetic acceleration.

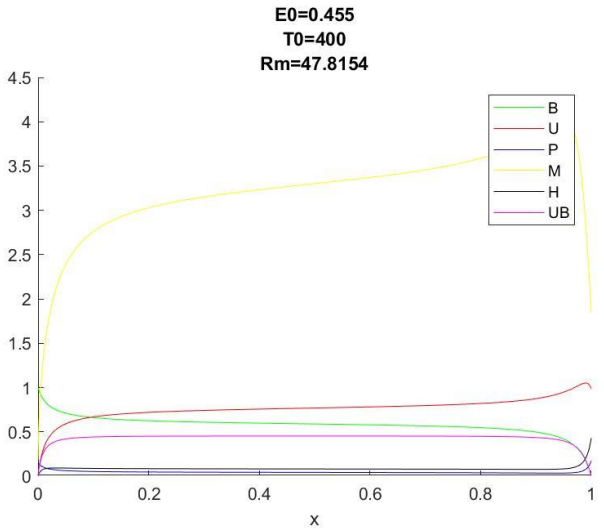

Figure 6-3: Trend of different parameters for $\tilde{E} = 0.455$ and $T = 400\ K$.

As we increase the Electric Field, the Magnetic Reynolds Number decreases and the Pressure Gradient at the end of the channel increases as well, finally leading to a thermal chocking for Magnetic Reynolds Number~3.4.

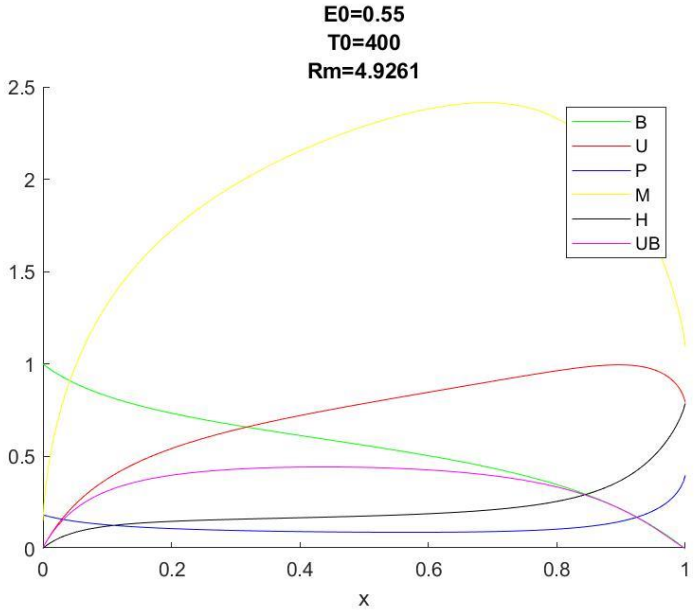

Figure 6-4: Trend of different parameters for $\tilde{E} = 0.55$ and $T = 400\ K$.

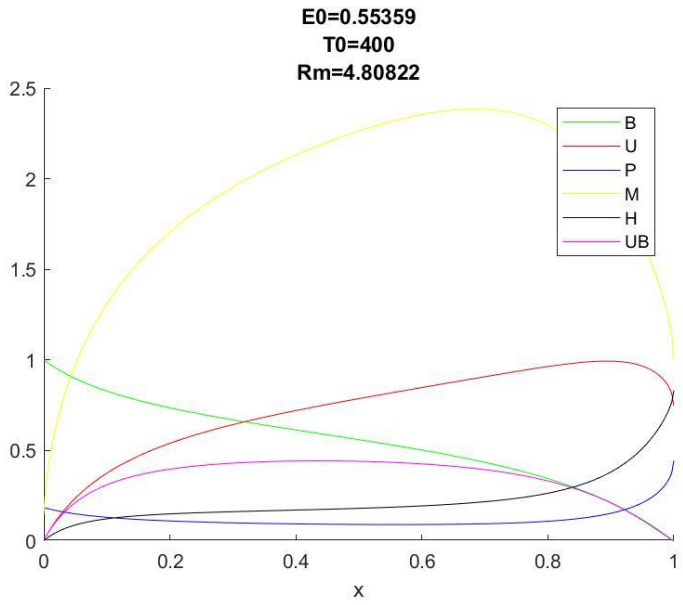

Figure 6-5: Trend of different parameters for $\tilde{E} = 0.55359$ and $T = 400\ K$.

From this point on, the graphs deriving from this matlab code are not very accurate any more.
According to the paper of Professor Martinez Sachez, there should be the formation of the Chocking a bit after the mid of the channel. However, in this small code, we were able to reproduce only the results arising before the thermal shock.
What really happens at this point is that there is the transition from the positive supersonic to the subsonic solution of the equation that we found before.
What we can see from the graphs, in fact, is that under that value of the Magnetic Reynolds Number a discontinuity arises, but the values of the respective Electric Field and Channel Lenght are quite higher than those calculated by Prof. Martinez Sanchez.

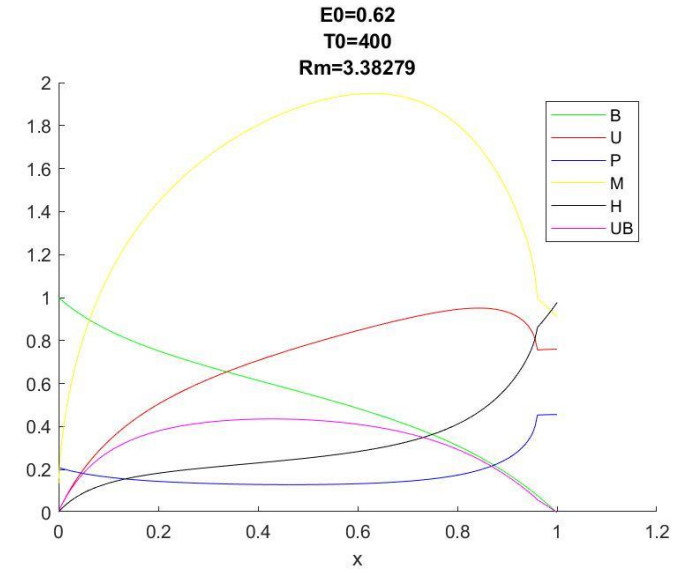

Figure 6-6: Trend of different parameters for $\tilde{E} = 0.62$ and $T = 400\ K$.

Finally, decreasing even more the Reynolds Magnetic Number, the graphs clearly diverge and are not reliable any more.

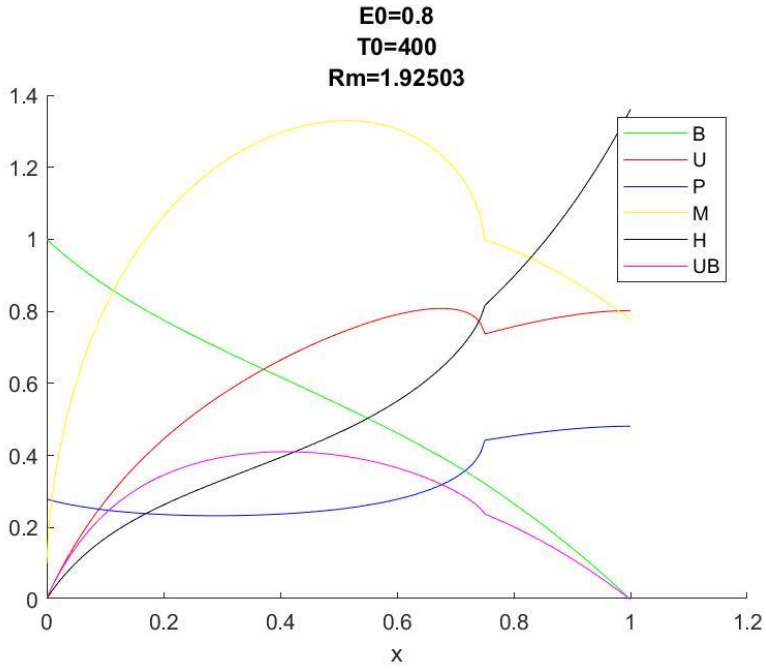

Figure 6-7: Trend of different parameters for $\tilde{E} = 0.8$ and $T = 400\ K$.

If we then run the Program increasing the value of the Temperature we can see that the trend of these different parameters is the opposite: the Reynolds Magnetic Number, in fact, increases and the other parameters will vary consequently.

For values of the Electromagnetic field higher than 0.5 the variation of the Temperature leads to a small variation in the Reynolds Magnetic Number.

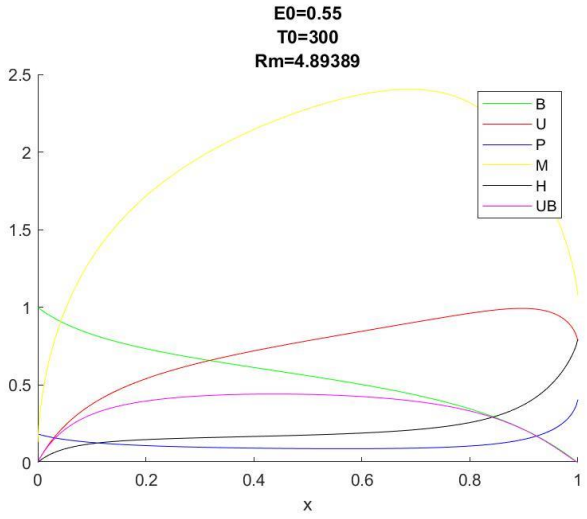

Figure 6-8: Trend of different parameters for $\tilde{E} = 0.55$ and $T = 300\ K$.

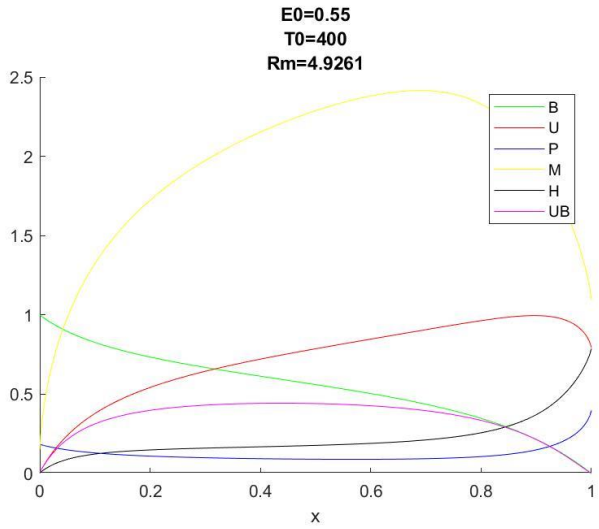

Figure 6-9: Trend of different parameters for $\tilde{E} = 0.55$ and $T = 400\ K$.

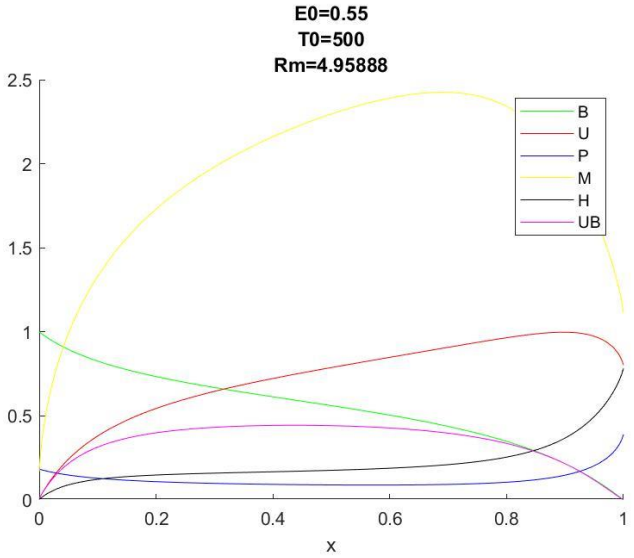

Figure 6-10: Trend of different parameters for $\tilde{E} = 0.55$ and $T = 500\ K$

However, if the Electromagnetic Field is too low an increase in the Temperature will lead to infinite values of the Reynolds Magnetic Number and the model is not accurate anymore, due to the strong localized heating typical of the Constant Area Geometry, as we can see in the figures below.

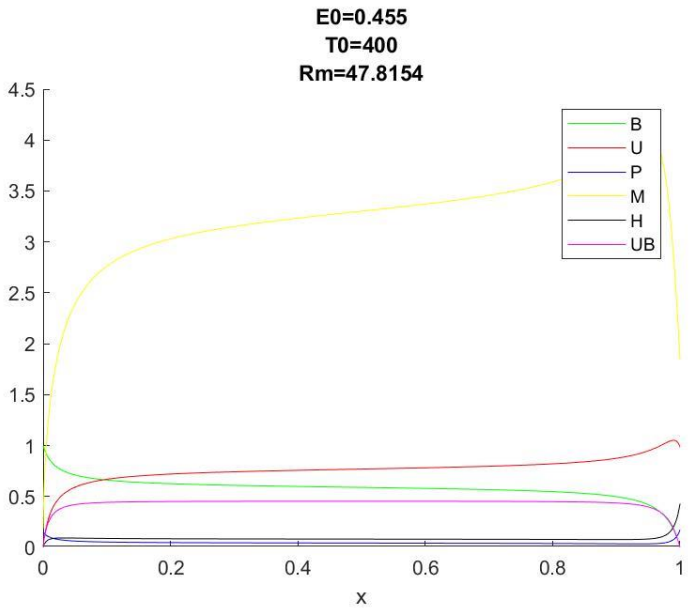

Figure 6-11: Trend of different parameters for $\tilde{E} = 0.455$and $T = 400\ K$.

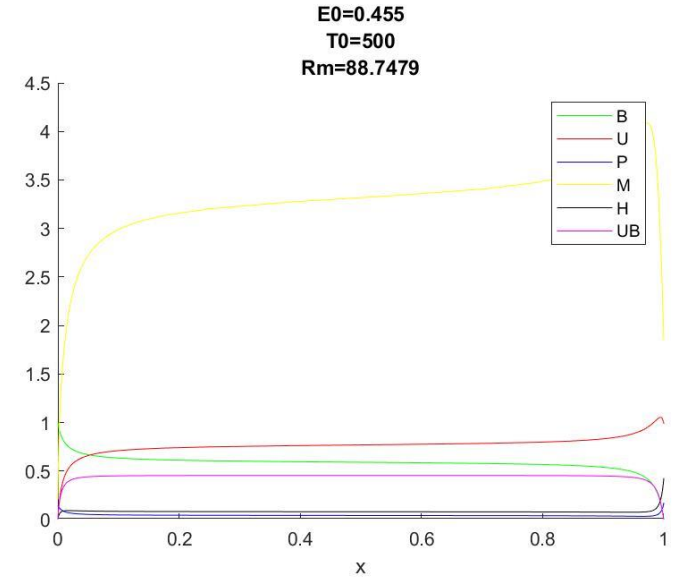

Figure 6-12: Trend of different parameters for $\tilde{E} = 0.455$ and $T = 500\ K$.

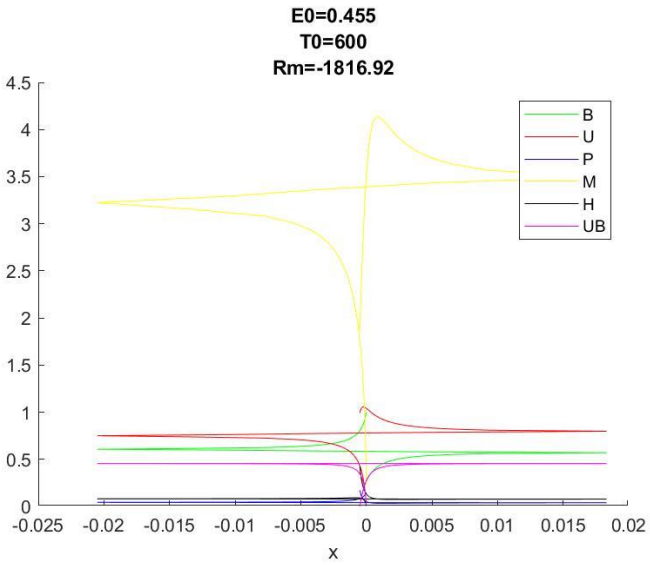

Figure 6-13: Trend of different parameters for $\tilde{E} = 0.455$ and $T = 500\ K$.

The results by Professor Martinez Sanchez, in the analysis of a Convergent Divergent Channel, using the same initial values show that:

- no current concentration is seen near the inlet or the exit and the current density is almost uniform along the channel;
- there is no positive pressure gradient near the exit, which means that the flow is never decelerated;
- the Mach-Alfven number is a bit less than one at the throat and increases above one in the divergent part of the channel.

What we can conclude from the results obtained from the graphs is that for big Reynolds Magnetic Numbers, geometrical throats are magnetosonically chocked and there is a predominance of the back electromagnetic field $\tilde{u}\tilde{B}$ over the ohmic drop $\tilde{E}$-$\tilde{u}\tilde{B}$ for almost all the channel.

Then, we also saw that the strong inlet and outlet current concentrations produce important thermal effects for a constant area channel, while for a convergent divergent channel there are no pressure gradients near the exit, so the flow is not decelerated.

These results are in agreement with those obtained by Prof. Martinez Sanchez for the Constant Area Channel until the Magnetic Reynolds Number decreases to 3.4. After that, we saw that the results are not so accurate any more. This is most likely due to limitations arising from the code itself which does not simulate perfectly the shock wave.

CHAPTER 7: CONCLUSIONS

With this thesis we investigated the operations of a Magneto Plasma Dynamic Thruster with a MatLab code that has been created to reproduce the conclusions drawn by Professor Martinez Sanchez in the paper "***The Structure of Self-Field Accelerated Plasma Flows***".

After a brief mathematical analysis of the basic equations which describe the MPD, some important parameters such as thrust, efficiency and exhaust velocity of the engine were calculated, then a simplified ***quasi-one-dimensional model*** of the plasma flow, in which the magnetic field has been assumed to be transversal to x, was formulated.

We then calculated, in particular, a steady state solution where we assumed:

- constant voltage along the channel,
- no pressure contribution,
- constant area channel,

and for this specific case, a MatLab code was created to reproduce the trend of some important parameters such as the magnetic field, the exhaust velocity and the current density.

What we could see was that our results are in agreement with those obtained by Prof. Martinez Sanchez for the constant area channel until the magnetic Reynolds number decreases to 3.4. After that, we saw that the results are not so accurate any more, most likely due to limitations arising from the code itself which does not perfectly simulate the shock wave.

For future work it would be interesting to create a Matlab code to simulate the convergent divergent channel and then to perform some simulations with a Multiphysics Software to compare the quasi-one-dimensional model with a 2D model.

BIBLIOGRAPHY

[1] Leiter, H. J. ,et al., Development and performance of the advanced radio frequency ion thruster RIT-XT [online] Available at < http://erps.spacegrant.org/uploads/images/images/iepc_articledownload_1988-2007/2003index/0115-0303iepc-full.pdf> [accessed 27 November 2017]

[2] Shtyrlin, A. F., 1995. State of the art and future prospects of colloidal electric thrusters. *IEPC*. [Online] Available at < http://erps.spacegrant.org/uploads/images/images/iepc_articledownload_1988-2007/1995index/IEPC1995-103.pdf> [accessed 27 November 2017]

[3] Chen, F.F., *Introduction to plasma physics and controlled fusion.* Second edition. New York: Plenum Press.

[4] Mikellides, P.G., Pulsed Inductive Thruster PIT Modeling and Validation Using the MACH2 Code. [Online] Available at <https://www.researchgate.net/publication/24373674_Pulsed_Inductive_Thruster_PIT_Modeling_and_Validation_Using_the_MACH2_Code> [accessed 27 November 2017]

[5] Bosia, G., Lezione 11 Equazioni Magneto-idrodinamiche [online] Available at <http://personalpages.to.infn.it/~gbosia/Fisica_Tecnologie%20Avanzate/LEZIONI%20FISICA%20DEL%20PLASMA%20CONFINATO/Lezione%2011%20Equazioni%20MHD.ppt.pdf> [accessed 27 November 2017]

[6] Gallina, G. 2014. Simulazioni PIC di sorgenti di plasma per applicazioni spaziali e di fusione. [online] Available at <http://tesi.cab.unipd.it/46633/1/Gallina_Giacomo.pdf> [accessed 27 November 2017]

[7] C Francescangeli, C. 2011. Aspetti fisici della propulsione spaziale al plasma. [online] Available at <http://cdlfbari.cloud.ba.infn.it/wp-content/uploads/file-manager/CIF/Triennale/Tesi%20di%20laurea/10-11-FRANCESCANGELI%20Claudia.pdf> [accessed 27 November 2017]

[8] Zakrzwski, C., Benson, S., 2001. Pulsed Plasma Thruster (PPT). [online] Available at <https://eo1.gsfc.nasa.gov/new/miscPages/TechForumPres/25-PPT.pdf> [accessed 27 November 2017]

[9] Mathworks. [online] Available at <www.mathworks.com> [accessed 27 November 2017]

[10] Wikipedia. [online] Available at <www.wikipedia.org> [accessed 27 November 2017]

[11] Hirsch, C., 2007 *Numerical Computation of Internal and External Flows.* Second edition. Elsevier Ltd

[12] Landau, L.D. Lifshitz, E.M., *Course on Theoretical Physics vol III*.

[13] Powell, K. G. 1997 An Approximate Riemann Solver for Magnetohydrodynamics (That works in more than one dimension)". Berlin: Springer-Verlag

[14] Martinez-Sanchez, M., The Structure of Self-Field Accelerated Plasma Flows. [online] Available at <https://arc.aiaa.org/doi/abs/10.2514/3.23294> [accessed 27 November 2017]

[15] Martinez-Sanchez, M., Mission Requirements for Space Propulsion, 16.522, {Course material], unpublished

[16] Plasma Rockets., [online] Available at <http://orbitalvector.com/Deep%20Space%20Propulsion/Plasma%20Rockets/Plasma%20Rockets.htm> [accessed 27 November 2017]

[17] Manente, M., Laboratorio di propulsione aerospaziale. Università degli Studi di Padova, Unpublished.